Technische Universität München
Fakultät für Medizin

Nuclear Pore Complex clustering in HGPS and Replicative Senescence

Jennifer Marie Röhrl

Vollständiger Abdruck der von der Fakultät für Medizin der Technischen Universität München zur Erlangung einer

Doktorin der Naturwissenschaften (Dr. rer. nat.)

genehmigten Dissertation.

Vorsitz: Prof. Dr. Carsten Schmidt-Weber

Prüfer*innen der Dissertation:

1. Prof. Dr. Karima Djabali
2. Prof. Dr. Thomas Brück

Die Dissertation wurde am 04.05.2022 bei der Technischen Universität München eingereicht und durch die Fakultät für Medizin am 09.08.2022 angenommen.

ACKNOWLEDGEMENTS

While working on my thesis, I received a great deal of support from a multitude of people, without whom I would have never been able to finish.

First of all, I would like to thank Professor Karima Djabali for granting me the opportunity to work on this thesis in her laboratory. Her guidance and insight helped me immeasurably to complete my dissertation and I will be forever grateful.

I also wish to thank Professor Thomas Brück and Dr. Alexander Konstantinow for their support throughout the course of my thesis.

I want to thank my fellow PhD students as well, without whom life in the lab would not have been nearly as much fun or as successful. You were the best colleagues I could hope for, and I already miss you so much.

Rouven, you are without the doubt the Master of the Western Blot and SingStar. Farah, you were the best office partner I could wish for! I will miss your questions and your never-ending optimism. Chang was one of the best discussion partners I ever had, and I really miss our little political skirmishes. Elena, I will miss our little chats and your ability to create fun out of nowhere. Peter, I will miss your wild stories, you definitely expanded my horizons! Last but not least, I want to thank Leithe, Lu Xiang, Eva and Hannah, you are awesome!

In addition, I would like to thank my entire family for their support, sympathetic ear, and wise counsel. Without your faith in my abilities, I would have never made it this far and I cannot thank you enough.

Lastly, I wish to dedicate this thesis to my grandfather. To my never-ending regret he cannot be here to witness the completion of my dissertation.

ABSTRACT

Hutchinson-Gilford progeria Syndrome (HGPS) is a rare premature aging disease in which patients have an average lifespan of only 14.6 years, with the major cause of death being cardiovascular defects. The disease is caused by a single-base mutation in the *LMNA* gene G608G (GGC→GGT), which introduces a cryptic splice site into exon 11 of *LMNA*. Aberrant splicing of the mutated Lamin A gene deletes 50 amino acids from the C-terminus of pre-LA, removing the recognition site of the protease Zmpste24. As a result, pre-Lamin A is not processed correctly and remains permanently farnesylated and therefore erroneously attached to the nuclear envelope. This mutant version of pre-Lamin A is called progerin and it causes a variety of cellular defects such as nuclear dysmorphism, loss of heterochromatin, premature senescence, faulty DNA repair, and clustering of Nuclear Pore Complexes (NPCs).

To identify the mechanism behind NPC clustering in HGPS, I first evaluated postmitotic NPC reassembly in control and HGPS fibroblasts and could not identify any defects in mitotic HGPS cells. Unlike progerin, the components of the NPC I analyzed did not aggregate and incorporation into the nuclear envelope was not delayed.

Since I found no defects in post-mitotic NPC reassembly, I examined the incidence of NPC clustering in control and HGPS fibroblasts undergoing replicative senescence. I observed that NPC clustering solely occurred in dysmorphic nuclei of control and HGPS fibroblasts. In addition, I detected a higher number of clustered NPCs in young (<5% senescence) or early passage HGPS fibroblasts, compared to control fibroblasts. In old cultures (>30% senescence) with a similar senescence index, the number of clustered NPCs was nearly identical in control and HGPS. To determine why a higher number of NPCs clustered in dysmorphic HGPS nuclei, I evaluated the relationship of progerin content and NPC clustering. I discovered that on average 87% of dysmorphic nuclei with clustered NPCs had an elevated progerin signal independent of cellular senescence. This observation offered an explanation as to why more pores cluster in young HGPS cells than in control.

However, the control fibroblasts I analyzed did not express progerin, raising the question, why NPCs clustered in them as well. This led to the conclusion that the disruption of the NE composition by mechanisms of replicative senescence e.g., downregulation of LB1 was the likely cause of NPC clustering in dysmorphic control nuclei.

In conclusion, I determined that NPC distribution depends on an intact nuclear envelope and any changes to its composition, such as the presence of progerin or reduction of LB1, can result in abnormal NPC localization or clustering.

ZUSAMMENFASSUNG

Hutchinson-Gilford-Progerie-Syndrom (HGPS) ist eine seltene Krankheit des vorzeitigen Alterns, bei der die Patienten eine durchschnittliche Lebenserwartung von nur 14,6 Jahren haben, wobei die Haupttodesursache kardiovaskuläre Defekte sind. Die Krankheit wird durch eine Basen-Mutation im LMNA-Gen G608G (GGC→GGT) verursacht, die eine kryptische Splicestelle in Exon 11 der LMNA einführt. Durch das abweichende Splicen des mutierten Lamin-A-Gens werden 50 Aminosäuren aus dem C-Terminus von pre-LA entfernt, wodurch die Erkennungsstelle der Protease Zmpste24 wegfällt. Infolgedessen wird prä-Lamin A nicht korrekt prozessiert und bleibt permanent farnesyliert und daher fälschlicherweise an der Kernhülle befestigt. Diese mutierte Version von Pre-Lamin A wird Progerin genannt und verursacht eine Reihe von Zelldefekten wie Zellkern-dysmorphismus, Verlust von Heterochromatin, vorzeitige Seneszenz, fehlerhafte DNA-Reparatur und Clustern von Kernporenkomplexen (NPCs).

Um den Mechanismus hinter der NPC-Clusterung bei HGPS zu identifizieren, habe ich zunächst die postmitotische NPC-Neubildung in Kontroll- und HGPS-Fibroblasten untersucht und konnte in mitotischen HGPS-Zellen keine Defekte feststellen. Im Gegensatz zu Progerin aggregierten die Komponenten des von mir untersuchten NPC nicht und der Einbau in die Kernhülle war nicht verzögert.

Da ich keine Defekte in der postmitotischen NPC-Neuzusammensetzung fand, untersuchte ich das Auftreten von NPC-Clustering in Kontroll- und HGPS-Fibroblasten, die eine replikative Seneszenz durchlaufen. Ich stellte fest, dass NPC-Clustering ausschließlich in dysmorphen Kernen von Kontroll- und HGPS-Fibroblasten auftrat. Darüber hinaus entdeckte ich in jungen (<5% Seneszenz) oder frühen HGPS-Fibroblasten eine höhere Anzahl von NPC-Clustern im Vergleich zu Kontroll-Fibroblasten. In alten Kulturen (>30% Seneszenz) mit einem ähnlichen Seneszenz Index war die Anzahl der geclusterten NPCs in Kontroll- und HGPS-Fibroblasten fast identisch. Um herauszufinden, warum in dysmorphen HGPS-Nuklei eine höhere Anzahl von NPCs geclustert waren, untersuchte ich die Beziehung zwischen Progerin Gehalt und NPC-Clustering. Ich entdeckte, dass im Durchschnitt 87 % der dysmorphen Kerne mit geclusterten NPCs ein erhöhtes Progerin-Signal aufwiesen, unabhängig von der zellulären Seneszenz. Diese

Beobachtung bot eine Erklärung dafür, warum sich in jungen HGPS-Zellen mehr Poren anhäufen als in Kontrollzellen.

Die von mir untersuchten Kontroll-Fibroblasten exprimierten jedoch kein Progerin, was die Frage aufwirft, warum sich auch in ihnen NPCs anhäuften. Dies führte zu der Schlussfolgerung, dass die Störung der NE-Zusammensetzung durch Mechanismen der replikativen Seneszenz, z. B. die Herunterregulierung von LB1, die wahrscheinliche Ursache für die Anhäufung von NVZ in dysmorphen Kontrollkernen ist.

Zusammenfassend habe ich festgestellt, dass die Verteilung der NPC von einer intakten Kernhülle abhängt und dass jede Veränderung ihrer Zusammensetzung, wie z. B. das Vorhandensein von Progerin oder die Reduzierung von LB1, zu einer abnormalen NPC-Lokalisierung oder -Clusterung führen kann.

Table of Contents

1. Introduction 1

1.1 The nuclear Lamina 1

1.2 Hutchinson-Gilford progeria Syndrome 6

1.3 The Nuclear Pore Complex 10

1.3.1 Structure and function of the Nuclear Pore Complex 10

1.3.2 Assembly of the NPC 13

1.4 Replicative senescence 17

2. Materials and Methods 20

2.1 Materials 20

2.1.1 Chemicals 20

2.1.2 Instruments 20

2.1.3 Kits, cell lines and antibodies 21

2.2 Methods 24

2.2.1 Cell culture 24

2.2.2 Senescence associated β-Galactosidase assay 25

2.2.3 Immunocytochemistry 25

2.2.4 Image analysis 26

2.2.5 Statistical evaluation of NPC clustering and progerin levels via immunocytochemistry 26

3. Results 28

3.1 Analysis of post-mitotic NPC assembly in control and HGPS fibroblasts 28

3.1.1 Unlike NUP107, progerin aggregated in the cytoplasm of mitotic HGPS cells 29

3.1.2 Seeding of post-mitotic NPCs by ELYS was not affected in HGPS 32

3.1.3 Mitotic localization of the basket nucleoporin NUP153 was not altered in HGPS 36

3.1.4 SUN1 aggregates did not influence POM121 recruitment or localization in post-mitotic NPC assembly 39

3.2 Analysis of nuclear morphology, progerin protein levels and NPC clustering in replicative senescence in control and HGPS fibroblasts 46

3.2.1 Nuclear morphology in replicative senescence 47

3.2.2 Detection of senescent HGPS and control fibroblasts 50

3.2.3 Progerin in replicative senescence 54

3.2.4 NPC clustering in replicative senescence 59

4. Discussion 70

4.1 NPC assembly in HGPS 70
4.1.1 Post-mitotic NPC reassembly in HGPS 70
4.1.2 De novo interphase NPC assembly in HGPS 74
4.2 Replicative senescence, nuclear morphology and NPC clustering in HPGS 77
4.2.1 Nuclear morphology and replicative senescence 77
4.2.2 Progerin and replicative senescence 80
4.2.3 Replicative senescence and NPC clustering 82
5. Appendix 85
5.1 Supplementary information 85
5.1.1 Tables 85
5.2 List of figures 90
5.3 List of tables 92
6. References 93

1. Introduction

1.1 The nuclear Lamina

The nucleus is an essential compartment of eukaryotic cells that encapsulates our genetic information inside a double-lipid membrane. The outer nuclear membrane (ONM) facing the cytoplasm is continuous with the endoplasmic reticulum (ER) and is separated by the perinuclear space (PNS) from the inner nuclear membrane (INM). The ONM is similar in composition to the ER, whereas the INM has a unique set of peripheral and integral proteins e.g., lamins, emerin, Lap2β, MAN1, Lamin B receptor (LBR) and the Nuclear Pore Complex (NPC). The outer and inner nuclear membrane are fused at multiple sites, creating 'holes' in which NPCs are anchored, allowing for transport across the nuclear envelope (Lin and Hoelz 2019). Spacing of the PNS is regulated by the LINC complex (linker of the nucleoskeleton and cytoskeleton), which is also involved in mechanotransduction and connects the nuclear lamina to the cytoskeleton of the cell (Rothballer, Schwartz et al. 2013). Below is a schematic representation of some of the components found in the nuclear envelope (NE)(Figure 1.1).

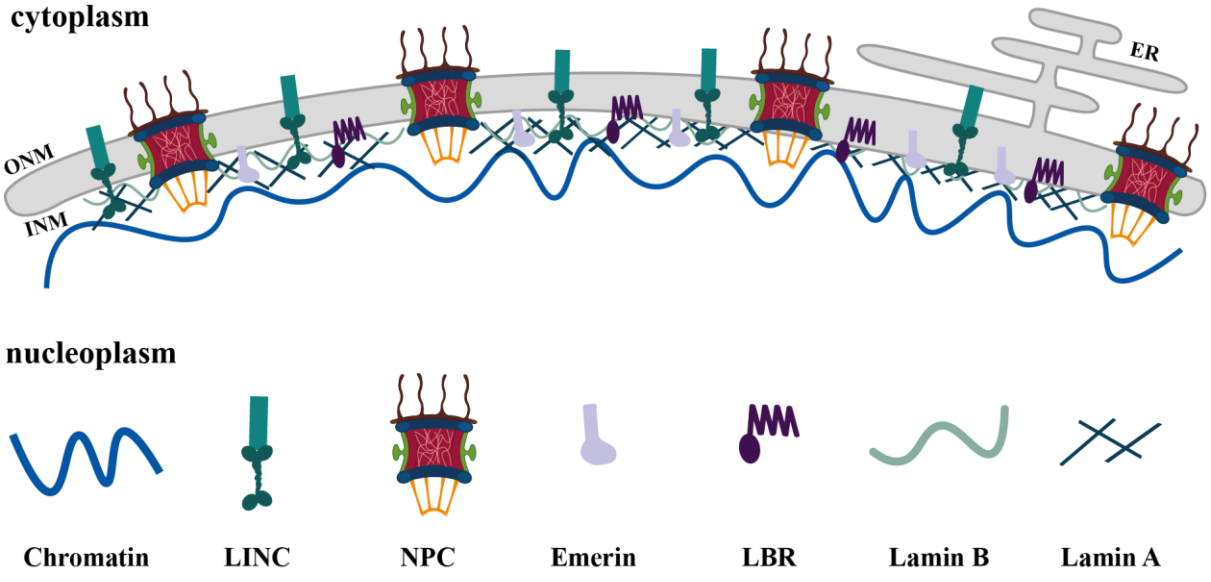

Figure 1.1 Schematic representation of the nuclear envelope

The lipid bilayer of the NE and ER is shown in grey. The LINC complex connects the lamina to the cytoskeleton, the NPC allows transport across the NE, emerin associates with the lamina, LBR anchors LB and chromatin (Olins, Rhodes et al. 2010) to the NE and Lamin B/A create the nuclear lamina. Not all components of the NE are depicted.

The nuclear lamina is a protein network made up by so-called lamins, creating a filamentous meshwork underlying the INM of the nuclear envelope, ensuring stability, flexibility and shape of the nucleus (Pappas 1956, Fawcett 1966, Aebi, Cohn et al. 1986, de Leeuw, Gruenbaum et al. 2017). Lamins are type V intermediate filament proteins with a short N-terminal head domain, a central rod domain composed of four α-helical domains that are separated by Linker regions and a globular C-terminal domain, containing motifs that distinguish lamins from other intermediate filaments: a nuclear localization sequence (NLS), an immunoglobulin (Ig) fold motif and a C-terminal CaaX motif (C = cysteine, a = aliphatic amino acid, X = any amino acid) (Fisher, Chaudhary et al. 1986, McKeon, Kirschner et al. 1986, Krohne, Wolin et al. 1987, Gruenbaum, Landesman et al. 1988). Mammalian cells have two types of lamins, Type-A and B. The two A-type lamins, Lamin A and C (LA, LC), are both encoded by the *LMNA* gene and generated by alternative splicing (Lin and Worman 1993). B-type Lamins Lamin B1 (LB1) and B2 are encoded by two different genes, namely *LMNB1* and *LMNB2* (Parry, Conway et al. 1986, Peter, Kitten et al. 1989, Vorburger, Lehner et al. 1989, Lin and Worman 1993). All mammalian cells express at least one B-type lamin, whereas A-type lamins are mainly expressed in differentiated cells (Lehner, Stick et al. 1987, Stewart and Burke 1987, Rober, Weber et al. 1989).

A- and B-type lamins create separate networks, but both assemble into 3.5 nm thick tetrameric filaments (Shimi, Kittisopikul et al. 2015, Turgay, Eibauer et al. 2017). A-type lamins stiffen the nucleus to protect it from deformation, whereas B-type lamins are involved in providing the nucleus with elastic properties. (Xie, Chojnowski et al. 2016, de Leeuw, Gruenbaum et al. 2017). Mutations or loss of A- and B-type lamins can cause nuclear abnormalities and have a negative effect on overall health. Reduction of LA/C increases susceptibility to mechanical stress, while LB1 reduction increases NE blebbing, but not mechanical stress (Sullivan, Escalante-Alcalde et al. 1999, Lammerding, Fong et al. 2006). *LMNA*$^{-/-}$ mice are born healthy, but soon suffer from severe muscle wasting and have an average lifespan of 8 weeks (Sullivan, Escalante-Alcalde et al. 1999). Their cells display increased nuclear fragility, deformability and impaired activation of transcription (Lammerding, Schulze et al. 2004). Mice with mutated

LMNB1 die at birth and their fibroblasts senesce prematurely, have abnormal nuclei and an increased incidence of polyploidy (Vergnes, Péterfy et al. 2004).

Both B-type lamins and Lamin A undergo post-translational modifications at their C-terminal CaaX motif (de Leeuw, Gruenbaum et al. 2017). Lamin A (LA) is synthesized as a precursor called pre-Lamin A (pre-LA) and is farnesylated and methylated at its' CaaX motif to ensure targeting to the nuclear membrane (Weber, Plessmann et al. 1989, Sinensky, Fantle et al. 1994) (Figure 1.2 a). Once pre-LA is properly localized to the INM, it is cleaved by the Zmpste24 metalloproteinase at Tyr646, which deletes 15 amino acids including the modified CaaX motif (Pendás, Zhou et al. 2002, Corrigan, Kuszczak et al. 2005) (Figure 1.2 a). Unlike

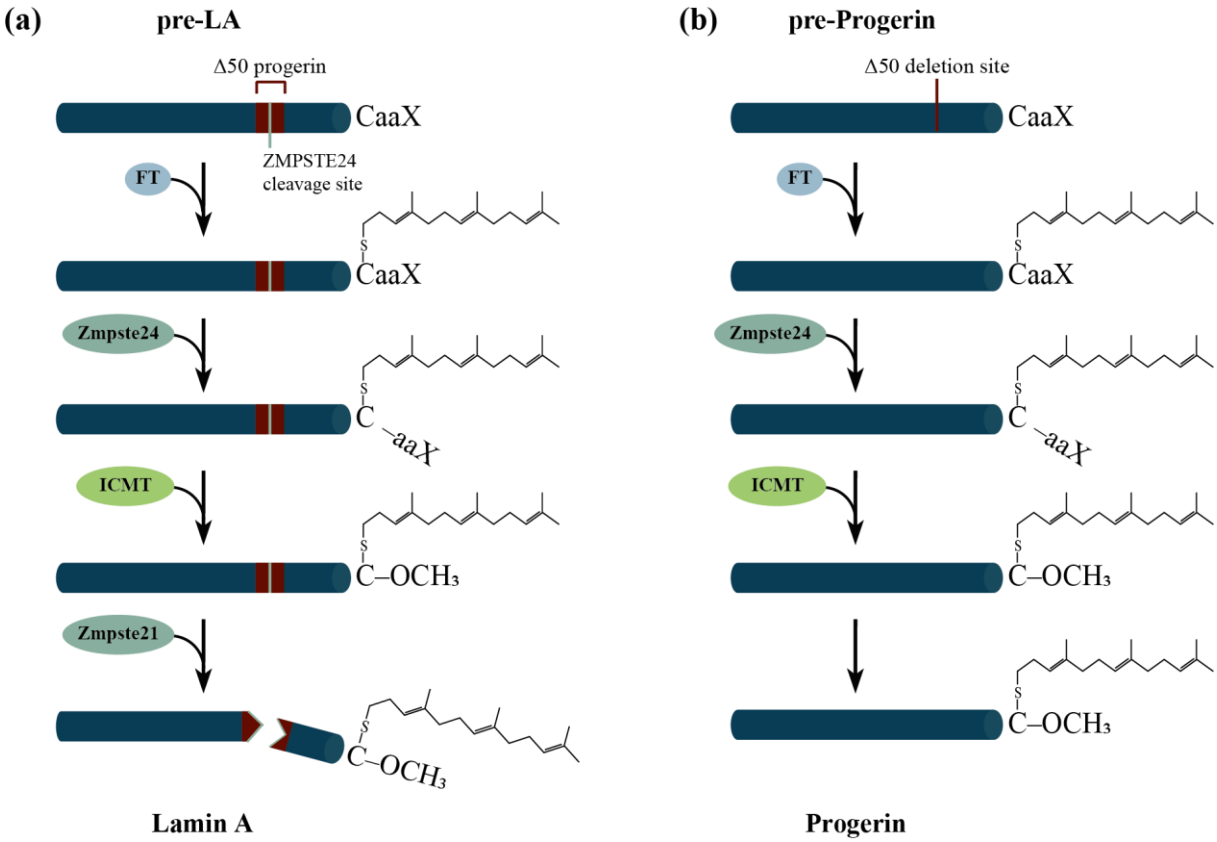

Figure 1.2 Schematic representation of the Lamin A and Progerin processing pathway

Lamina A is synthesized as a precursor called pre-LA. (a) Pre-LA is farnesylated by Farneslyltransferase (FT) and methylated by Isoprenylcysteine carboxyl methyltransferase (ICMT) at its CaaX motif before import into the nucleus. Once pre-LA is integrated into the nuclear lamina, the farnesyl- and methyl-group are cleaved by Zmpste24, and LA is no longer attached to the NE. (b) Due to the cryptic splice site in exon 11 of *LMNA* in HGPS patients, pre-Progerin lacks the recognition site of Zmpste24. Pre-progerin is methylated and farnesylated, but retains both groups and progerin permanently attaches to the NE.

Lamin A, B-type lamins retain the farnesyl- and methyl group following post-translational modification, permanently attaching them to the INM (Adam and Goldman 2012).

Lamins are not only structural components of the nuclear envelope, they interact with various proteins, such as LEM domain proteins, SUN1-domain proteins, Lamina-associated polypeptide 1 (LAP1) and LBR. These interactions allow mechanosignal transduction via their connection with the LINC complex and they are involved in chromatin organization (Swift, Ivanovska et al. 2013, de Leeuw, Gruenbaum et al. 2017). Mechanotransduction happens via the connection of the lamina to the LINC-complex. The LINC-complex is comprised of two transmembrane protein families in mammalian cells: two SUN domain proteins reside in the INM (SUN1/2) and the six KASH domain proteins in the ONM (Lee and Burke 2018). The SUN proteins create dimers, which bind to KASH domain proteins in the PNS (Crisp, Liu et al. 2006, Sosa, Rothballer et al. 2012). SUN1 and SUN2 associate with the nuclear lamina and KASH domain proteins connect to the cytoskeleton, allowing mechanosignal transduction across the NE (Crisp, Liu et al. 2006, Haque, Lloyd et al. 2006, Janota, Calero-Cuenca et al. 2020). Alterations in this relationship can disrupt nuclear and chromatin positioning, cell migration, gene expression, perinuclear actin and nuclear shape (Lombardi, Jaalouk et al. 2011, Banerjee, Zhang et al. 2014, Chen, Wang et al. 2014, Tajik, Zhang et al. 2016).

On the periphery of the nucleus one can find a dense layer of heterochromatin, close to the nuclear lamina. These so-called Lamina-associated domains (LADs) are usually heterochromatic with low transcriptional activity and often contain repressive histone modifications (Buchwalter, Kaneshiro et al. 2019). In some cases chromatin can bind directly to the lamina, whereas some interactions are regulated by other lamina-associated proteins such as LBR, MAN1, lamina-associated polypeptide 2 (LAP2) and emerin (Buchwalter, Kaneshiro et al. 2019). Changes in the interaction of the lamina with LADs can have dramatic effects e.g.: reduction of Lamin B1 during replicative senescence induces genome reorganization or mutations in *LMNA* can cause loss of heterochromatin (Shumaker, Dechat et al. 2006, Sadaie, Salama et al. 2013).

At least 15 diseases, so-called laminopathies, are linked to mutations in lamins or lamin-binding proteins, demonstrating their importance (Worman, Ostlund et al. 2010). They can be

divided into four major sub-types: one peripheral neuropathy, striated muscle disorders, lipodystrophy syndromes and pre-mature aging disorders. Examples include Charcot-Marie-Tooth Disorder Type 2B1, autosomal-dominant Emery-Dreifuss Muscular Dystrophy, Dunnigan-type Familial Partial Lipodystrophy, Atypical Werner Syndrome and Hutchinson-Gilford Progeria Syndrome (Worman and Bonne 2007). Intriguingly, laminopathies do not affect all tissues equally or at all, despite lamins being ubiquitously expressed. A factor might be that changes in the lamina affect chromatin organization and thereby alter gene expression, which would vary depending on the cell type/tissue (Gonzalo, Kreienkamp et al. 2017). Some also propose that the resulting changes in mechanotransduction would have a greater effect on tissues exposed to mechanical tension such as muscles and bones, as seen e.g., in Hutchinson-Gilford Progeria Syndrome.

1.2 Hutchinson-Gilford progeria Syndrome

Hutchinson-Gilford progeria Syndrome (HGPS) is a rare premature aging disease in which patients have an average lifespan of only 14.6 years (Ullrich and Gordon 2015). The syndrome occurs in about 1 in 8 million births (DeBusk 1972, Eriksson, Brown et al. 2003, Hennekam 2006) and the major cause of death is cardiac defects. Vascular smooth muscle cell degeneration and calcification leads to accelerated arteriosclerosis, resulting in stroke or myocardial infarction (Merideth, Gordon et al. 2008, Salamat, Dhar et al. 2010). Other symptoms include alopecia, lipodystrophy, osteoporosis, wrinkled skin, joint contractures and weakened muscles (Merideth, Gordon et al. 2008, Gerhard-Herman, Smoot et al. 2012, Gordon, Massaro et al. 2014, Ullrich and Gordon 2015). The cause is a single-base mutation in the *LMNA* gene G608G (GGC→GGT), which introduces a cryptic splice site into exon 11 (De Sandre-Giovannoli, Bernard et al. 2003, Eriksson, Brown et al. 2003). Aberrant splicing of mutated *LMNA* deletes 50 amino acids from pre-LA C-terminus, (Kreienkamp and Gonzalo 2019) removing the Zmpste24 recognition site and pre-LA cannot be processed correctly (Figure 1.2 b).

Since Zmpste24 no longer removes the farnesylated C-terminus of pre-LA, we now have a permanently farnesylated toxic pre-LA protein in the nucleus, which is called “progerin” (Capell, Erdos et al. 2005). Due to the farnesyl-anchor, progerin is stably attached to the nuclear envelope, unlike LA (Capell, Erdos et al. 2005, Young, Fong et al. 2005). This leads to an accumulation of progerin over time and consequent stiffening of the NE, resulting in a dysmorphic nuclear morphology (Goldman, Shumaker et al. 2004, Toth, Yang et al. 2005) (Figure 1.3, Figure 3.1 & Figure 3.2). Cellular symptoms of progerin include not only abnormal nuclear morphology, but also deregulated gene expression, binucleation, lagging chromosomes in mitosis, loss of peripheral heterochromatin, faulty DNA repair, shortened telomeres, mitochondrial dysfunction, premature senescence and clustering/altered distribution of multiple NE proteins (Figure 1.3) (Goldman, Shumaker et al. 2004, Cao, Capell et al. 2007, Chen, Chi et al. 2012, Rivera-Torres, Acín-Perez et al. 2013, Eisch, Lu et al. 2016).

Progerin is not exclusively detectable in HGPS patients, it also accumulates in aging dermal fibroblasts (McClintock, Ratner et al. 2007). Aberrant splicing can occur at low levels *in vivo* and while mRNA levels are low, progerin can accumulate in the skin of aging individuals (McClintock, Ratner et al. 2007). Pre-LA has also been detected in vascular smooth muscle cells (VSMC), where it interferes with mitosis and induces DNA damage, leading to genomic instability and premature senescence (Ragnauth, Warren et al. 2010, Cobb, Larrieu et al. 2016, Ashapkin, Kutueva et al. 2019).

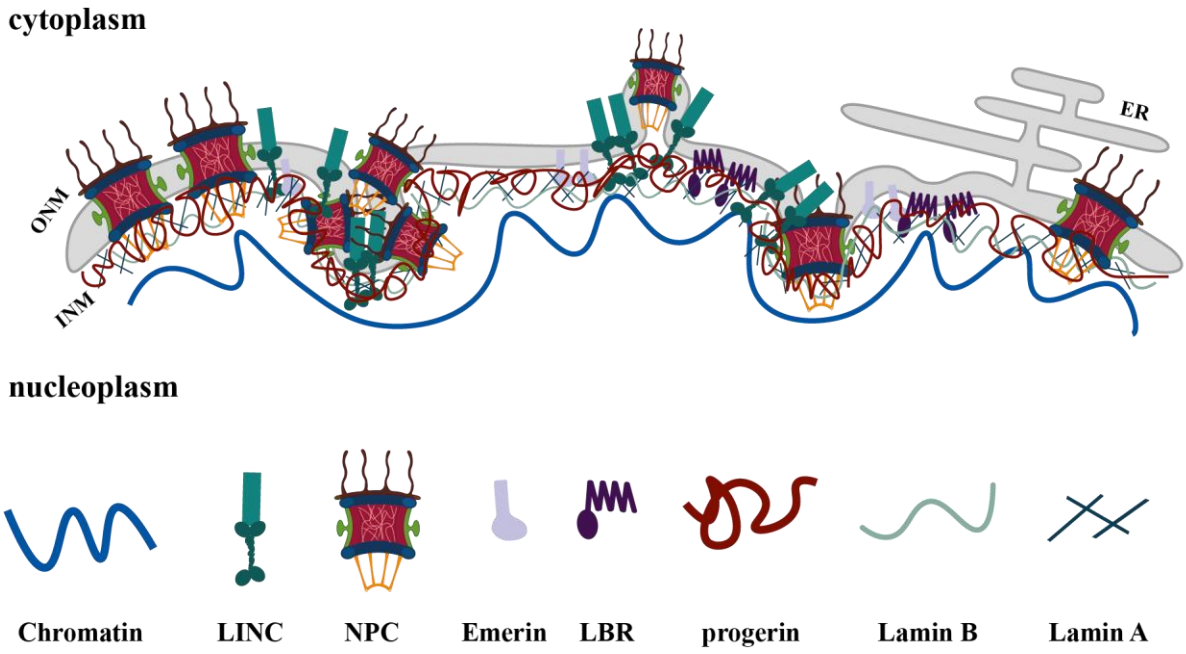

Figure 1.3 Schematic representation of the nuclear envelope in HGPS

The lipid bilayer of the NE and ER is shown in grey. Unlike in a healthy cell, the NE is deformed in HGPS cells. The LINC complex connects the lamina to the cytoskeleton, the NPC allows transport across the NE, emerin associates with the lamina, LBR anchors LB and heterochromatin to the NE (Olins, Rhodes et al. 2010) and Lamin B/A create the nuclear lamina. Progerin's presence stiffens the NE, leading to folds, blebs and invaginations of the NE. Numerous proteins cluster or are trapped in these folds, e.g., SUN1 and the NPC. Not all components of the NE are depicted, nor all proteins affected by progerin.

In 2013 López-Otín postulated nine hallmarks of aging: "[…] genomic instability, telomere attrition, epigenetic alterations, loss of proteostasis, deregulated nutrient sensing, mitochondrial

dysfunction, cellular senescence, stem cell exhaustion, and altered intercellular communication" (López-Otín, Blasco et al. 2013). HGPS represents most of these hallmarks, allowing researchers to use it as a model of accelerated aging.

However, there are a few key differences between natural aging and HGPS. HGPS can be called a segmental aging disease, since not all features of natural aging are present in this disease. Some notable exceptions are a healthy liver, lung, kidney and gastrointestinal tract (Ullrich and Gordon 2015, Gonzalo, Kreienkamp et al. 2017). In addition, HGPS patients do not suffer from neural degeneration and do not have an elevated cancer risk compared to their healthy peers, despite their increased DNA damage levels (Ashapkin, Kutueva et al. 2019). Not only does progerin not lead to an elevated incidence of cancer, overexpression of progerin in lung cancer cells inhibits proliferation, invasion, and migration of lung cancer cells (Hu, Song et al. 2020). It has also been shown that by altering distribution of the transcriptional regulator BRD4, progerin mediates cellular resistance to oncogenic challenges (Fernandez, Scaffidi et al. 2014). An explanation why progerin does not affect brain function in HGPS patients is the post-translational down-regulation of *LMNA* by miRNA 9, but further research is required to elucidate why progerin expression only affects some cell types and tissues (Jung, Coffinier et al. 2012).

In this thesis, the focus lies on the changes of the nuclear envelope following progerin expression. These nuclear abnormalities caused by progerin go hand in hand with increased nuclear stiffness and HGPS cells do not respond to mechanical strain in the same fashion as healthy cells (Dahl, Scaffidi et al. 2006, Verstraeten, Ji et al. 2008). The nuclear lamina in HGPS cells has a reduced ability to rearrange following mechanical stress and cannot return to its previous state after stretching. This does not translate into increased mechanical sensitivity of the nucleus, since HGPS nuclei are somewhat more resistant to pressure than healthy nuclei (Dahl, Scaffidi et al. 2006). However, upon application of mechanical strain HGPS fibroblasts display a higher number of apoptotic cells and do not activate cell cycle progression compared to control cells (Verstraeten, Ji et al. 2008). This increased sensitivity could potentially affect regeneration or repair of for example tissues that are regularly exposed to mechanical strain such as blood vessels, contributing to arteriosclerosis in HGPS.

Changes in nuclear morphology caused by progerin are dependent on farnesylation, since treatment with FTI (Lonafarnib) and mutation of the CaaX motif preventing farnesylation can restore nuclear shape (Capell, Erdos et al. 2005, Mallampalli, Huyer et al. 2005, Lu and Djabali 2018). Yet, FTI treatment does not improve resistance to mechanical strain-induced cell death (Verstraeten, Ji et al. 2008). This could have a direct effect on HGPS pathophysiology, as impacted nuclear mechanics due to progerin could be conducive to the development of arteriosclerosis due to loss of vascular smooth muscle cells (Stehbens, Wakefield et al. 1999, Stehbens, Delahunt et al. 2001). Since at the moment only Lonafarnib has been approved by the FDA as treatment of HGPS, additional measures have to be identified to completely ameliorate the sensitivity to mechanical strain (Dhillon 2021).

However not only the shape of the nucleus is altered, but also various nuclear and nuclear envelope proteins are mislocalized or clustered, such as emerin, nesprin-2, SUN1, Ran and the NPC (Goldman, Shumaker et al. 2004, Kelley, Datta et al. 2011, Chen, Wang et al. 2014, Sola-Carvajal, Revêchon et al. 2019).

One consequence of this clustering or mislocalization is that in HGPS cells the concentration of nuclear Ran is reduced, changing the ratio from 3:1 to 1:1 (nuclear/cytoplasmic Ran) (Kelley, Datta et al. 2011). Progerin reduces RCC1 (Ran guanine exchange factor) mobility, likely affecting RanGDP to RanGTP transformation in the nucleoplasm and thereby disrupting the Ran gradient. This mainly affects import of large proteins, such as the nucleoporin Tpr (535 kDa), that are imported to a lesser degree in HGPS (Kelley, Datta et al. 2011, Snow, Dar et al. 2013). However, not just the disruption of the Ran gradient could influence nuclear import/export, clustering of NPCs in HGPS cells might also play a role, raising the question how progerin causes NPC clustering.

1.3 The Nuclear Pore Complex

1.3.1 Structure and function of the Nuclear Pore Complex

The human NPC is a ~112 MDa large protein complex (Reichelt, Holzenburg et al. 1990) spanning the nuclear envelope to ensure transport between the nucleus and cytoplasm, while preserving the integrity of nuclear compartmentalization (LIN AND HOELZ 2019) (Figure 1.4). Human NPCs are made up of 32 subunits, so-called nucleoporins (NUP) and it has an eightfold rotational symmetry (Gall 1967, Hoelz, Glavy et al. 2016) occupying a ~ 800 Å 'hole' created by the fusion of outer and inner nuclear membrane (Watson 1959). The NPC has 6 major subcomplexes: eight cytoplasmic filaments, the inner/outer rings (Nup107-160 complex),

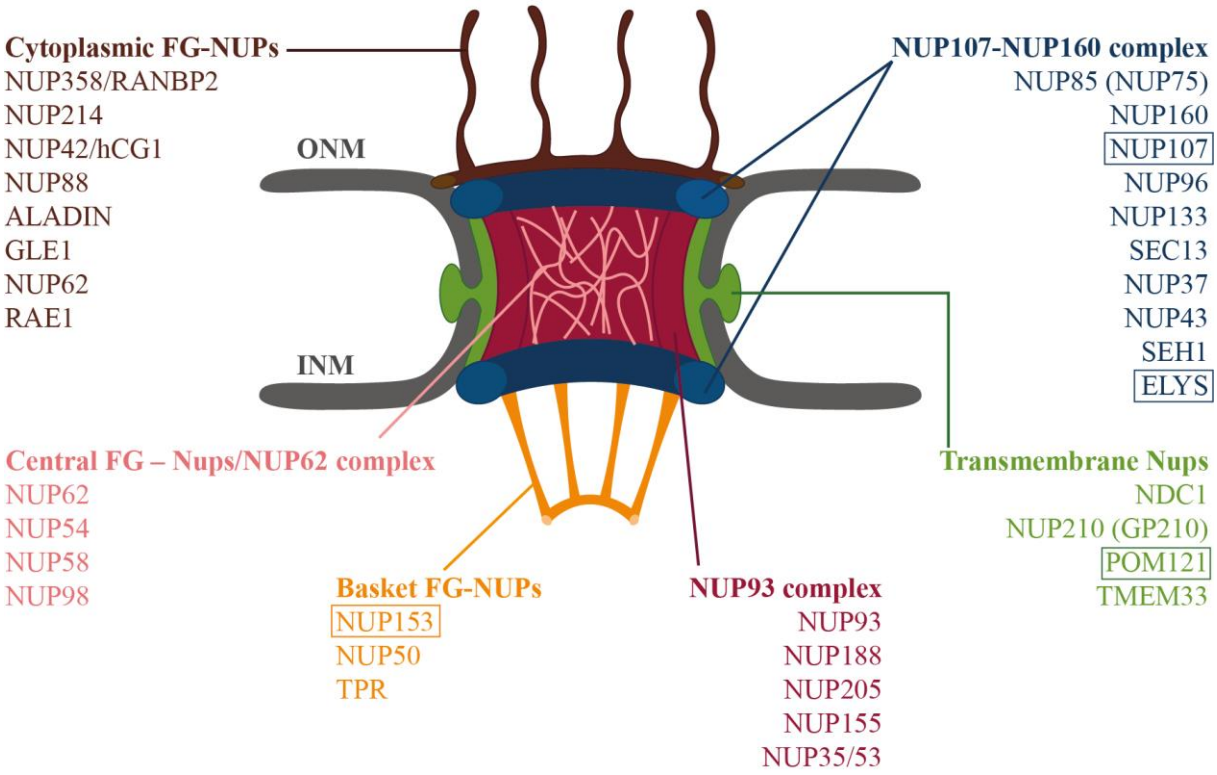

Figure 1.4 Schematic representation of the Nuclear Pore Complex structure

The cyto- and nucleoplasmic rings (NUP107-160 complex, blue) and the central channel (NUP93, red) are the scaffolding subunits of the NPC. The transmembrane nucleoporins (green), anchor the pore withing the NE. The cytoplasmic filaments (brown) are attached to the cytoplasmic ring, the nuclear basket (orange) is connected to the nucleoplasmic ring. The central FG-NUPs line the channel creating a permeability barrier. Boxes indicate NUPs analyzed in this thesis.

the central channel (Nup93 complex) lined with Phenylalanine-Glycine-repeat NUPs (FG-repeat NUPs) (Nup62 complex), the transmembrane NUPs and the nuclear basket (Beck and Hurt 2017) (Figure 1.4).

The architecture of the pore is created by the scaffolding subunits, that make up the central channel (NUP93) within the NE, which is enclosed by the inner and outer ring complex (NUP107-160). Attached to the cytoplasmic ring are the cytoplasmic filaments and to the nucleoplasmic ring the so-called nuclear basket. The transmembrane NUPs anchor the NPC in the NE (Mitchell, Mansfeld et al. 2010) and the FG-repeat nucleoporins line the central channel creating a permeability barrier to ensure proper transport across the NE.

For a long time, it was assumed that the stoichiometry of the NPC was the same in all cells, however more recent results have revealed that stoichiometry of the NPC is tissue dependent and NUPs such as GP210, NUP133 and NUP358 are involved in myogenesis and neuronal differentiation (Raices and D'Angelo 2012). What is more, mutations in some NUPs cause tissue-specific diseases, e.g., a mutation in mouse *NUP155* causes atrial fibrillation leading to cardiac death, patients with a mutation in *ALADIN* suffer from adrenal insufficiency and various neurological symptoms (Triple A syndrome), and *Nup96* heterozygous mice have a defective adaptive and innate immune response (Huebner, Kaindl et al. 2004, Faria, Levay et al. 2006, Zhang, Chen et al. 2008). The NPC has also been implicated in various other diseases e.g., amyotrophic lateral sclerosis, Parkinson's, Huntington's and Alzheimer's disease and it is involved in cancer development (Sakuma and D'Angelo 2017).

Some of these diseases are caused by problem in nucleocytoplasmic transport, which involves two different mechanisms: passive diffusion and active transport.

Passive diffusion through the NPC channel is possible for molecules up to 5 nm diameter or ~40 kDa in size, mediated by the FG-repeat nucleoporins that create a barrier to prevent uncontrolled import/export of macromolecules (Timney, Raveh et al. 2016). FG-repeat NUPs are rich in phenylalanine (F) and glycine residues (G) and are intrinsically disordered, creating a 'hydrogel' responsible for the NPCs transport specificity (Ribbeck and Görlich 2001, Denning, Patel et al. 2003, Frey and Görlich 2007, Timney, Raveh et al. 2016).

Larger macromolecules require active transport by nuclear transport receptors (NTRs) (Knockenhauer and Schwartz 2016, Schmidt and Gorlich 2016, Timney, Raveh et al. 2016).

Active transport is mediated by the Ran-gradient (Melchior, Paschal et al. 1993, Moore and Blobel 1993, Izaurralde, Kutay et al. 1997), the requisite transport receptors (importins/exportins) (Görlich, Prehn et al. 1994, Imamoto, Shimamoto et al. 1995, Bernad, van der Velde et al. 2004, Port, Monecke et al. 2015) and the transient interactions of the transport receptors with the hydrogel created by FG-repeat NUPs (Bayliss, Ribbeck et al. 1999, Frey, Richter et al. 2006, Frey and Görlich 2007, Frey and Görlich 2009, Schmidt and Gorlich 2016).

The Ran gradient is dependent on Ran, a small GTPase that exists in two conformations: RanGTP or RanGDP (Melchior, Paschal et al. 1993). The change from one conformation to the other is mediated by the Ran GTPase-activating protein (RanGAP) and the Ran guanine exchange factor RCC1 (Bischoff and Ponstingl 1991, Izaurralde, Kutay et al. 1997). Both are restricted in their localization, RanGAP to the cytoplasm and RCC1 to the nucleus. RanGTP is transformed to RanGDP in the cytoplasm by RanGAP and is returned to the nucleoplasm via its dedicated transport receptor Ntf2, where it released from Ntf2 by the exchange of GDP to GTP, mediated by RCC1. This mechanism creates a Ran-gradient with a much higher Ran concentration in the nucleus than in the cytoplasm (Kalab, Weis et al. 2002).

Cargo import into the nucleus requires a nuclear localization sequence, which is recognized by β-karyopherin's either directly or indirectly (Christie, Chang et al. 2016). Once cargo and transport receptor (importin) have entered the nucleus via the NPC, the cargo is released by binding of RanGTP to importin (Görlich, Panté et al. 1996, Izaurralde, Kutay et al. 1997, Christie, Chang et al. 2016). The cargo-free importin-RanGTP complex returns to the cytoplasm, where RanGTP is hydrolyzed to RanGDP with the help of RanGAP, importin is released and can now bind new cargo (Floer, Blobel et al. 1997, Lounsbury and Macara 1997).

Export requires a nuclear export sequence within the cargo, which is bound by a karyopherin-RanGTP export complex. Once the export complex emerges into the cytoplasm, RanGTP returns to its' GDP-bound state with the help of RanGAP and RanBP1/2 and the cargo is released from exportin (Kutay, Bischoff et al. 1997, Stade, Ford et al. 1997, Matsuura 2016).

RanGDP is then transported to the nucleus via Ntf2, ensuring that the cycle of import/export is maintained.

Besides its primary purpose controlling nuclear transport, the NPC also fulfills multiple other roles.

For example the NPC is involved in chromatin modulation and gene expression (Raices and D'Angelo 2017). NPCs are surrounded by decondensed chromatin, which is regulated by TPR (Krull, Dörries et al. 2010) and therefore NPCs could modulate gene expression in these regions, by preventing formation of heterochromatin in these areas.

In mitotic cells, nucleoporins play a role in regulating kinetochore-microtubule attachment, the spindle assembly checkpoint and mitotic progress (Salina, Enarson et al. 2003, Joseph, Liu et al. 2004, Orjalo, Arnaoutov et al. 2006, Zuccolo, Alves et al. 2007, Mackay, Elgort et al. 2009, Lussi, Shumaker et al. 2010, Cross and Powers 2011).

In addition, the NPC interacts with the nuclear lamina, the LBR and the LINC complex (Smythe, Jenkins et al. 2000, Lu, Gotzmann et al. 2008, Al-Haboubi, Shumaker et al. 2011, Funakoshi, Clever et al. 2011). Interaction with e.g., the LINC complex is crucial for *de novo* interphase assembly of the NPC, which will be detailed in the following section and the discussion.

1.3.2 Assembly of the NPC

To be able to fulfill its' myriad functions, the NPC must be assembled first. It has two modes of assembly, post-mitotic reassembly following open mitosis and *de novo* NPC insertion into the NE during interphase (Otsuka and Ellenberg 2018).

Post-mitotic re-assembly is a highly ordered sequence of events, resulting in fully functional pores by early G1. The current theory of reassembly is that pre-pores form on chromatin and are enclosed by the reforming NE membrane (Otsuka and Ellenberg 2018). At the onset of mitosis the NPC is disassembled into its subunits (Figure 1.4) from pro- to metaphase, and most of them remain stably assembled until reformation (Belgareh, Rabut et al. 2001, Loiodice, Alves et al. 2004, Dultz and Ellenberg 2010). The subcomplexes are either diffused in the cytoplasm or, in the case of the transmembrane NUPs, localize to the ER membrane. Disassembly

begins in prophase and is mediated by phosphorylation of several NUPs (Dultz, Zanin et al. 2008, Laurell, Beck et al. 2011). Phosphorylation is reverted by phosphatases, which allows NPC reassembly to proceed (Schellhaus, De Magistris et al. 2016).

Starting in early anaphase, ELYS initiates post-mitotic assembly, by binding to the separating chromosomes with its' AT-hook DNA binding domain (Kimura, Takizawa et al. 2002, Rasala, Orjalo et al. 2006, Franz, Walczak et al. 2007). It recruits the remainder of the Nup107-160 complex forming a pre-pore complex on chromatin, followed by partial binding of Nup153/Nup50 (Bodoor, Shaikh et al. 1999, Hase and Cordes 2003, Dultz, Zanin et al. 2008, Rasala, Ramos et al. 2008). In a next step, two transmembrane NUPs, NDC1 and POM121 (Antonin, Franz et al. 2005, Mansfeld, Guttinger et al. 2006, Rasala, Ramos et al. 2008) are recruited by ELYS, as well as Nup53 by NDC1 in early telophase (Vollmer, Schooley et al. 2012, Eisenhardt, Redolfi et al. 2014). Central channel Nup155 is incorporated via its interaction with Nup53 (Eisenhardt, Redolfi et al. 2014), it in turn recruits the other central channel NUPs (Nup205/188/93). In telophase Nup93 adds the Nup62 complex, at which point partial transport across the NE is established (Dultz, Zanin et al. 2008, Sachdev, Sieverding et al. 2012). The remainder of the nuclear basket NUPs (Nup153/50, TPR) and cytoplasmic filaments are assembled in early G1 (Dultz, Zanin et al. 2008), which concludes post-mitotic NPC reassembly.

Interestingly this process is not only controlled via phosphorylation/dephosphorylation of NUPs but is also mediated by two factors normally involved in nucleocytoplasmic transport: importins β1/β2 and a Ran gradient (Hetzer, Bilbao-Cortés et al. 2000, Walther, Askjaer et al. 2003, Forbes, Travesa et al. 2015). Usually, importins transport cargo from the cytoplasm to the nucleus, in mitotic cells they bind to several proteins and prevent them from interacting with others (Forbes, Travesa et al. 2015). A few examples are: LB1, LBR, spindle assembly factors, the NUPs 62, 98, 153 214, 358, the NUP107-160 complex and ELYS (Forbes, Travesa et al. 2015). These proteins are only released by binding of RanGTP to the transport receptors (Görlich, Panté et al. 1996). RanGTP is only present adjacent to chromatin, since its' guanine-exchange factor RCC1 is bound to chromatin during mitosis (Hetzer, Bilbao-Cortés et al. 2000). Consequently, NPC reformation is restricted to the area surrounding the dividing chromosomes

beginning with ELYS in anaphase, positively regulated by RanGTP and negatively regulated by importins (Hetzer, Bilbao-Cortés et al. 2000, Rasala, Ramos et al. 2008, Rotem, Gruber et al. 2009).

During interphase NPC numbers increase approximately 2-fold in preparation for cell division (Maul, Maul et al. 1972) and new NPCs need to be inserted into the intact NE. This process is governed by Cdk1/2 activity and the basket nucleoporin TPR, which regulate localization, number and expression of certain NUPs involved in *de novo* NPC assembly (Maeshima, Iino et al. 2010, McCloskey, Ibarra et al. 2018).

De novo NPC requires the following elements for insertion: the basket nucleoporin NUP153 which recruits NUP107-160 (Vollmer, Lorenz et al. 2015), POM121 and SUN1 interaction (Funakoshi, Clever et al. 2011, Talamas and Hetzer 2011), the DP1/Yop1p reticulon family protein (Dawson, Lazarus et al. 2009), NUP53's membrane-deforming ability (Vollmer, Schooley et al. 2012) and NUP133 membrane-curvature sensing capability (Doucet, Talamas et al. 2010). Insertion proceeds via an inside-out extrusion, which requires deformation and then fusion of the double membrane (Otsuka, Bui et al. 2016, Otsuka and Ellenberg 2018). The first structure to be detected at the insertion site is an eight-fold symmetric ring, which is likely the nucleoplasmic ring (NUP107-160 complex), since NUP107-160 is recruited to the INM by NUP153 (Vollmer, Lorenz et al. 2015.). Recruitment of NUP107-160 to the INM is also facilitated by the membrane-curvature sensing ability of one of its' components, NUP133 (Doucet, Talamas et al. 2010). The resulting pre-pore structure is then further pushed into the double membrane until the INM and ONM fuse and a mature pore is formed. The exact mechanism of how this fusion is achieved still remains to be identified (Otsuka, Bui et al. 2016). However, the interaction of POM121 and SUN1 is thought to be essential for reducing the distance of the INM and ONM, which would facilitate the fusion event (Funakoshi, Clever et al. 2011, Talamas and Hetzer 2011).

Once NPCs are inserted into the NE, they are fairly immobile, which is dependent on NUP153s interaction with the nuclear lamina (Walther, Fornerod et al. 2001). NUP153 interacts with Lamin A and B1 and in Xenopus egg extract it needs the lamina to incorporate into the NPC (Smythe, Jenkins et al. 2000, Al-Haboubi, Shumaker et al. 2011). At the same time down-

regulation of TPR affects lamina organization, as does NUP153 knockdown (Fiserova, Maninova et al. 2019, Kittisopikul, Shimi et al. 2021). In addition to being involved with the lamina, the NPC also associates with a member of the LINC complex, SUN1 and the LBR (Funakoshi, Maeshima et al. 2007, Liu, Pante et al. 2007).

1.4 Replicative senescence

In this study NPCs were not just analyzed during cellular division, I also looked into the relationship of NPC distribution and replicative senescence, since HGPS cells senesce prematurely, and senescent cells exhibit nuclear changes as well. Replicative senescence was discovered by Hayflick *et al.* (Hayflick and Moorhead 1961, Hayflick 1965), when they observed that cells cultured *in vitro* have a limited lifespan. Senescent cells no longer proliferate and have an altered metabolism and their state is attributed to various factors such as shortened telomers, DNA damage, genotoxic drugs, irradiation, oxidative stress, nutrient deprivation, mitochondrial dysfunction, hypoxia, oncogenic stress etc. (Childs, Durik et al. 2015, Gorgoulis, Adams et al. 2019). Senescent cells also become resistant to apoptosis and can persist, if not removed by e.g. natural killer cells (Ryu, Oh et al. 2007, Krizhanovsky, Yon et al. 2008).

What is more, cellular senescence is not just an artefact of *in vitro* cell culture, it has both beneficial and deleterious effects on organisms (Di Micco, Krizhanovsky et al. 2021). Senescence plays a role in embryonic development, tumor suppression, wound healing, tissue repair, insulin secretion and age-associated degeneration (Baker, Wijshake et al. 2011, de Magalhães and Passos 2018) (Di Micco, Krizhanovsky et al. 2021).

In mammalian cells, the irreversible cell cycle arrest of senescent cells is driven by the p53-p21 and $p16^{INK4A}$-RB tumor suppressor pathways (Childs, Durik et al. 2015), which both lead to the activation of pRb (retinoblastoma protein) family members resulting in cell cycle arrest. p21 and $p16^{INK4A}$ (p16) are both cyclin dependent kinase (CDK) inhibitors, however p21 is thought to initiate senescence, whereas p16 maintains the terminal stage of senescence (Alcorta, Xiong et al. 1996, Stein, Drullinger et al. 1999). Both p21 and p16 upregulation first induces pRB hypo-phosphorylation, which then associates with the transcriptions factor E2F, preventing E2F activation and consequent G1 to S-phase transition is inhibited (Chellappan, Hiebert et al. 1991, Dyson 1998), leading to the irreversible senescent cell cycle arrest.

Senescent cells exhibit various morphological changes, e.g. an irregular and enlarged cellular shape, increased lysosomal content, accumulation of mitochondria and nuclear changes (Hernandez-Segura, Nehme et al. 2018). Nuclear changes include an increase in size, downregulation of LB1, inhibition of signal molecule nuclear translocation and old NPCs become more

permeable to passive diffusion (Mitsui and Schneider 1976, D'Angelo, Raices et al. 2009, Kim, Ryu et al. 2010, Freund, Laberge et al. 2012, Hänzelmann, Beier et al. 2015).

Another characteristic of senescent cells is the senescence-associated secretory phenotype (SASP) (Di Micco, Krizhanovsky et al. 2021). Senescent cells secrete various molecules f. ex. cytokines, chemokines, growth factors and extracellular matrix proteases, which can affect the surrounding environment. The SASP can reinforce or spread senescence and can attract the immune response to eliminate senescent cells (Krizhanovsky, Yon et al. 2008, Acosta, Banito et al. 2013, Sagiv and Krizhanovsky 2013, Gorgoulis, Adams et al. 2019).

Cellular senescence also plays a role in disease progression of HGPS. HGPS cells enter replicative senescence prematurely due to progerin's deleterious effect on cellular health, f. ex. DNA damage, replication stress, JAK/STAT overactivation and accelerated telomere shortening (Liu, Wang et al. 2005, Huang, Risques et al. 2008, Benson, Lee et al. 2010, Wheaton, Campuzano et al. 2017, Liu, Arnold et al. 2019). Forced progerin expression can induce premature senescence in VSMCs, possibly contributing to arterial VSMC loss in HGPS patients and premature senescence interferes with adipocyte differentiation in HGPS as well(Kinoshita, Nagasawa et al. 2017, Najdi, Krüger et al. 2021). Premature senescence of HGPS can be rescued f. ex. by telomerase expression or inhibition of the JAK/STAT pathway (Kudlow, Stanfel et al. 2008, Benson, Lee et al. 2010, Liu, Arnold et al. 2019), potentially offering a novel therapeutic strategy besides detaching progerin from the NE with FTI.

One problem researchers' face when analyzing cellular senescence is that so far, no universal marker for cellular senescence has been identified. Common markers that are used at the moment are increased lysosomal content, elevated p16 or p21 content, reduced LB1, γ-H2AX nuclear foci, phosphorylated p53, BCL-2 expression etc. (Hernandez-Segura, Nehme et al. 2018). However, none of these are just involved in senescence, they also have roles during the cell cycle, depend on the cell type, the factor initiating cellular senescence and more. Consequently, a careful analysis needs to be performed before choosing the appropriate markers, before starting any experiments.

AIM AND SCOPE OF THIS THESIS

The aim of thesis was to shed light on the cause for abnormal NPC distribution in the nuclear envelope of HGPS fibroblasts and potentially enable development of new treatment strategies for this debilitating disease. Previous work in the laboratory of Professor Djabali demonstrated how progerin interferes with mitotic progression of HGPS cells. In addition, progerin caused the mislocalization of various proteins throughout mitosis e.g., Lamin B1, Lamin A, SUN1, emerin, CENP-F and Aurora B. A slight delay in recruitment of different nucleoporins labelled by mAb414 was also detected, which raised the question, if clustering of NPCs in HGPS cells was caused by a defect in post-mitotic NPC reassembly. To answer this question, the distribution of progerin and various nucleoporins in mitotic cells was analyzed in combination with Lamin A and SUN1. SUN1 is a known interaction partner of progerin and the NPC and progerin's negative influence on SUN1 might also impact the NPC. What is more, nucleoporins from different parts of the NPC were analyzed in mitotic HGPS and control fibroblasts, to be able to observe the sequential step of post-mitotic NPC reassembly.

Not only did I analyze post-mitotic NPC reassembly, I also looked into the distribution of NPCs in cells undergoing replicative senescence and how senescence affected the morphology of the nuclear envelope.

The discovery of the mechanism for NPC in HGPS could potentially help ameliorate some of the cellular symptoms of HGPS, for example the disturbed Ran gradient and premature senescence.

2. Materials and Methods

2.1 Materials

2.1.1 Chemicals

Chemicals, Kits and antibodies were purchased from the following companies:
Abcam (Cambridge, UK), Bethyl (Montgomery, USA), Biolegend (San Diego, USA), Bio-Rad Laboratories (Munich, Germany), Biozol (Eching, Germany), GE Healthcare (Munich, Germany), Jackson Immuno Research (Westgrove, USA), Luminex (Austin, USA), Merck Biosciences (Darmstadt, Germany), Merck Millipore (Burlington, USA), Proteintech (Manchester, UK), Roche (Mannheim, Germany, Roth (Karlsruhe, Germany), Santa Cruz Biotechnology, Inc. (Dallas, USA), Sigma-Aldrich (Taufkirchen, Germany), Thermo Fisher Scientific Inc. (Waltham, USA), VWR (Radnor, USA).

2.1.2 Instruments

Instrument	**Producer**
CO2 incubator CB	Binder GmbH, Tuttlingen, Germany
ChemiDocTM MP	Bio-Rad Laboratories, München, Germany
Mini Trans-Blot® Cell	Bio-Rad Laboratories
Trans-Blot Turbo Transfer System	Bio-Rad Laboratories
Mini-PROTEAN II electrophoresis system	Bio-Rad Laboratories,
Rocking Shaker	Biozym, Hessisch Oldendorf, Germany
FLUOstar® Omega	BMG LABTECH, Ortenberg, Germany
Axio Imager D2 fluorescence microscope	Carl Zeiss, Oberkochen, Germany
Eppendorf Research® plus pipettes	Eppendorf, Hamburg, Germany
Eppendorf thermomixer comfort	Eppendorf
Eppendorf centrifuge Minispin, 5810	Eppendorf
IKA Mixer Vortex Shaker Model MS 2	IKA, Staufen, Germany
NanoDrop ND-1000 spectrophotometer	PEQLAB, Erlangen, Germany

2.1.3 Kits, cell lines and antibodies

Kits: Senescence Detection Kit I (PromoCell, PK-CA577-K320)

Table 2.1 Cell lines used in this study

Name	Condition	Donor	Biopsy	Mutation	Source
GM01652c	Normal	11 Y Female	Skin	none	Coriell Institute
GM01651c	Normal	13 Y Female	Skin	none	Coriell Institute
HGADFN003	HGPS	3 Y Female	Skin	LMNA Exon 11, heterozygous c.1824C>T (p.Gly608Gly)	Progeria Research Foundation
HGADFN127	HGPS	2 Y Male	Skin	LMNA Exon 11, heterozygous c.1824C>T (p.Gly608Gly)	Progeria Research Foundation

Table 2.2 Primary antibodies used in this study

Name	origin	Cat#	Supplier	weight [kDa]	dilution IF	Fixation	Incuba-tion IF	2nd AB IF	dilution WB	Incuba-tion WB	2nd AB WB
ELYS	RAB	A300-166A	Bethyl	256	1:500	MeOH	4°C ON or 2h RT	1:1000	1:2000	4°C ON	1:3000
LA	MAB	133A2	Abcam	78	1:500	4% PFA or MeOH	4°C ON	1:1000			
Lamin A/C	MAB	(E-1): sc-376248	Santa Cruz	78 63				1:1000	1:1000	1 h RT or 4°C ON	1:5000
Lamin A/C	RAB	H-110, SC-20681	Santa Cruz	78 63				1:1000	1:10000	1 h RT or 4°C ON	1:3000
Lamin B	Goat	M-20, sc-6217	Santa Cruz	66	1:50	MeOH	4°C ON	1:800			
Lamin B1	MAB	66095-1-Ig, clone 3C10G12	Pro-teintech	66				1:1000	1:500	4°C ON	1:5000
NPC 414	MAB	MMS-120P	Biolegend	358, 214, 153, 98, 62	1:2000	4% PFA or MeOH	4°C ON or 2h RT	1:1000	1:1000	4°C ON	1:5000
NUP107	MAB	MA1-10031	Thermo Fisher	107	1:500 1:300	4% PFA or MeOH	4°C ON or 2h RT	1:800	no good		
NUP153	RAB	A301-788A	Bethyl	153	1:500 1:400	4% PFA or MeOH	4°C ON or 2h RT	1:1000	1:1000	4°C ON	1:5000
p16-INK4A	MAB	P 0968	Santa Cruz	16	1:250	MeOH	4°C ON	1:800			
p21	MAB	(F-5), sc-6246	Santa Cruz	21	1:250	MeOH	4°C ON	1:800			
POM121	RAB	SAB2700248	Sigma-Al-drich	121	1:800 1:600	4% PFA or MeOH	4°C ON or 2h RT	1:800	1:1000	1 h RT or 4°C ON	1:3000

progerin-S5	RAB		Home-made	70	none	2% PFA or MeOH	ON at RT	1:800	none	4°C ON	1:3000
progerin-S9	RAB		Home-made	70	none	2% PFA or MeOH	ON at RT	1:800	none		1:3000
SUN1	RAB	HPA008346	Sigma-Aldrich	90	1:400	4% PFA or MeOH	4°C ON or 2h RT	1:1000	1:500	1 h RT or 4°C ON	1:3000

Table 2.3 Secondary antibodies used in this study

Type	**origin**	**Cat#**	**Supplier**	**dilution**
Alexa® 488	Donkey αMAB	A21202	Thermo Fisher	1:800 or 1:1000
Alexa® 488	Donkey αRAB	A21206	Thermo Fisher	1:800 or 1:1000
Alexa® 488	Donkey αGAB	A11055	Thermo Fisher	1:800 or 1:1000
Alexa® 555	Donkey αRAB	A31572	Thermo Fisher	1:800 or 1:1000
Alexa® 555	Donkey αMAB	A31570	Thermo Fisher	1:800 or 1:1000

2.2 Methods

2.2.1 Cell culture

HGPS fibroblast cell lines carrying the *LMNA* mutation G608G, HGADFN127 and HGADFN003, were supplied by The Progeria Research Foundation Cell and Tissue Bank (https://www.progeriaresearch.org/). Control fibroblasts GMO1651 and GMO1652 were supplied by the Coriell Institute for Medical Research (Camden, NJ, USA). All cells were cultured at 37°C, 5% CO_2 in DMEM high glucose, GlutaMAX (TM), pyruvate supplemented with 15% fetal bovine serum (FBS), 1% penicillin, 1% glutamine and 0.5% gentamicin (growth medium). Media, Trypsin, supplements and PBS (Phosphate buffered saline) were all supplied by Thermo Fisher Scientific Inc. (Waltham, USA).

To split cells, they were first washed with PSB and then incubated for ~3 min at 37°C in Trypsin. The detached cells were resuspended in 2-7 ml media, depending on size of the dish. They were then counted using a Muse™ Cell analyzer (Merck Millipore; Burlington, USA). The cell suspension was diluted 1:1 in Muse™ Count & Viability Reagent and incubated for 5 minutes (min) at room temperature (RT) before counting. Following counting, cells were seeded at density appropriate for maintenance or immunofluorescent/western blot experiments. For storage, cell pellets were resuspended and stored in FBS supplemented with 10% DMSO at -80°C.

To maximize the number of mitotic cells per glass coverslip, cells (passage 15-19) were seeded at a density of 3000 cells/cm^2 and fixed after 48 h. To further increase the number of mitotic cells, cells were synchronized by serum starvation. 4000 cells/cm^2 were seeded on glass coverslips and cultured in growth medium for 24 h, followed by 72 h incubation in starvation medium, containing only 0.1% instead of 15% FBS. After 72 h, growth medium was reintroduced, and cells were fixed 28 to 31 h following release from starvation.

For statistical analysis of young and old cells, 2000 cells/cm^2 were seeded in growth medium on coverslips and fixed on day 4. Before seeding, cells were evaluated by a senescence associated β-Galactosidase assay (see 2.2.2).

2.2.2 Senescence associated β-Galactosidase assay

To evaluate replicative senescence of cell cultures, the Senescence Detection Kit I (PromoCell, PK-CA577-K320) was used according to the manufacturer's instructions:

1. 20 mg X-Gal was diluted in 1 ml DMSO resulting in a 20 mg/ml stock solution (20x).
2. The staining solution was prepared as follows, before each new experiment:
    - 47% v/v Staining Solution (1x)
    - 0.01% v/v Staining Supplement (100x)
    - 0.05% v/v 20 mg/ml X-Gal in DMSO → final concentration of1 µg/µl X-Gal

Cell culture medium was aspirated, cells washed 1x with PBS and then fixed in 1 ml fixation solution for 10 min at RT. After fixation, cells were washed 2x with PBS, the staining solution was added, and the samples were incubated ON at 37°C. Following staining, cells were washed 1x with PBS and at least 300 cells per experiment were counted manually, distinguishing normal ("young") and blue cells ("old").

To analyze progerin levels concomitant with senescence associated β-Galactosidase increase, HGPS cells were stained using the Senescence Detection Kit I. Cells were then permeabilized with ice-cold Methanol (MeOH) at -20°C for 10 min. Following permeabilization, cells were blocked and treated as in 2.2.3.

2.2.3 Immunocytochemistry

Cells were grown on glass coverslips and fixed with either 2/4% paraformaldehyde (PFA) solution in PBS for 15 min at RT or in ice-cold MeOH for 10 min at -20°C. Following fixation, coverslips were washed 3x with PBS. 2/4% PFA-fixed cells were permeabilized with 0.2% Triton-X-100 in PBS 10 min at RT and washed 3x with phosphate-buffered-saline (PBS). Coverslips were then stored in PBS at 4°C until used. The primary and secondary antibodies used in this study are listed in Table 2.2 and Table 2.3. Samples were blocked with 10% FBS in PBS for 1 h at RT in a humidity chamber, before adding primary antibodies diluted in blocking buffer (see Table 2.2). Incubation times are listed in Table 2.2 and were followed by washing 3x with PBS, before adding secondary antibody diluted in blocking buffer (see Table 2.3) for 1 h at RT. Then samples were washed 4x with PBS, before counterstaining and mounting with

VECTASHIELD® Antifade Mounting Medium with DAPI (Vector Inc., VEC-H-1200). Images were acquired with an Axio Imager D2 fluorescence microscope (AxioCam MRm, Objective X63 oil NA 1.4 or X40 oil NA 1.3, Carl Zeiss, Oberkochen, Germany) or a Leica SP8 Lightning confocal microscope (objective X63 oil NA 1.4, Leica, Wetzlar, Germany).

2.2.4 Image analysis

Images were analyzed, cropped and brightness/contrast adjusted with Fiji ImageJ (Schindelin, Arganda-Carreras et al. 2012), followed by import into Adobe Photoshop CC 2017 or Adobe Illustrator (Adobe Inc., San José, USA) for presentation. Once imported into Adobe Photoshop CC or Adobe Illustrator, images were not altered further.

2.2.5 Statistical evaluation of NPC clustering and progerin levels via immunocytochemistry

NPC clustering and progerin levels were analyzed in all four cell lines listed in Table 2.1. At least three replicates were performed for each experiment, with 300 nuclei counted per technical replicate, adding up to ~900 nuclei per condition (see Table 5.3). Prior to statistical evaluation of cells by immunocytochemistry, primary fibroblast cultures were analyzed by senescence associated β-Galactosidase assay and only "young" cells (≤ 5% β-Galactosidase positive cells) or "old" cells (≥ 30% β-Galactosidase positive cells) were evaluated. Cells were analyzed visually and evaluated by inspecting signal intensity and morphology in the field of view of a X40 oil objective (see 2.2.3). Antibodies used to assess progerin levels, cellular senescence and NPC distribution were progerin S5, p16, p21, LB1 and POM121 (for details see Table 2.2). The same homemade progerin S5 lot was used for all statistical experiments, to ensure uniform results.

The results from visual analysis were transferred to MS Excel (Microsoft, Redmond, USA) for overview and calculation of the percentages. To calculate the mean and the standard deviation, the percentages were transferred to GraphPad Prism 6.01 (GraphPad, San Diego, CA, USA). All graphs in the results section were prepared in GraphPad Prism 6.01 (GraphPad, San Diego, CA, USA) as well. All results are compared with a tow-tailed Student's t-test, repeated measures one-way or two-way ANOVA, depending on the type of comparison and presented

with mean ±SD. Which test was performed, is specified in the legend of the corresponding figure. The symbols used to indicate statistical significance are: ns, not significant, $p > 0.05$, *$p \leq 0.05$, **$p \leq 0.01$, and ***$p \leq 0.001$.

3. Results

3.1 Analysis of post-mitotic NPC assembly in control and HGPS fibroblasts

Characteristic defects observed in HGPS are clustered NPCs, co-localizing with progerin trapped in invaginations of the NE (Goldman, Shumaker et al. 2004, Paradisi, McClintock et al. 2005)(Figure 1.3). Progerin has been shown to affect localization of various proteins during mitosis, therefore I investigated post-mitotic NPC assembly, to determine the cause of irregular NPC distribution in HGPS. I used immunofluorescence to track protein localization in two HGPS and control fibroblast cell lines (see 2.2.1). A list of how many fixed cells were analyzed per mitotic phase, per cell line and antibody combination, can be found in the appendix (Table 5.1).

In the following figures, examples of NPC clustering in two HGPS cell lines are depicted, using five different antibodies binding to different subunits of the NPC: ELYS, mAb414, NUP107, NUP153 and POM121 (see schematic representation in Figure 1.4 and IF analysis in

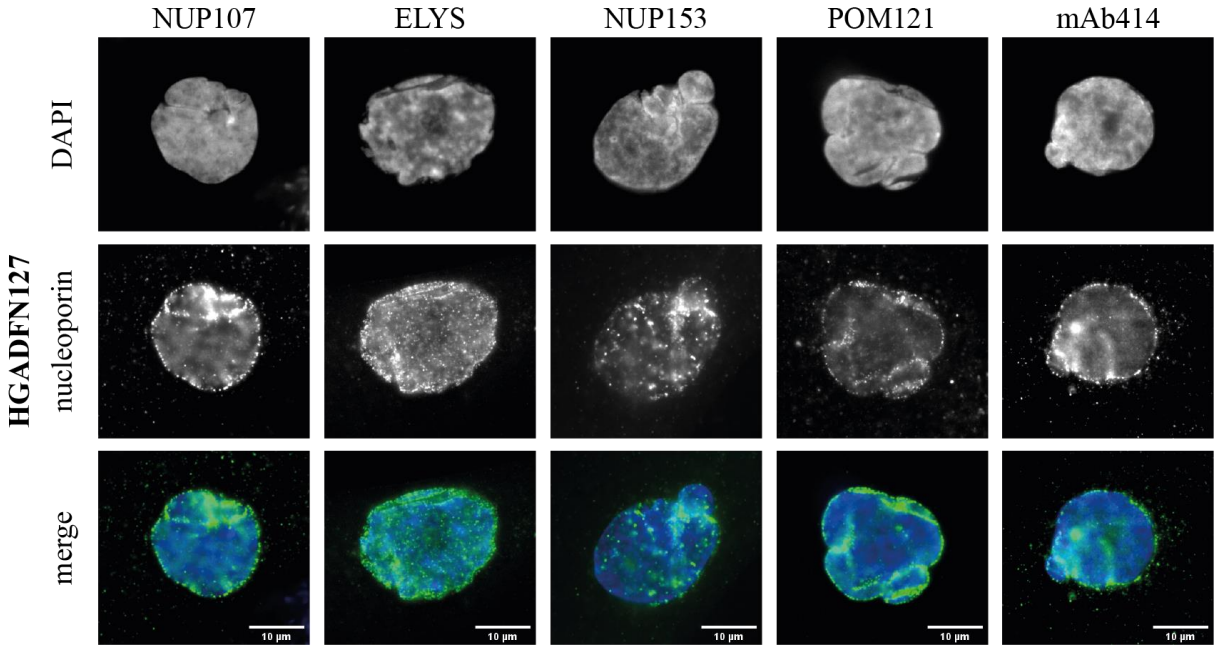

Figure 3.1 NPCs clustered in dysmorphic HGADFN127 nuclei

Representative images of dysmorphic HGADFN127 nuclei with clustered NPCs, labeled with α-NUP107/ ELYS/NUP153/POM121 or α-mAb414 (green), counterstained with DAPI (blue). Scalebar 10 µm.

Figure 3.1 and Figure 3.2). In both HGPS cell lines the different NUPs collect and cluster mostly in the folds and invaginations of the nuclear envelope (Figure 3.1 & Figure 3.2.).

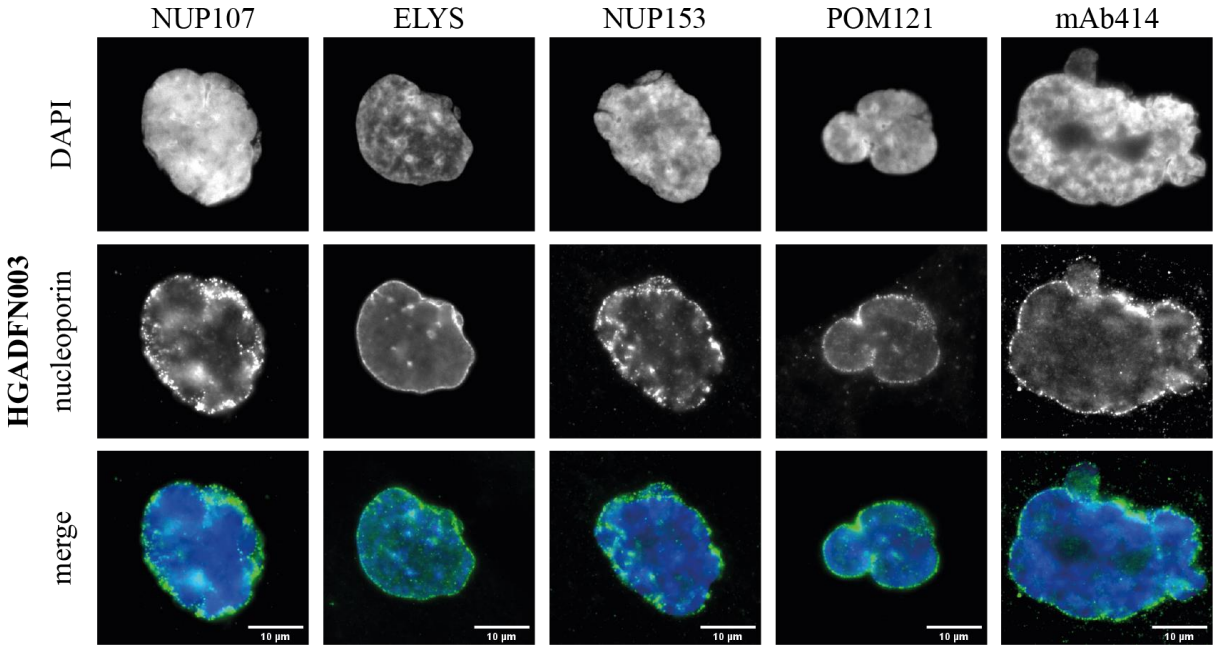

Figure 3.2 NPCs clustered in dysmorphic HGADFN003 nuclei

Representative images of dysmorphic HGADFN003 nuclei with clustered NPCs, labeled with α-NUP107/ ELYS/NUP153/POM121 or α-mAb414 (green), counterstained with DAPI (blue). Scalebar 10 µm.

3.1.1 Unlike NUP107, progerin aggregated in the cytoplasm of mitotic HGPS cells

Progerin accumulates with age, deforms the NE and collects in its' folds (Figure 3.3 a, b) (Goldman, Shumaker et al. 2004). In mitotic cells progerin does not disperse in the cytoplasm from metaphase to telophase and large quantities remained trapped in the ER of cytokinetic cells (Eisch, Lu et al. 2016). In contrast, LA is usually dispersed evenly in the cytoplasm, starts to collect at the periphery of telophase chromosomes and is fully assembled in cytokinesis/G1 (Moir, Yoon et al. 2000). Since progerin ER aggregates also de-localize other NE proteins during mitosis, such as LA, LB1, SUN1 and emerin (Eisch, Lu et al. 2016), I looked into the location of NUP107 in relation to progerin in mitotic cells, one of the first nucleoporins recruited to the reforming nuclear envelope (Figure 3.3 a, b). NUP107 is part of the NUP107-160-complex, which remains mostly associated throughout mitosis (Loiodice, Alves et al. 2004) and

diffuses in the cytoplasm after NE breakdown in prophase (Belgareh, Rabut et al. 2001). Therefore, following NUP107 would give a good overview of the entire NUP107-160 complex and any aggregates would indicate a perturbation of its' function during mitosis.

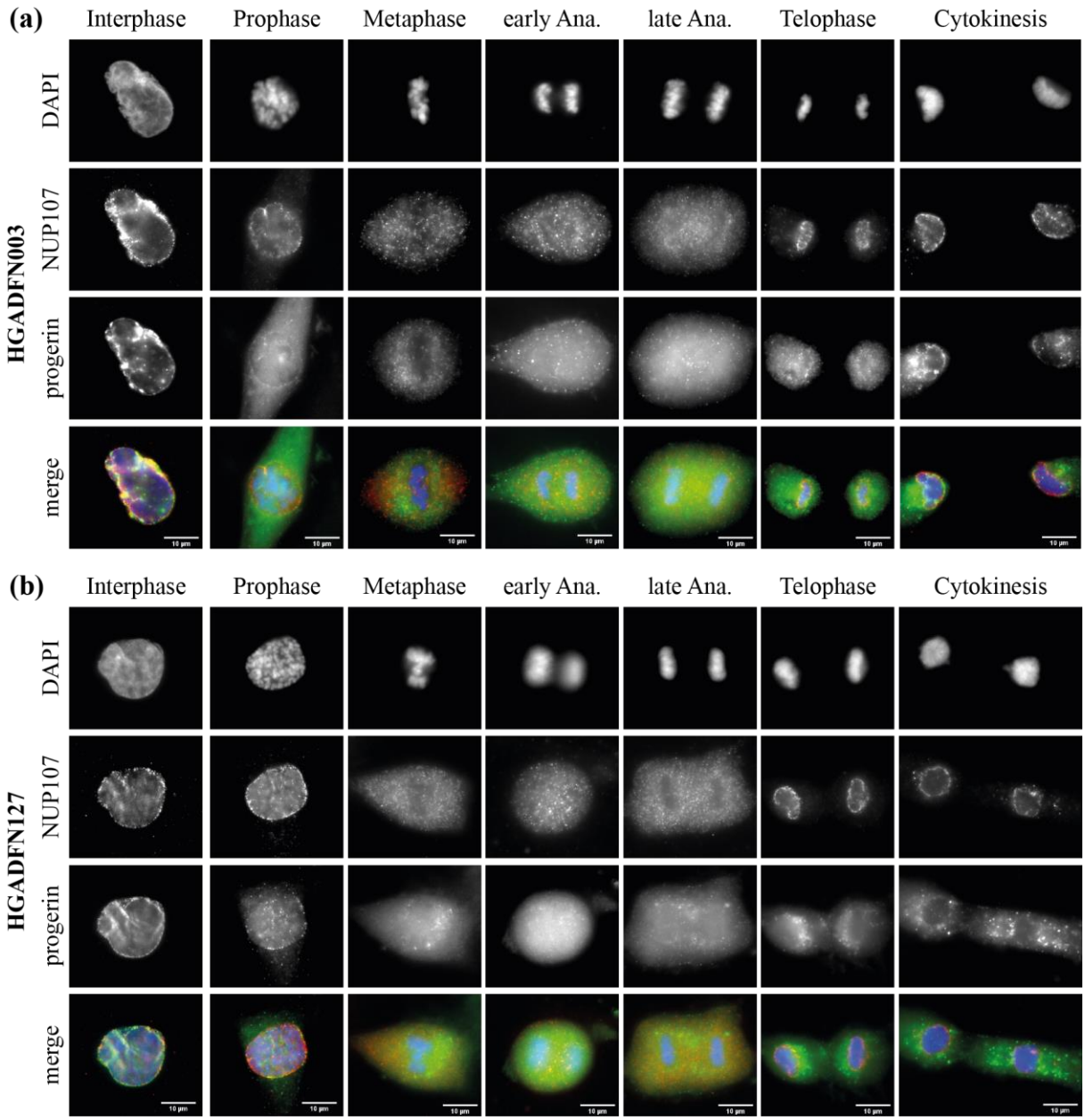

Figure 3.3 NUP107 did not colocalize with progerin aggregates in mitotic HGPS cells

Representative images of two HGPS cell lines: (a) HGADFN003 and (b) HGADFN127 labeled with α-NUP107 (red) and α-progerin (green), counterstained with DAPI (blue). From metaphase to cytokinesis progerin was aggregated in the cytoplasm of HGPS cells. Large aggregates were still visible in the cytoplasm of cytokinetic cells, so incorporation of progerin into the NE was delayed. NUP107 did not aggregate in mitotic HGPS cells, it dispersed evenly in the cytoplasm from metaphase to early anaphase. NUP107 recruitment to the dividing chromosomes in late anaphase/telophase was not delayed. n≥3, Scalebar 10 µm.

The nuclear envelope began to dissolve in prophase and NUP107 started to dissociate from the NE into the cytoplasm (Figure 3.3 a, b). In both metaphase and early anaphase HGPS cells, NUP107 was distributed evenly across the cytoplasm, whereas progerin accumulated adjacent to metaphase and anaphase chromosomes (Figure 3.3 a, b). Of note, since progerin retains its farnesyl anchor, it remains associated with the ER membrane in mitotic cells from prophase to cytokinesis (Eisch, Lu et al. 2016).

In late anaphase NUP107 began to form a rim at the core region of the separating chromosomes, which continued in telophase, where chromatin was now completely surrounded by NUP107 (Figure 3.3 a, b). By cytokinesis, NUP107 was fully incorporated into the daughter NE, with only background signal detectable in the cytoplasm (Figure 3.3 a, b). Progerin, however, remained attached to the ER membrane after NE dissolution in prophase and aggregated close to aligned metaphase chromosomes (Figure 3.3 a, b). In anaphase and telophase progerin was still aggregated and did not form a detectable rim at the dividing chromosomes (Figure 3.3 a, b). In addition, large progerin aggregates remained trapped in the cytoplasm of the daughter nuclei in cytokinesis and progerin was not properly incorporated into the NE (Figure 3.3 a, b).

In conclusion, progerin aggregated in dividing mitotic cells from metaphase to cytokinesis and incorporation into the reforming nuclear envelope was delayed. NUP107 recruitment to the NE did not appear to be affected and it did not colocalize with progerin aggregates. To confirm that progerin did not have a deleterious effect on overall post-mitotic NPC assembly, I analyzed further nucleoporins from different subunits of the NPC (highlighted in Figure 1.4).

3.1.2 Seeding of post-mitotic NPCs by ELYS was not affected in HGPS

ELYS is the first NUP recruited to the reforming NE, binding to the separating chromosomes in early anaphase via its' AT-hook domain (Rasala, Orjalo et al. 2006, Rasala, Ramos et al. 2008). If progerin interfered at the beginning of post-mitotic NPC assembly, as it does with other NE proteins (Eisch, Lu et al. 2016), we should be able to observe a defect at this first step. At the time only an ELYS antibody (AB) of the same species as our progerin AB was available, therefore a co-stain of ELYS and LA was performed. In healthy dividing cells both ELYS and LA should be diffused in the cytoplasm or in the case of ELYS, partially localized to kinetochores of metaphase chromosomes (Moir, Yoon et al. 2000, Rasala, Orjalo et al. 2006, Zuccolo, Alves et al. 2007). Progerin delocalizes the centromere protein CENP-F from kinetochores, therefore I was also interested if ELYS would properly bind to kinetochores in HGPS (Eisch, Lu et al. 2016). To elucidate, if ELYS localization is changed in HGPS, mitotic cells of two control and two HGPS cell lines were analyzed from prophase to cytokinesis (Figure 3.4 & Figure 3.5, Table 5.1).

In control and HGPS prophase the NE begins to dissolve and ELYS signal started to become more diffuse (Figure 3.4 & Figure 3.5 a, b). ELYS was partially localized to metaphase kinetochores in control and HGPS cell, with no obvious difference between the two (Figure 3.4 & Figure 3.5 a, b). LA, however, was only properly dispersed in the cytoplasm of metaphase control cells, whereas it formed aggregates close to the aligned chromosomes comparable to progerin in HGPS cells (Figure 3.3 a, b, Figure 3.4 & Figure 3.5 a, b). In control and HGPS early anaphase, we could observe that ELYS started to form a rim-like pattern surrounding the dividing chromosomes, which continued from late anaphase to telophase (Figure 3.4 & Figure 3.5 a, b). By the time control and HGPS cells had reached cytokinesis, ELYS was completely assembled into new pores in the NE of their daughter nuclei (Figure 3.4 & Figure 3.5 a, b). Yet LA assembly remained perturbed in HGPS fibroblasts, where aggregates could still be detected in the cytoplasm from anaphase up until cytokinesis, just as for progerin (Figure 3.4 & Figure 3.5 b, Figure 3.3 b).

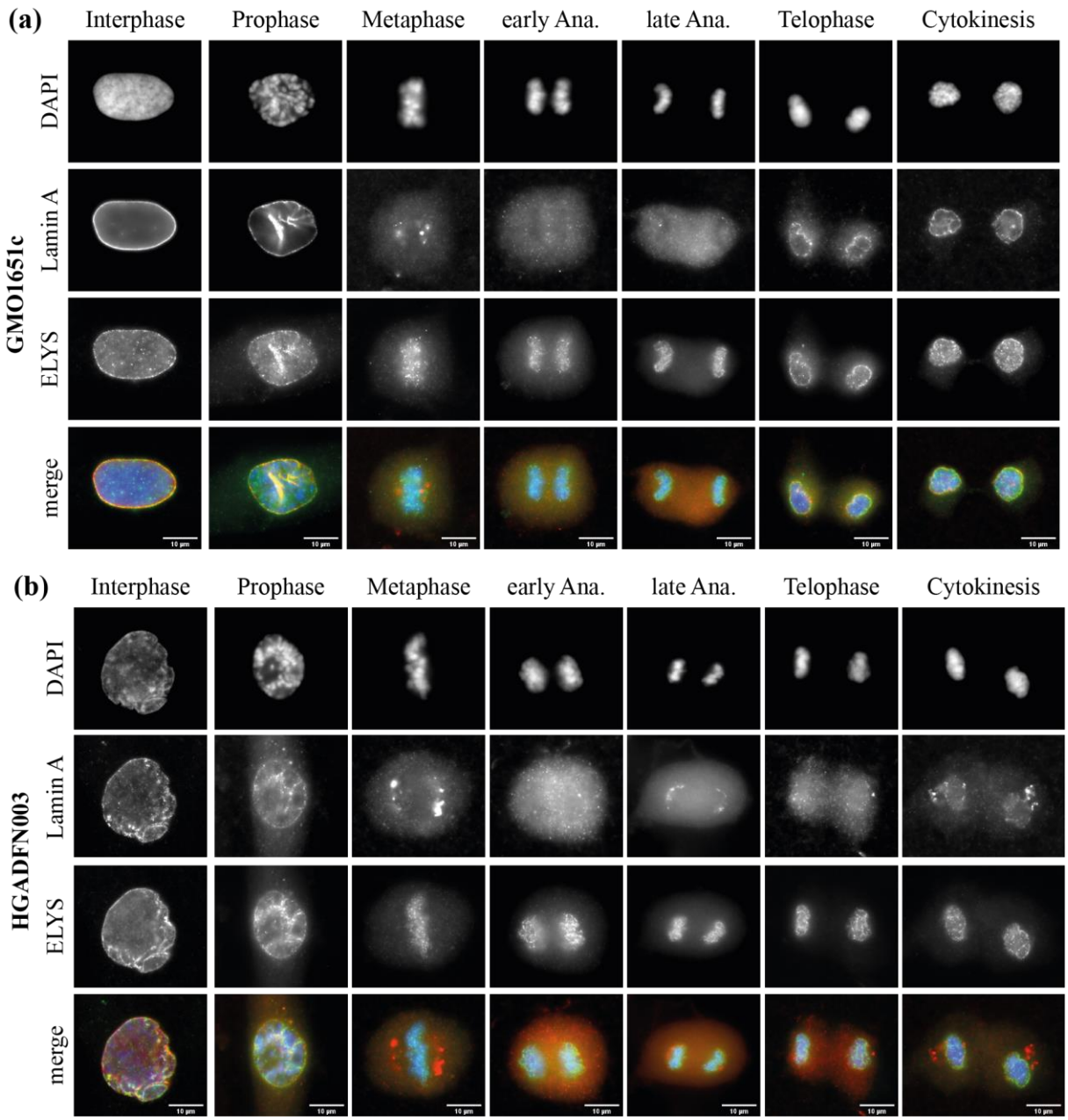

Figure 3.4 Seeding of NPCs by ELYS on anaphase chromosomes was not delayed in HGADFN003 compared to GMO1651c

Representative images of (a) GMO1651c (control) and (b) HGADFN003 (HGPS) labeled with α-LA (red) and α-ELYS (green), counterstained with DAPI (blue). From metaphase to cytokinesis LA was aggregated adjacent to the chromosomes in the cytoplasm of HGPS cells and incorporation into the NE was delayed. In mitotic control, LA was evenly dispersed from metaphase to anaphase and properly recruited to the separating chromosomes starting in telophase. ELYS was not affected in HGPS, it partially localized to the kinetochores on metaphase chromosomes and beginning in anaphase started to form a rim around the separating chromosomes. It was fully incorporated into the NE by cytokinesis in control and HGPS. n≥4, Scalebar 10 µm.

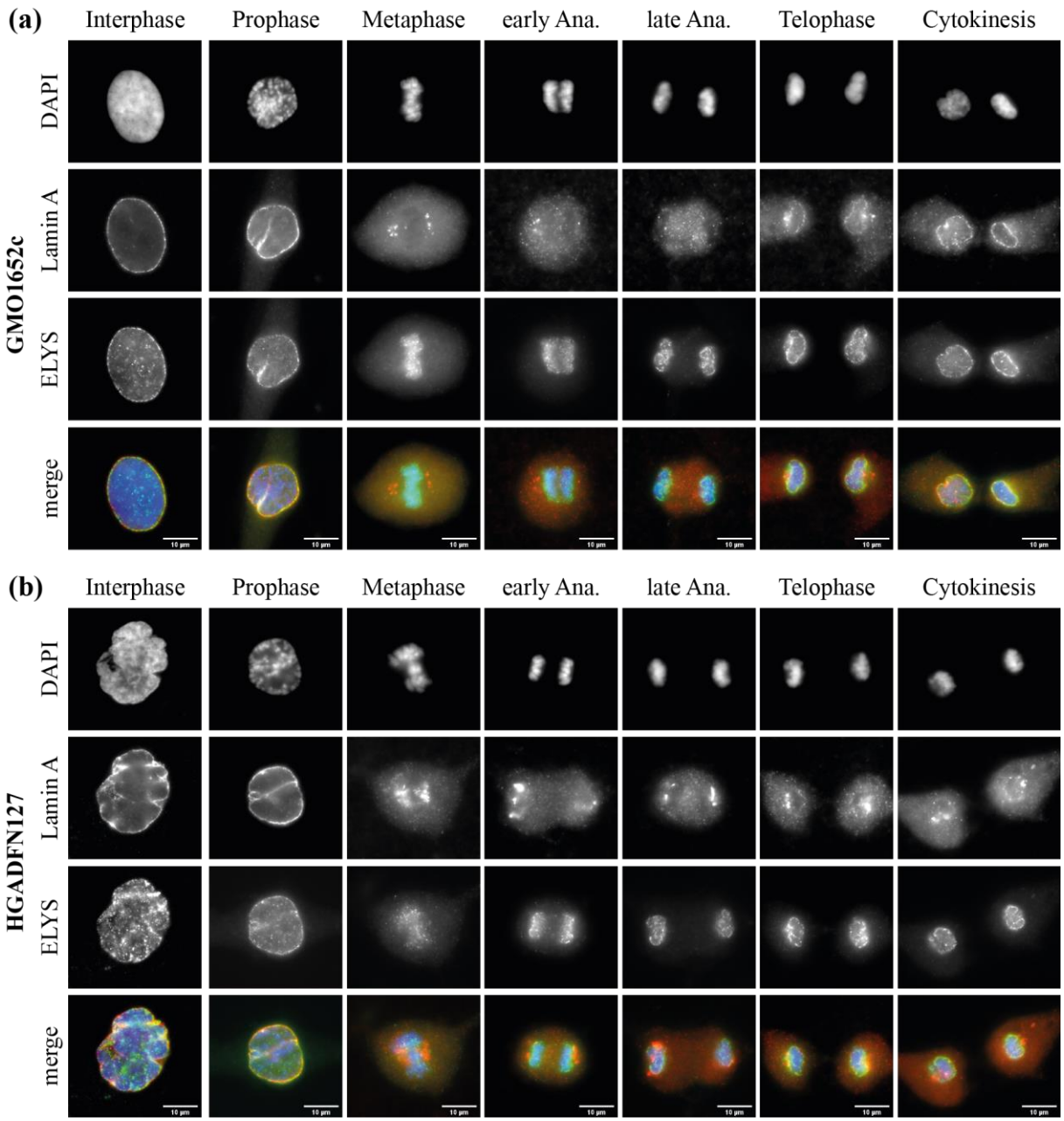

Figure 3.5 Seeding of NPCs by ELYS on anaphase chromosomes was not delayed in HGADFN127 compared to GMO1652c

Representative images of (a) GMO1652c (control) and (b) HGADFN127 (HGPS) labeled with α-LA (red) and α-ELYS (green), counterstained with DAPI (blue). From metaphase to cytokinesis LA was aggregated adjacent to the chromosomes in the cytoplasm of HGPS cells and incorporation into the NE was delayed. In mitotic control, LA was evenly dispersed from metaphase to anaphase and properly recruited to the separating chromosomes starting in telophase. ELYS was not affected in HGPS, it partially localized to the kinetochores on metaphase chromosomes and beginning in anaphase started to form a rim around the separating chromosomes. It was fully incorporated into the NE by cytokinesis in control and HGPS. n≥4, Scalebar 10 µm.

In control, LA started to form a rim surrounding telophase chromosomes, which was barely detectable in HGPS telophase (Figure 3.4 & Figure 3.5 a, b). LA was completely assembled in control cytokinesis, whereas it was still delayed in HGPS, similar to progerin (Figure 3.3, Figure 3.4 & Figure 3.5 a, b).

To conclude, ELYS localization was not affected in HGPS, unlike LA. It was not de-localized from metaphase chromosomes, unlike CENP-F, and properly seeded post-mitotic NPC assembly at anaphase onset. In HGPS cells, LA was aggregated in the cytoplasm from metaphase to cytokinesis and lamina assembly at the reforming NE was delayed. Large quantities of LA seemed to be trapped in the cytoplasm of cytokinetic HGPS daughter cells (see Table 5.2), and it remained unclear how this issue is resolved.

3.1.3 Mitotic localization of the basket nucleoporin NUP153 was not altered in HGPS

NUP153 is part of the NPC basket and is partially recruited to the reforming NPC in anaphase, similar to NUP107, a member of the NUP107-160 complex (Dultz, Zanin et al. 2008). NUP153 associates with Lamin A and B1 (Al-Haboubi, Shumaker et al. 2011) binding to their IG-fold and lack of NUP153 increases NPC mobility, which causes clustering (Walther, Fornerod et al. 2001). Therefore, I chose NUP153 as a further nucleoporin to analyze in mitotic HGPS and control cells, in combination with NUP107 (Figure 3.7 & Figure 3.6 a, b, Table 5.1).

Like NUP107, NUP153 is dispersed in the cytoplasm following dissolution of the NE in prophase (Bodoor, Shaikh et al. 1999, Dultz, Zanin et al. 2008), which was observed in control and HGPS (Figure 3.7 & Figure 3.6). Notably, NUP107 was detectable in the cytoplasm of prophase cells before NUP153, likely due to NUP153 as part of the NPC basket, still being present inside the barely disassembled NE (Figure 3.7 & Figure 3.6).

In metaphase both NUPs were diffused in the cytoplasm and excluded from the region of aligned chromosomes (Figure 3.7 & Figure 3.6 a, b). Once the chromosomes began to separate in early anaphase, a faint accumulation of NUP153 started to form at the core region (Figure 3.7 & Figure 3.6 a, b). This rim became stronger in late anaphase and completely enclosed control and HGPS chromatin by telophase (Figure 3.7 & Figure 3.6 a, b). NUP107 could first be detected at the chromosomes in late anaphase, with a complete rim visible in telophase (Figure 3.7 & Figure 3.6 a, b). In cytokinetic cells, both NUP107 and NUP153 were assembled completely, with no visible cytoplasmic aggregates at any time in either control or HGPS (Figure 3.7 & Figure 3.6 a, b).

Therefore, even though NUP153 associates with the lamina in interphase (Al-Haboubi, Shumaker et al. 2011), progerin's presence did not hinder its' function nor incorporation during post-mitotic NPC assembly.

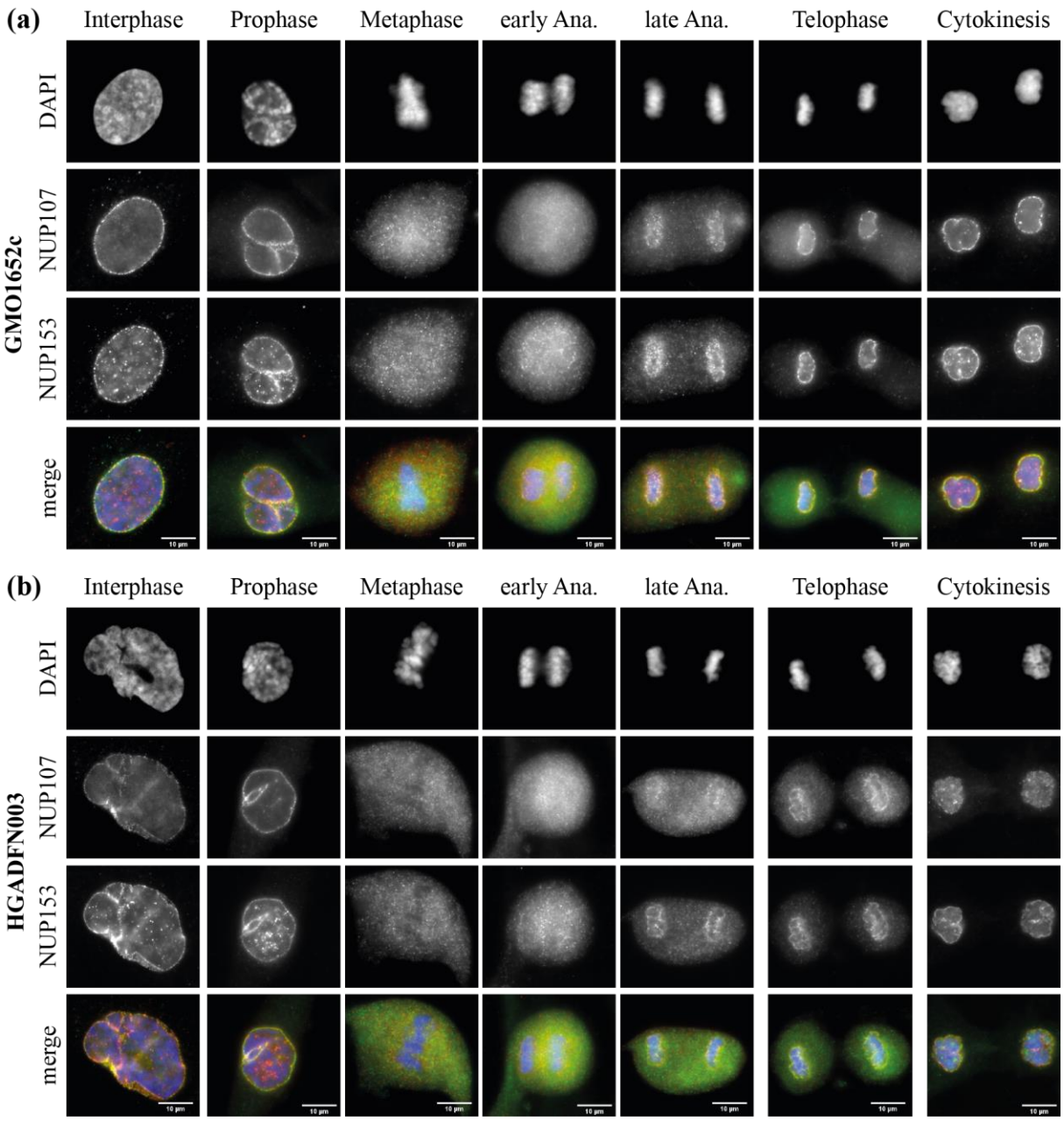

Figure 3.6 NUP153 and NUP107 recruitment and localization was not affected in HGADFN003 compared to GMO1652c

Representative images of (a) GMO1652c (control) and (b) HGADFN003 (HGPS) labeled with α-NUP153 (red) and α-NUP107 (green), counterstained with DAPI (blue). Neither NUP153 nor NUP107 aggregated in the cytoplasm of mitotic HGPS or control cells. Both NUP107 and NUP153 were properly incorporated into the NE starting in early anaphase for NUP153 and late anaphase for NUP107. By cytokinesis both were fully incorporated into the NE of the daughter nuclei. n≥5, Scalebar 10 µm.

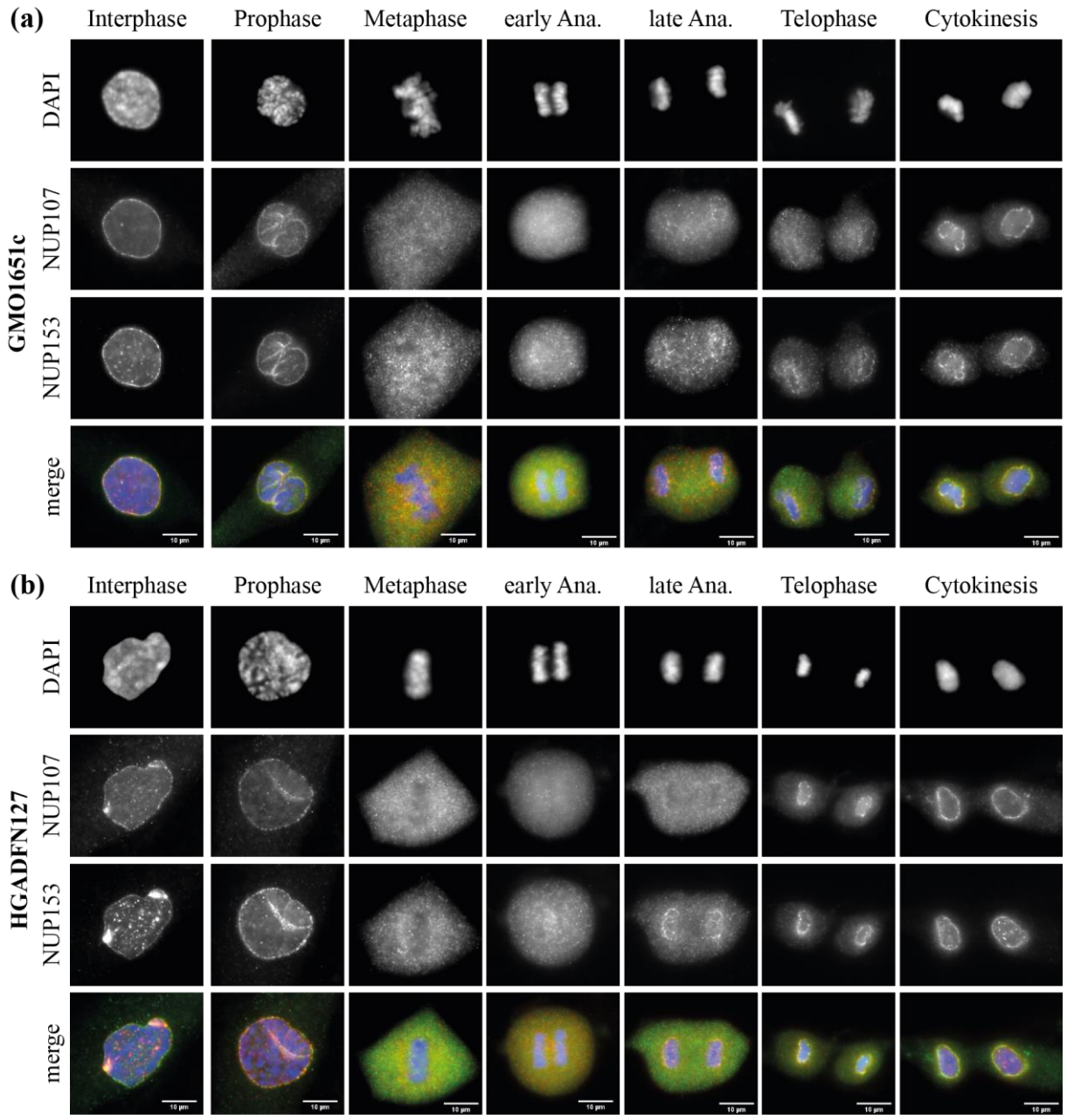

Figure 3.7 NUP153 and NUP107 recruitment and localization was not affected in HGADFN127 compared to GMO1651c

Representative images of (a) GMO1651c (control) and (b) HGADFN127 (HGPS) labeled with α-NUP153 (red) and α-NUP107 (green), counterstained with DAPI (blue). Neither NUP153 nor NUP107 aggregated in the cytoplasm of mitotic HGPS or control cells. Both NUP107 and NUP153 were properly incorporated into the NE starting in early anaphase for NUP153 and late anaphase for NUP107. By cytokinesis both were fully incorporated into the NE of the daughter nuclei. n≥5, Scalebar 10 µm.

3.1.4 SUN1 aggregates did not influence POM121 recruitment or localization in post-mitotic NPC assembly

SUN1 localization is affected by progerin in both mitotic and interphase HGPS cells (Chen, Wang et al. 2014, Eisch, Lu et al. 2016). Progerin decreases SUN1 mobility, it causes SUN1 to accumulate in replicating cells and SUN1/progerin aggregates overlap in dividing cells (Chen, Wang et al. 2014, Eisch, Lu et al. 2016). Since progerin strongly affects the INM protein SUN1, we decided to take a closer look at the transmembrane nucleoporin, POM121 as well (Table 5.1, Figure 3.10 & Figure 3.11 a, b). We chose POM121, because it associates with SUN1 during *de novo* interphase NPC assembly (Talamas and Hetzer 2011) and may consequently be negatively influenced by progerin as well. It was not possible to combine SUN1 and POM121 in the same immunofluorescence experiment, since at the time both antibodies were only available from the same species. Hence, we chose to label cells with either POM121 or SUN1 in combination with mAb414. mAb414 recognizes glycosylated FG-repeat NUPs, such as NUP358, NUP214, NUP153, NUP98 and NUP62 (Davis and Blobel 1986, Lin and Hoelz 2019) and thus gives a good overview over multiple other NUPs, which we would not have had if I had combined POM121 and SUN1 directly.

First, I looked at SUN1 in control and HGPS cells, to clarify the relative localization of SUN1 and NUPs bound by mAb414 from prophase to cytokinesis (Figure 3.8 & Figure 3.9, Table 5.1). Since SUN1 is a transmembrane protein, it localizes to the dissociated ER membrane, as does POM121 (Daigle, Beaudouin et al. 2001, Chen, Wang et al. 2014), whereas NUPs bound by mAb414 diffuse in the cytoplasm, since none of them are transmembrane NUPs (Figure 1.4). SUN1 remains bound to the dissolving NE in prophase, later redistributing to the ER(Chen, Wang et al. 2014) and therefore no SUN1 background signal was visible in the prophase cytoplasm of control or HGPS.

In metaphase control cells, SUN1 is excluded from the region surrounding the aligned chromosomes, whereas in HGPS cells SUN1 aggregated close to them (Figure 3.8 & Figure 3.9 a, b, Table 5.2). Aggregated SUN1 could still be observed in early anaphase HGPS cells, in control it remained dispersed (Figure 3.8 & Figure 3.9 a, b). In late anaphase of control cells, SUN1 is

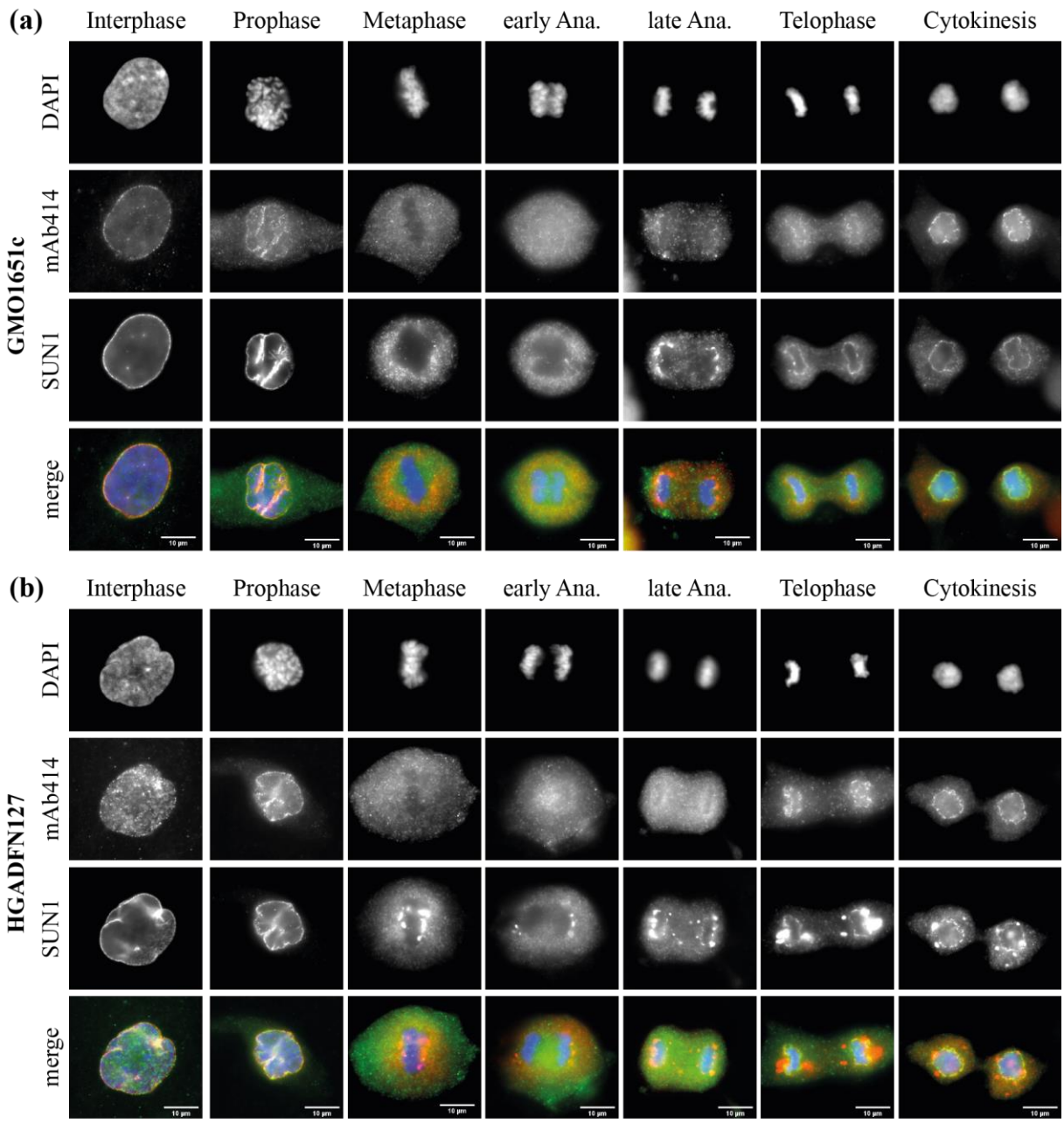

Figure 3.8 mAb414 did not colocalize with aggregated SUN1 in mitotic HGADFN127 cells

Representative images of (a) GMO1651c (control) and (b) HGADFN127 (HGPS) labeled with α-SUN1 (red) and α-mAb414 (green), counterstained with DAPI (blue). From metaphase to cytokinesis SUN1 was aggregated in the ER of HGPS cells and incorporation into the NE was delayed. In mitotic control, SUN1 was evenly dispersed from metaphase to anaphase and properly recruited starting in late anaphase. In cytokinetic control nuclei SUN1 was fully incorporated into the NE. NUPs bound by mAb414 did not colocalize with SUN1 aggregates in HGPS. The signal was dispersed in the cytoplasm from metaphase to early anaphase, with a faint rim surrounding late anaphase chromosomes. Not all NUPs bound by mAb414 were fully incorporated in cytokinesis in control and HGPS. n≥10, Scalebar 10 µm.

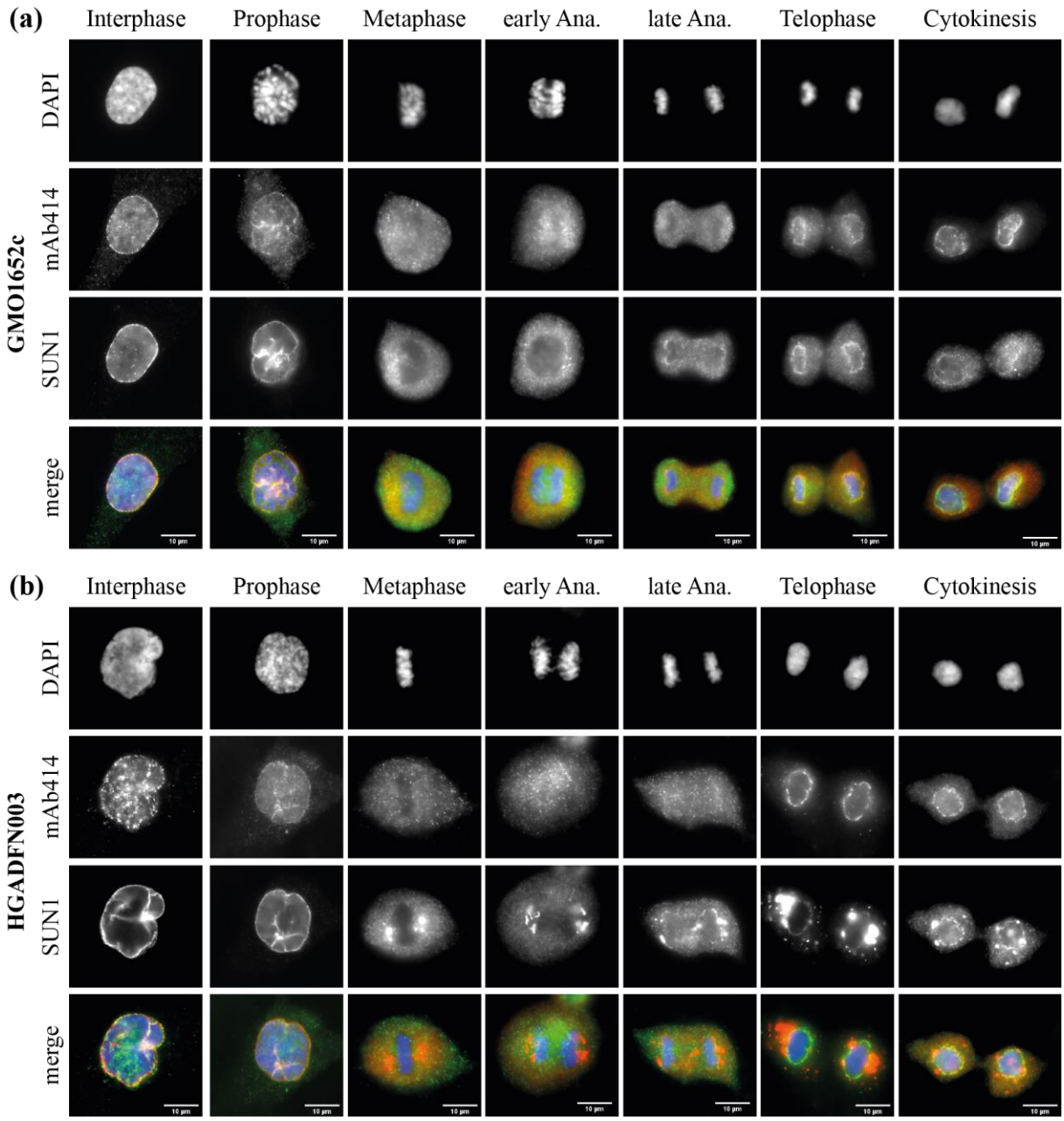

Figure 3.9 mAb414 did not colocalize with aggregated SUN1 in mitotic HGADFN003 cells

Representative images of (a) GMO1652c (control) and (b) HGADFN003 (HGPS) labeled with α-SUN1 (red) and α-mAb414 (green), counterstained with DAPI (blue). From metaphase to cytokinesis SUN1 was aggregated in the ER of HGPS cells and incorporation into the NE was delayed. In mitotic control, SUN1 was evenly dispersed from metaphase to anaphase and properly recruited starting in late anaphase. In cytokinetic control nuclei SUN1 was fully incorporated into the NE. NUPs bound by mAb414 did not colocalize with SUN1 aggregates in HGPS. The signal was dispersed in the cytoplasm from metaphase to early anaphase, with a faint rim surrounding late anaphase chromosomes. Not all NUPs bound by mAb414 were fully incorporated in cytokinesis in control and HGPS. n≥10, Scalebar 10 µm.

recruited to the core region of the separating chromosomes and began to form a rim, which fully enclosed chromatin in telophase (Figure 3.8 & Figure 3.9 a).

Cytokinetic control displayed an even distribution of SUN1encompassing the two daughter nuclei (Figure 3.8 & Figure 3.9 a). In HGPS, a faint SUN1 rim became visible in late anaphase, which continued in telophase (Figure 3.8 & Figure 3.9 b). However, the rim was uneven compared to control and large aggregates remained trapped in the ER from anaphase until cytokinesis (Figure 3.8 & Figure 3.9 b).

mAb414 NUPs began to dissociate from the NE in prophase, in contrast to SUN1, which was still associated with the NE. The NUPs bound by mAb414 remained evenly distributed in the cytoplasm until late anaphase, in both control and HGPS (Figure 3.8 & Figure 3.9 a, b). Beginning in late anaphase, the signal accumulated at the chromosomal core region. A full rim became visible in telophase and fully surrounded cytokinetic nuclei. Unlike the previous NUPs analyzed, we could detect remaining signals in the cytoplasm of cytokinetic cells. This was expected, since some NUPs bound by mAb414 , such as the cytoplasmic filament NUP358, do not fully integrate into the NPC until early G1 (Dultz, Zanin et al. 2008). Just as with the previous NUPs analyzed, no difference in mAb414 localization could be detected in HGPS, compared to control (Figure 3.8 & Figure 3.9 a, b).

Lastly, I observed POM121 behavior in concert with mAb414 in control and HGPS (Table 5.1, Figure 3.10 & Figure 3.11 a, b). Like SUN1, POM121 remains associated with the ER membrane in mitosis (Daigle, Beaudouin et al. 2001) and did not begin to detach from the NE like mAb414 in control and HGPS prophase (Figure 3.10 & Figure 3.11 a, b).

POM121 was excluded from the region of aligned chromosomes in metaphase and the separating chromosomes in anaphase control and HGPS cells and unlike SUN1 did not aggregate in HGPS (Figure 3.10 & Figure 3.11 a, b). In late anaphase, POM121 had begun to encircle the separating chromosomes, which continued in telophase where only residual POM121 remained associated with the ER in the cytoplasm of both control and HGPS (Figure 3.10 & Figure 3.11 a, b).

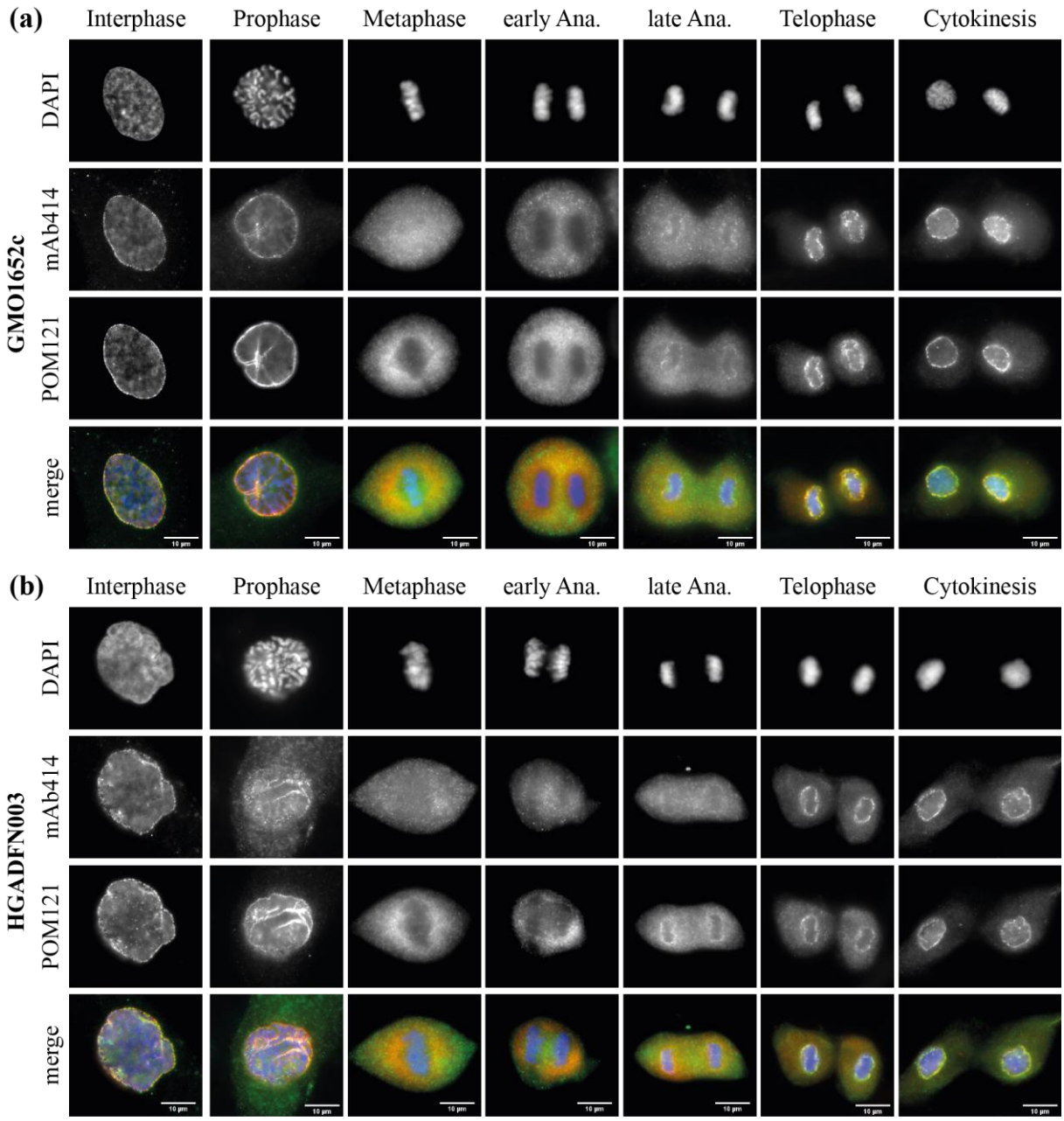

Figure 3.10 The transmembrane nucleoporin POM121 did not aggregate in mitotic HGADFN003 cells and incorporation into the NE was not delayed.

Representative images of (a) GMO1652c (control) and (b) HGADFN003 (HGPS) labeled with α-POM121 (red) and α-mAb414 (green), counterstained with DAPI (blue). Neither POM121 nor mAb414 recruitment or localization was altered in mitotic HGPS cells, compared to control. POM121 dispersed in the ER, excluded from the region of the chromosomes, until it began to form a rim surrounding the chromosomes in late anaphase. By cytokinesis it was fully incorporated into the NE. NUPs bound by mAb414 did not colocalize with SUN1 aggregates in HGPS. The signal was dispersed in the cytoplasm from metaphase to early anaphase, with a faint rim surrounding late anaphase chromosomes. Not all NUPs bound by mAb414 were fully incorporated in cytokinesis in control and HGPS. n≥6, Scalebar 10 µm.

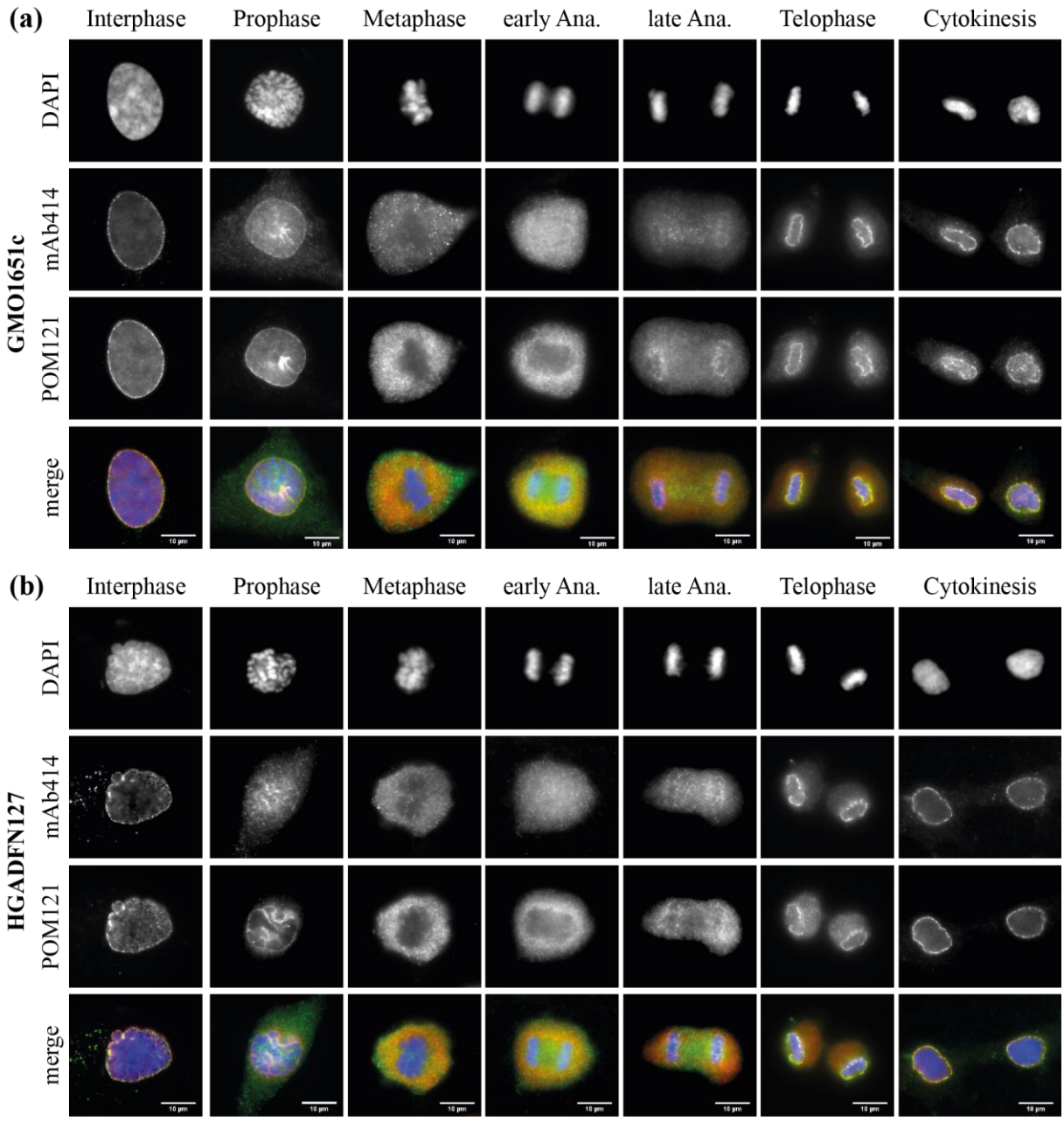

Figure 3.11 The transmembrane nucleoporin POM121 did not aggregate in mitotic HGADFN127 cells and incorporation into the NE was not delayed.

Representative images of (a) GMO1651c (control) and (b) HGADFN127 (HGPS) labeled with α-POM121 (red) and α-mAb414 (green), counterstained with DAPI (blue). Neither POM121 nor mAb414 recruitment or localization was altered in mitotic HGPS cells, compared to control. POM121 dispersed in the ER, excluded from the region of the chromosomes, until it began to form a rim surrounding the chromosomes in late anaphase. By cytokinesis it was fully incorporated into the NE. NUPs bound by mAb414 did not colocalize with SUN1 aggregates in HGPS. The signal was dispersed in the cytoplasm from metaphase to early anaphase, with a faint rim surrounding late anaphase chromosomes. Not all NUPs bound by mAb414 were fully incorporated in cytokinesis in control and HGPS. n≥6, Scalebar 10 µm.

Once the dividing cells had reached cytokinesis, POM121 was fully incorporated into the NE of control and HGPS daughter nuclei (Figure 3.10 & Figure 3.11 a, b). This was in direct opposition to the observations concerning SUN1 (Figure 3.8 & Figure 3.9 a, b; Figure 3.10 & Figure 3.11 a, b), where large aggregates of SUN1 were still detectable in the cytoplasm of cytokinetic HGPS cells. mAb414 behaved in the same fashion as in the co-stain of mAb414 and SUN1 (Figure 3.8, Figure 3.9, Figure 3.10 & Figure 3.11 a, b), no delay or aggregation could be detected in HGPS cells at any point.

Therefore, contrary to SUN1, POM121 localization or recruitment to the NE was not affected throughout mitosis in HGPS cells. Given that progerin did not interfere with any of the various NUPs analyzed in this study, we can posit that defective or altered post-mitotic NPC assembly was likely not the cause for NPC clustering in HGPS.

3.2 Analysis of nuclear morphology, progerin protein levels and NPC clustering in replicative senescence in control and HGPS fibroblasts

Throughout the course of my experiments with mitotic cells, I noticed that with increasing replicative senescence or passage number, my control fibroblast nuclei began to exhibit similar morphological features as my HGPS fibroblasts. Therefore, I investigated the possibility that NPC clustering does not just occur in HGPS, but in aged control cells as well. To analyze NPC distribution in relation to replicative senescence, I had to determine which senescence markers would be suitable for my experiments. Commonly used hallmarks of senescence are increased lysosomal content, nuclear alterations, reduced LB1 levels and elevated $p16^{INK4A}$ (p16) or p21 (Dimri, Lee et al. 1995, Alcorta, Xiong et al. 1996, Mehta, Figgitt et al. 2007, Freund, Laberge et al. 2012, Hernandez-Segura, Nehme et al. 2018). Increased lysosomal content can be ascertained by a senescence-associated β-Galactosidase assay (SA β-Gal) (Dimri, Lee et al. 1995), which I used to predetermine senescence levels, before advancing to immunofluorescent analysis (see 2.2.2 & 2.2.5). Predetermination of SA β-Gal levels were necessary, since HGPS cells age prematurely (Liu, Wang et al. 2005, Huang, Risques et al. 2008, Benson, Lee et al. 2010, Wheaton, Campuzano et al. 2017, Liu, Arnold et al. 2019). Therefore, passage numbers cannot accurately reflect cellular age (Liu, Arnold et al. 2019), distorting any results dependent on cellular health and age. Additionally, I cultured all four cell lines in the exact same manner, to ensure all results I gathered would not be influenced by different handling. Cells were split at the same time each week and seeded with the same density (cells/cm^2). Generally, FN127 and FN003 reached a senescence index of ≥30% (SNS >30%) at an earlier passage number than GMO1651c and GMO1652c (see caption Figure 3.14), which highlights the importance of using SNS to compare HGPS with control cells and not passage number.

3.2.1 Nuclear morphology in replicative senescence

One hallmark of HGPS cells is the distinct change in nuclear morphology, compared to healthy control cells (Figure 1.1 versus Figure 1.3) (Goldman, Shumaker et al. 2004). First, I evaluated if abnormal nuclear morphology was dependent on replicative senescence and how control and HGPS cells differed from each other. I evaluated nuclear shape, distinguishing between 'normal' and 'dysmorphic' based on the DAPI signal (Figure 3.12).

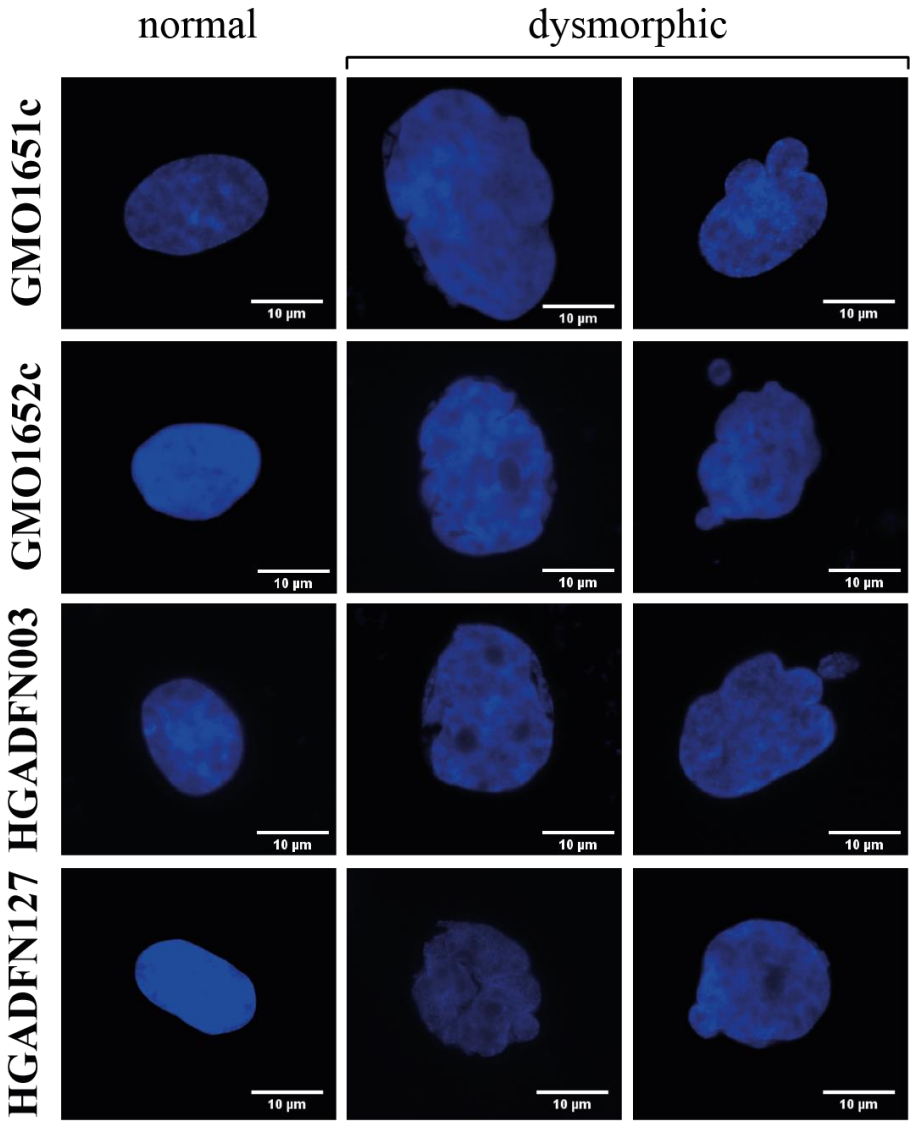

Figure 3.12 Dysmorphic nuclei in replicative senescence

Representative images of normal and dysmorphic GMO1651c/GMO1652c (control) and HGADFN003/HGADFN127 (HGPS) nuclei counterstained with DAPI. Scalebar 10 µm.

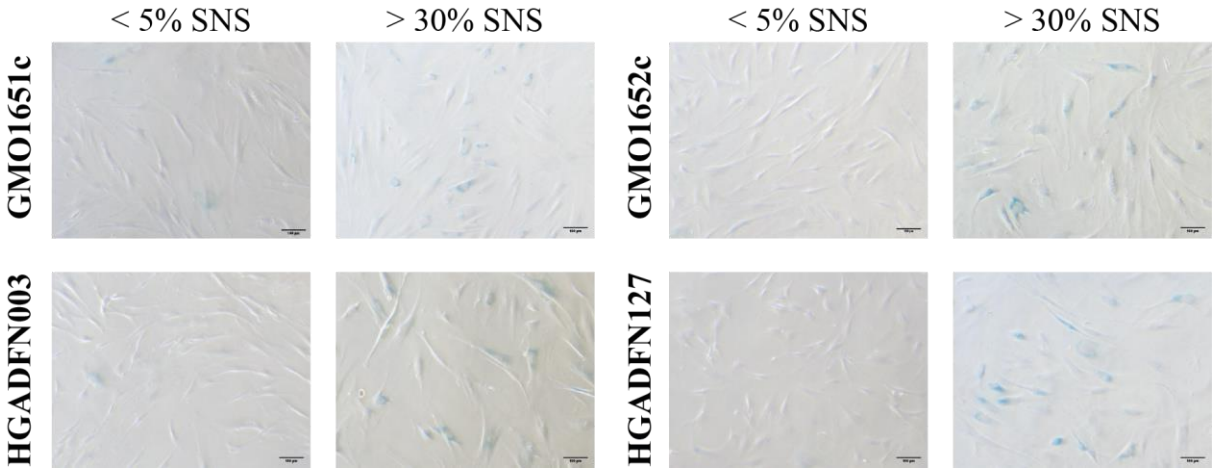

Figure 3.13 Determination of senescence index using a Senescence associated β-Galactosidase assay

Representative images of GMO1651c/GMO1652c (control) and HGADFN003/HGADFN127 (HGPS) stained for lysosomal content using SA β-Gal assay (see 2.2.2). Scalebar 100 µm.

To determine, if replicative senescence had an influence on the occurrence of nuclear dysmorphism, I compared nuclear morphology in control and HGPS cells with low (<5%) and high (>30%) SNS, determined by SA β-Gal (Figure 3.13), using immunofluorescence (Figure 3.12).

I found that the number of dysmorphic nuclei increased significantly in both control and HGPS with rising senescence (Figure 3.14). At high SNS an average of 61% of control nuclei were dysmorphic and 54% of HGPS nuclei (Figure 3.14). The difference between control and HGPS at SNS >30% was not statistically significant or only to a small degree (Figure 3.14). In young cells with low SNS, this was not the case (Figure 3.14). Here HGPS cells had a significantly higher number of dysmorphic nuclei compared to control; ~18,2 % vs. 11,2 % (Figure 3.14).

I concluded that the higher number of nuclear abnormalities in young HGPS cells was likely due to progerin's influence, which I further investigated in 3.2.3. The similar levels of dysmorphic nuclei in aged control and HGPS cells were probably caused by down-regulation of LB1 due to replicative senescence in both and increased progerin accumulation in HGPS (Goldman, Shumaker et al. 2004, Freund, Laberge et al. 2012).

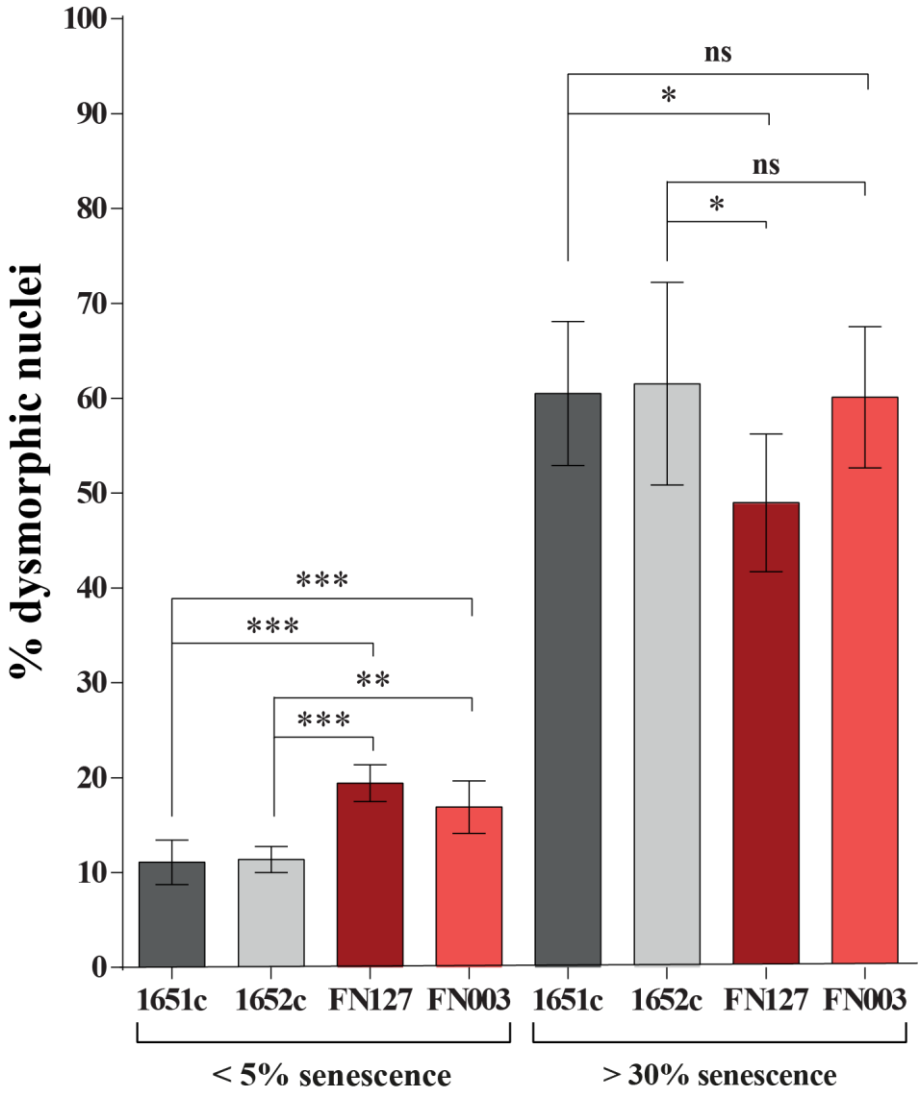

Figure 3.14 Nuclear abnormalities increase with rising replicative senescence in control and HGPS fibroblasts

Number of control (1651c/1652c) and HGPS (FN127/FN003) dysmorphic nuclei <5% and >30%SNS was determined by counting nuclei counterstained with DAPI. SNS of control and HGPS cultures was pre-determined with SA β-Gal. Values were analyzed with a one-way ANOVA with Tukey's multiple comparison test and are presented as mean ± SD: not significant (ns) $p > 0.05$, * $p < 0.05$, ** $p < 0.01$, *** $p < 0.001$ (n≥3). Differences between young and old cells within each cell line were significant. Passage number <5% SNS was ≤P18 for HGPS and ≤P21 for control. Passage number >30% SNS was ≥P21 for HGPS and ≥P25 for control.

3.2.2 Detection of senescent HGPS and control fibroblasts

However, predetermining SNS by SA β-Gal and observing nuclear morphology by counterstaining with DAPI did not allow me to link progerin content and mechanisms of senescence directly to changes in single control or HGPS nuclei. To precisely visualize these effects, I had to find the right marker to fluorescently label cells, which would enable me to evaluate single cells. Hence, I prepared samples with young (<5% SA β-Gal positive = young) or old cells (>30% SA β-Gal positive = old) and labeled them with α-p16, α-p21 or α-LB1 antibodies to distinguish senescent from proliferating or quiescent cells via immunofluorescence (Figure 3.15). Both p16 and p21 are also expressed in non-senescent cells (Jung, Qian et al. 2010, Witkiewicz, Knudsen et al. 2011), so I only considered cells to be senescent, if they were positive for one of the senescence markers and nuclear morphology was altered as well (Figure 3.15 arrows).

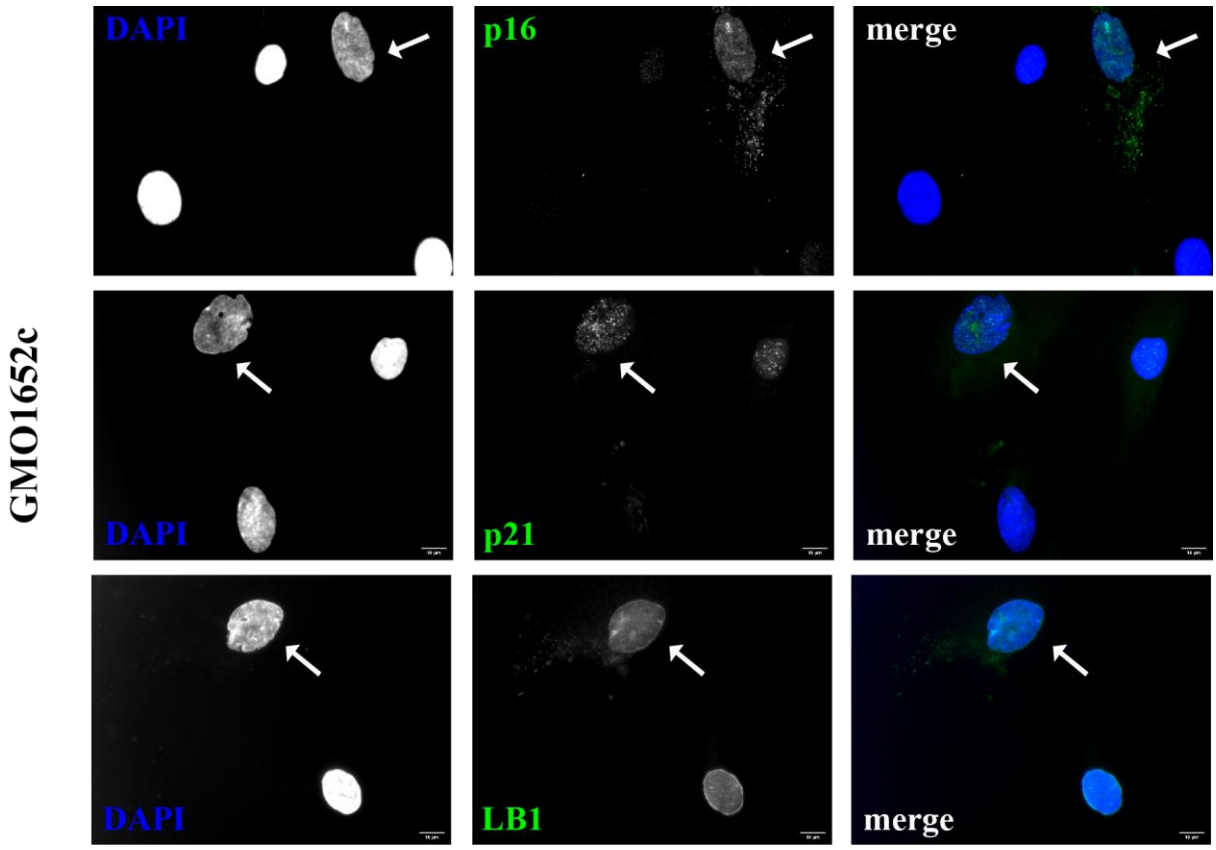

Figure 3.15 Immunofluorescent determination of replicative senescence with p16, p21 or LB1

Representative images of GMO1652c stained with α-p16, α-p21, or α-LB1, counterstained with DAPI. Arrows point out dysmorphic nuclei with elevated p16 or p21 or reduced LB1. Scalebar 10 µm.

I deemed nuclear dysmorphism to be a proper measure to prevent misidentification of healthy nuclei as senescent, since I observed a significant increase concomitantly with rising age of my cultures, in line with previous findings (Figure 3.14) (Mitsui and Schneider 1976, Hänzelmann, Beier et al. 2015).

Just as with nuclear dysmorphism, more dysmorphic HGPS nuclei <5% SNS were positive for one of three senescent markers (p16/p21/LB1) compared to young dysmorphic control nuclei, even though senescence levels were pre-matched with SA β-Gal (Figure 3.16). On average ~5% more dysmorphic HGPS nuclei in young cultures were senescent than in the two young control fibroblast cultures.

In addition, in young control and HGPS cultures I generally detected more senescent dysmorphic nuclei than SA β-Gal positive cells (Figure 3.16). In old cultures the number of senescent dysmorphic nuclei was similar to the number of SA β-Gal positive cells. This discrepancy is likely due to SA β-Gal being a later stage senescence marker (Dimri, Lee et al. 1995), compared to p16, p21 and LB1.

Not all dysmorphic control or HGPS nuclei were positive for one of the three markers, highlighting that just changes in nuclear morphology were not sufficient to determine SNS (Figure 3.16).

When comparing p16, p21 and LB1 within one control or HGPS cell line, I detected a similar number of senescent nuclei in young cultures, which changed in old cells (Figure 3.16). Control or HGPS cells with a SNS greater than 30%, did not significantly differ in nuclear dysmorphism, however, p21 appeared to be elevated in fewer dysmorphic nuclei than p16 (Figure 3.16). This was not surprising, since p21 only plays a role at the induction of senescence and instead p16 is required for maintenance (Alcorta, Xiong et al. 1996). Consequently, a significantly higher amount of dysmorphic control nuclei displayed elevated levels of p16 in old cultures (Figure 3.16). In old HGPS cells the difference between dysmorphic nuclei labeled by p21 or p16 was not significantly different, likely due to the high standard deviation in old HGPS cells (Figure 3.16).

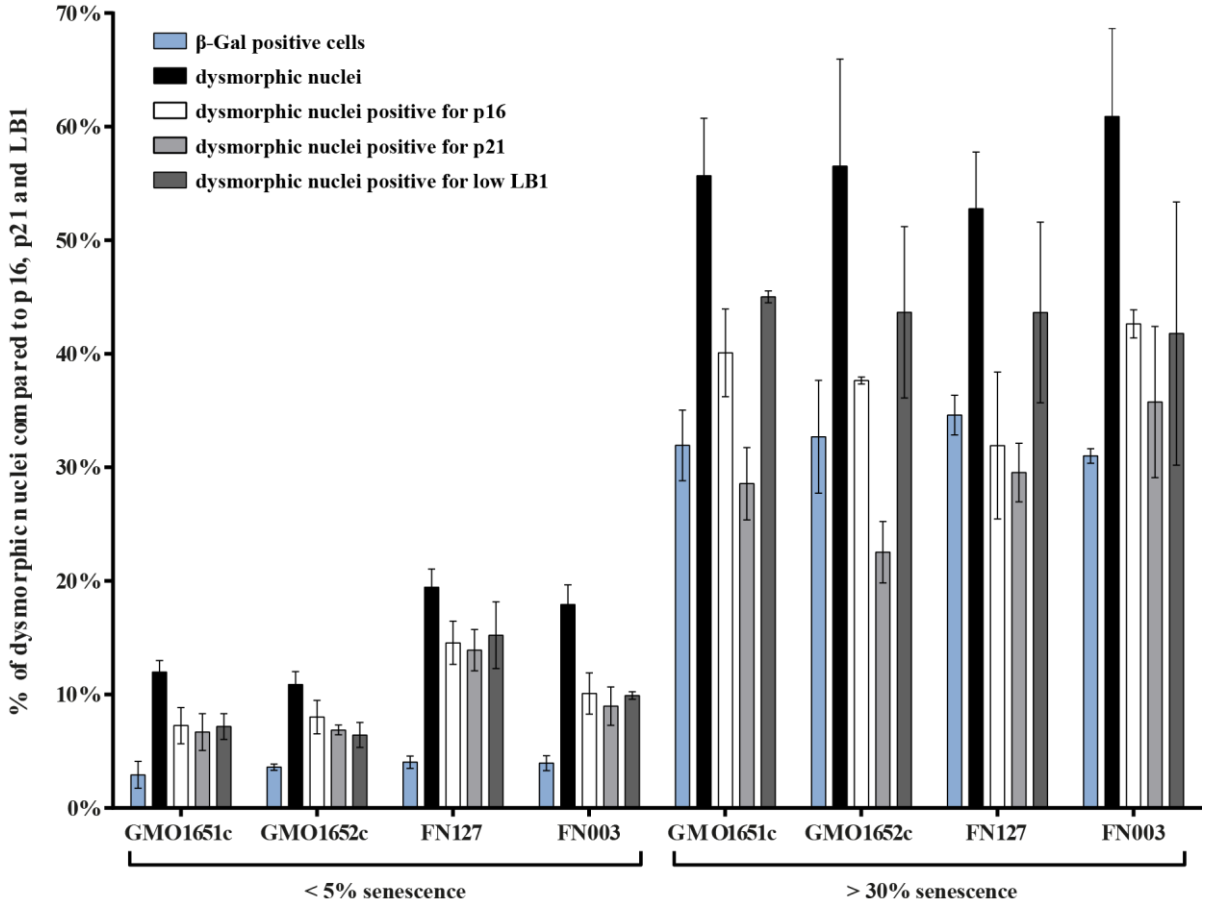

Figure 3.16 Comparison of the senescence markers p16, p21 and LB1 in young or old control and HGPS fibroblasts

Control (GMO1651c/GMO1652c) and HGPS (FN127/FN003) cells were sorted into young/old based on the result of a SA β-Galactosidase assay: <5% SA β-Gal positive = young; >30% SA β-Gal positive = old. They were then stained with α-p16, α-p21 or α-LB1, counterstained with DAPI and evaluated for senescence markers and nuclear morphology (see Figure 3.15). Values are presented as mean ± SD (n≥3) and were analyzed using a two-way ANOVA with Tukey's multiple comparison test. Differences between young and old cells within each cell line were significant. Significance was not depicted in this graph, because it could not be clearly shown. Passage number <5% SNS was ≤P18 for HGPS and ≤P21 for control. Passage number >30% SNS was ≥P21 for HGPS and ≥P25 for control. Values are presented as mean ± SD (n≥3).

Generally, the standard deviation was higher in experiments performed in cells with a high SNS, possibly indicating a higher variance within a population of older cells than in young cultures. In conclusion control and HGPS only significantly differed in their behavior in young cultures, whereas in older cultures they displayed similar levels of nuclear dysmorphism and incidence of elevated p16/p21 or reduced LB1.

In total the results of this comparison highlight the need to use multiple senescence markers to be able to accurately judge the SNS. Therefore, in the following sections I used at least three senescence indicators: I pre-matched the SNS of my cultures with SA β-Gal and used nuclear dysmorphism and one additional senescence marker to determine SNS in my immunofluorescence analysis.

3.2.3 Progerin in replicative senescence

To my knowledge, nobody has directly linked the SNS index to progerin levels and nuclear dysmorphism, by observing young and old HGPS nuclei labeled with α-progerin AB. Therefore, I analyzed how increased progerin signal in HGPS nuclei related to changes in nuclear morphology and, if increasing replicative senescence played a role in this relationship. To confirm that progerin was the cause of increased nuclear dysmorphism in young HGPS cultures, I analyzed how many abnormal HGPS nuclei also had high levels of progerin (Figure 3.17).

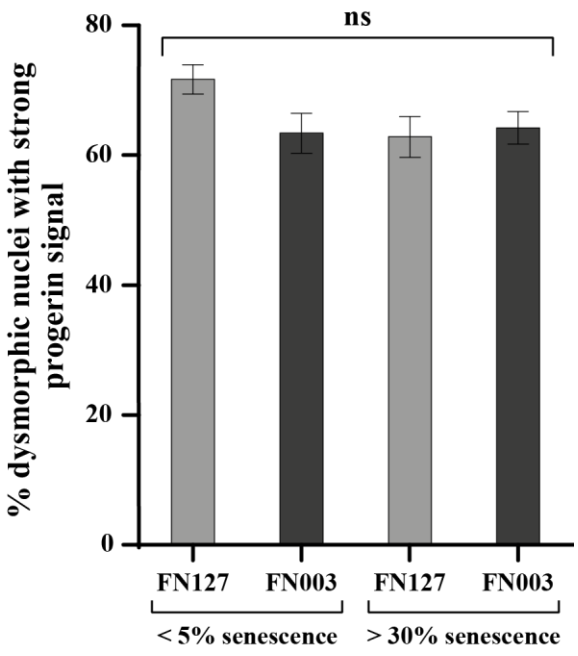

Figure 3.17 Progerin was elevated in most dysmorphic HGPS nuclei independent of replicative senescence

Number of HGPS dysmorphic nuclei with elevated progerin <5% and >30%SNS was determined by counting HGPS nuclei labelled with α-progerin, counterstained with DAPI. Values were analyzed with a one-way ANOVA with Tukey's multiple comparison test and are presented as mean ± SD: not significant (ns) $p > 0.05$, * $p < 0.05$, ** $p < 0.01$, *** $p < 0.001$ ($n \geq 3$). Passage number <5% SNS was ≤P18 and >30% SNS was ≥P21.

An average of 65% of dysmorphic HGPS nuclei had elevated progerin levels in both young and old cultures (Figure 3.17). The difference between young and old was not significant and both FN127 and FN003 behaved similarly. This demonstrated that progerin accumulation had a greater impact on nuclear morphology than mechanisms inherent to cellular aging, f. ex. downregulation of LB1. However, 35% of abnormal nuclei did not have elevated progerin, indicating that HGPS cells might also age in a manner independent of progerin or that not all nuclear abnormalities are caused by progerin or aging (Figure 3.17). Therefore, I took a closer look at the relationship of progerin content and nuclear shape in relation to replicative senescence in HGPS fibroblasts. I performed immunofluorescence of young and old HGPS cells, combining progerin with the following senescence markers: SA β-Gal, LB1, p16 and p21 (Figure 3.18). For statistical evaluation, I

counted how many dysmorphic nuclei were positive for one of the above SNS markers and then how many of these had high levels of progerin as well.

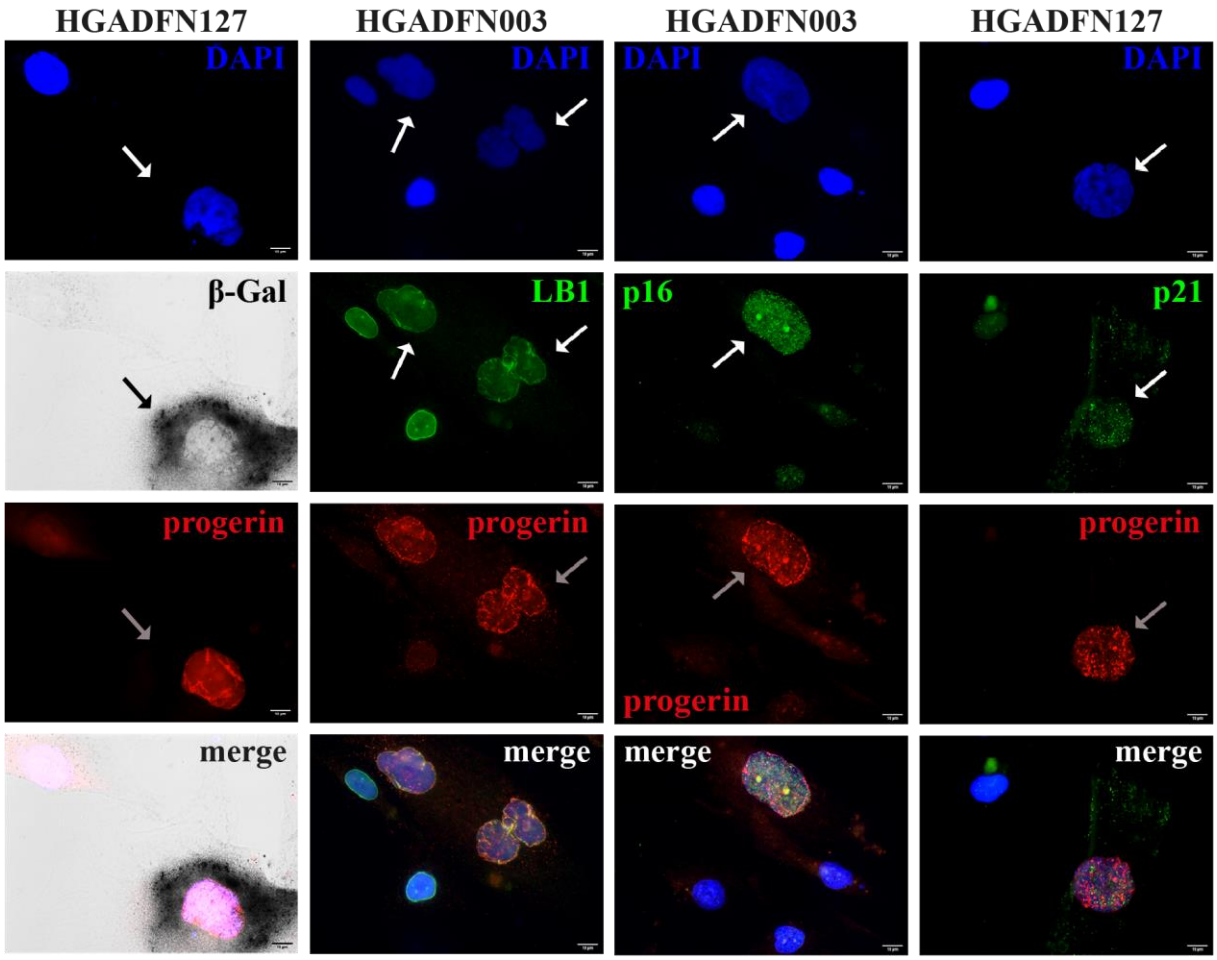

Figure 3.18 HGPS fibroblasts with elevated progerin levels were positive for one of four different indicators of replicative senescence

Representative images of HGADFN003 or HGADFN127 labeled with α-progerin (red) and SA β-Gal (grey) or α-LB1/p16/p21 (green), counterstained with DAPI (blue). Arrows indicate dysmorphic HGPS nuclei with elevated progerin and positive for SA β-Gal, low LB1 or increased p16/p21. Scalebar 10 µm.

In general, the number of senescent dysmorphic nuclei rose with SNS (Figure 3.19 a, b), albeit to a different degree, depending on the senescence marker used.

All percentages in the following paragraph are given as the calculated average ($\bar{x}$) of the results for FN127 and FN003 (see Table 5.4).

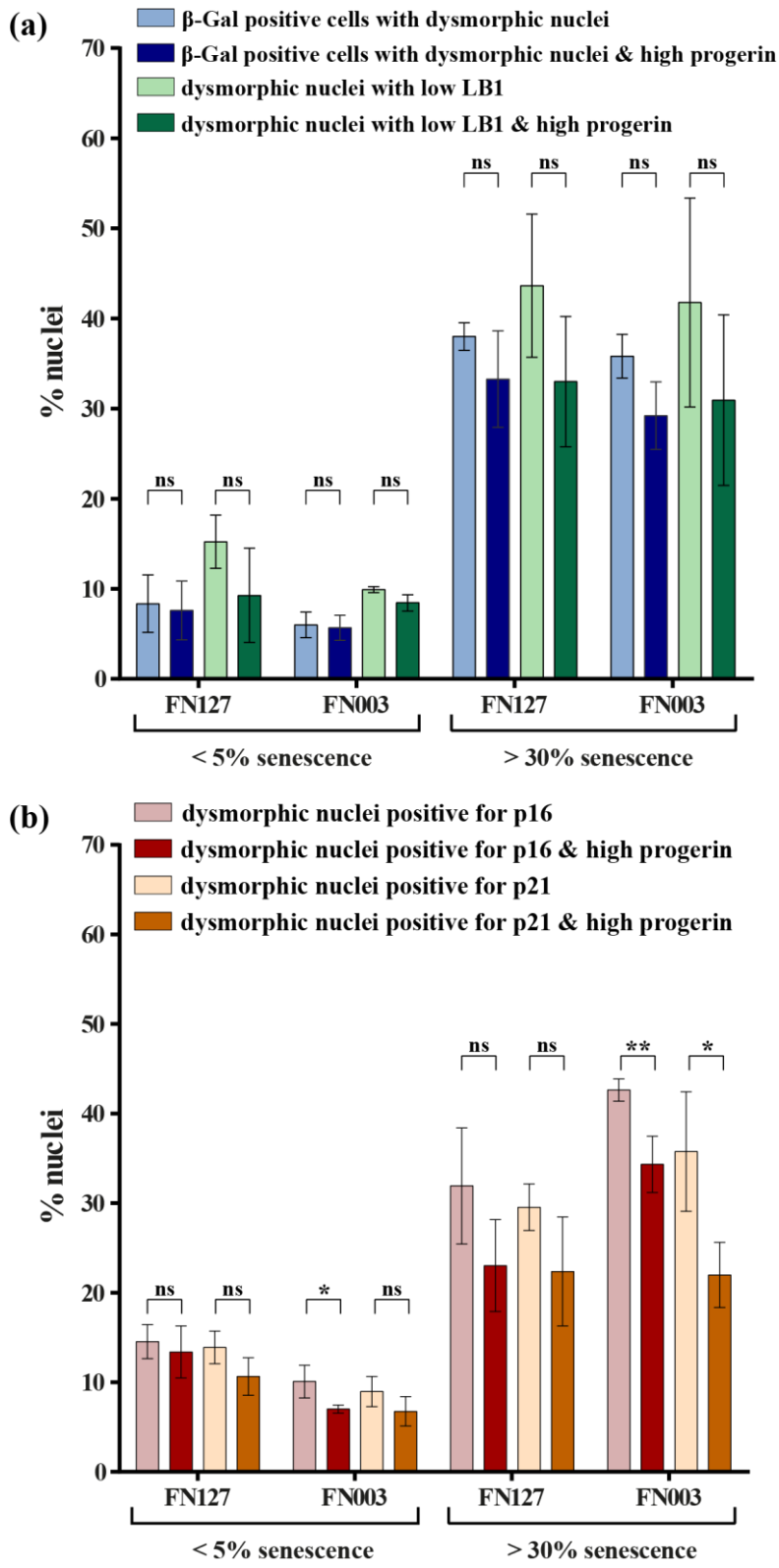

Figure 3.19 HGPS fibroblasts with elevated progerin were senescent independent of cellular age

Number of HGPS dysmorphic nuclei positive for one of four senescence markers and elevated progerin <5% and >30%SNS was determined by counting dysmorphic HGPS nuclei labelled with α-progerin and SA β-Gal/LB1/p16/p21, counterstained with DAPI. The number of dysmorphic nuclei with strong progerin signal (a) positive for SA β-Gal, low LB1 or (b) elevated p16/p21; increased during replicative senescence. Values were analyzed with an unpaired *t*-test and are presented as mean ± SD: not significant (ns) $p > 0.05$, * $p < 0.05$, ** $p < 0.01$, *** $p < 0.001$ (n≥3). Passage number <5% SNS was ≤P18 & >30% SNS was ≥P21.

The percentage of SA β-Gal positive abnormal nuclei in young cells ($\bar{x}$ =7,2%) was similar to the number of nuclei also harboring a strong progerin signal (6,6%) (Figure 3.19 a). In old cells a five-fold increase to 36,9% and 31,2% could be observed, again with only a small difference between only SA β-Gal and those with elevated progerin as well. The difference of SA β-Gal positive abnormal nuclei without or with elevated progerin was not significant in young or old HGPS cells (Figure 3.19 a).

For low LB1 the numbers were slightly higher <5% SNS, compared to SA β-Gal (Figure 3.19 a). In young cells, an average of 12,6% of HGPS nuclei were dysmorphic with reduced LB1 levels, and 8,7% also had increased progerin levels. In old cells dysmorphic nuclei with low LB1 rose 3-fold to 42,7% and 31,9%, which was similar to the results for SA β-Gal (Figure 3.19 a). Again, the difference between dysmorphic nuclei with low LB1 and high progerin was not significant independent of SNS (Figure 3.19 a).

p16 behaved similarly to LB1, in young HGPS cells an average of 12,31% nuclei were dysmorphic and had increased p16 signal, 10,2% also had a strong progerin signal (Figure 3.19 b). As with low LB1, the number of senescent dysmorphic nuclei rose 3-fold to 37,3% and 28,7% (Figure 3.19 a, b). Unlike with LB1 and SA β-Gal, I could detect a significant difference between p16 positive dysmorphic nuclei without or with elevated progerin in HGADFN003 cells. However, the difference was low and only detectable in one out of two HGPS fibroblast cell lines.

p21 had similar results to LB1 and p16 in young cells, 11,4% of nuclei were dysmorphic and had elevated p21 levels, 8,7% also had increased progerin signal (Figure 3.19 a, b). However, the increase from young to old was only ~2,8-fold, from 11,4% to 32,7% and from 8,7% to 22,2% (Figure 3.19 b). Considerably fewer dysmorphic nuclei with high progerin content had elevated p21 levels (22,2%) in old HGPS cells, compared to SA β-Gal, LB1 and p16 (28,7% – 31,9%) (Figure 3.19 a, b). This was likely due to p21 being an early senescence marker and therefore it would be less active in older cells. In addition, significantly less old dysmorphic FN003 positive for p21 had elevated progerin levels, which was not the case for FN127.

When analyzing all four senescence markers, SA β-Gal detected fewer abnormal nuclei in young cells than LB1, p16 and p21 (Figure 3.19 a, b). However, in old HGPS cells no difference

could be seen in nuclei with increased lysosomal content, elevated p16 or low LB1 (Figure 3.19 a, b). Only p21 indicated fewer dysmorphic nuclei as senescent in old cells, likely due to it being an early marker of replicative senescence that does not persist (Figure 3.19 a, b). This discrepancy is likely due the different dynamics each of these senescent markers have during replicative senescence.

To conclude, most dysmorphic HGPS nuclei positive for the four senescence markers had elevated levels of progerin, while only a few abnormal senescent nuclei were negative for progerin. These results indicated that progerin potentially induced premature senescence by accumulating in individual aging cells.

3.2.4 NPC clustering in replicative senescence

During the course of my mitotic experiments, I also noticed that in later passages cells clustering of NPCs increased, and I detected irregular NPC distribution in older control cells as well. Since I could not detect any defects in post-mitotic NPC assembly, we postulated that the disturbance of the NE caused by progerin in interphase cells might be the cause for clustered pores. In addition, it is well known that replicative senescence affects the composition of the nuclear lamina, as LB1 is downregulated (Freund, Laberge et al. 2012). This could explain my aforementioned observation and I analyzed NPC clustering in the context of replicative senescence accordingly.

First, I imaged z-stacks of nuclei stained with POM121/NUP107 and lamin A/C/progerin, to visualize pores trapped in NE invaginations (Figure 3.20 a, b). In normal ovoid control and ovoid HGPS nuclei with low progerin signal, NPCs were distributed evenly across the nuclear envelope, with no abnormalities visible (Figure 3.20 a). This changed when looking at dysmorphic nuclei, here we observed NUP107 trapped in nuclear invaginations in both HGPS and control (Figure 3.20 a, b white arrows). In HGPS nuclei, accumulated or clustered NUP107 overlapped with aggregated progerin, which was even more apparent in the zoomed in image (Figure 3.20 b). We observed the same phenomena in control with NUP107 and LA/C, with multiple NPCs trapped in the folds of the abnormal nucleus and increased LA/C signal in the same area (Figure 3.20 a, white arrows).

To corroborate our observations further, the transmembrane nucleoporin POM121 was imaged in combination with LA/C, with the same results as for NUP107 (Figure 3.21 a, b). POM121 collected in the folds of the deformed NE and overlapped with increased LA/C signal in dysmorphic control and HGPS nuclei (Figure 3.21 a, b white arrows). In normal ovoid nuclei POM121 was evenly dispersed across the NE, as was LA/C which formed an even ring (Figure 3.21 a, b). Hence, we concluded that the aforementioned clusters were indeed situated in the deformed NE and were not nuclear foci, since POM121 resides in the membrane of the nucleus.

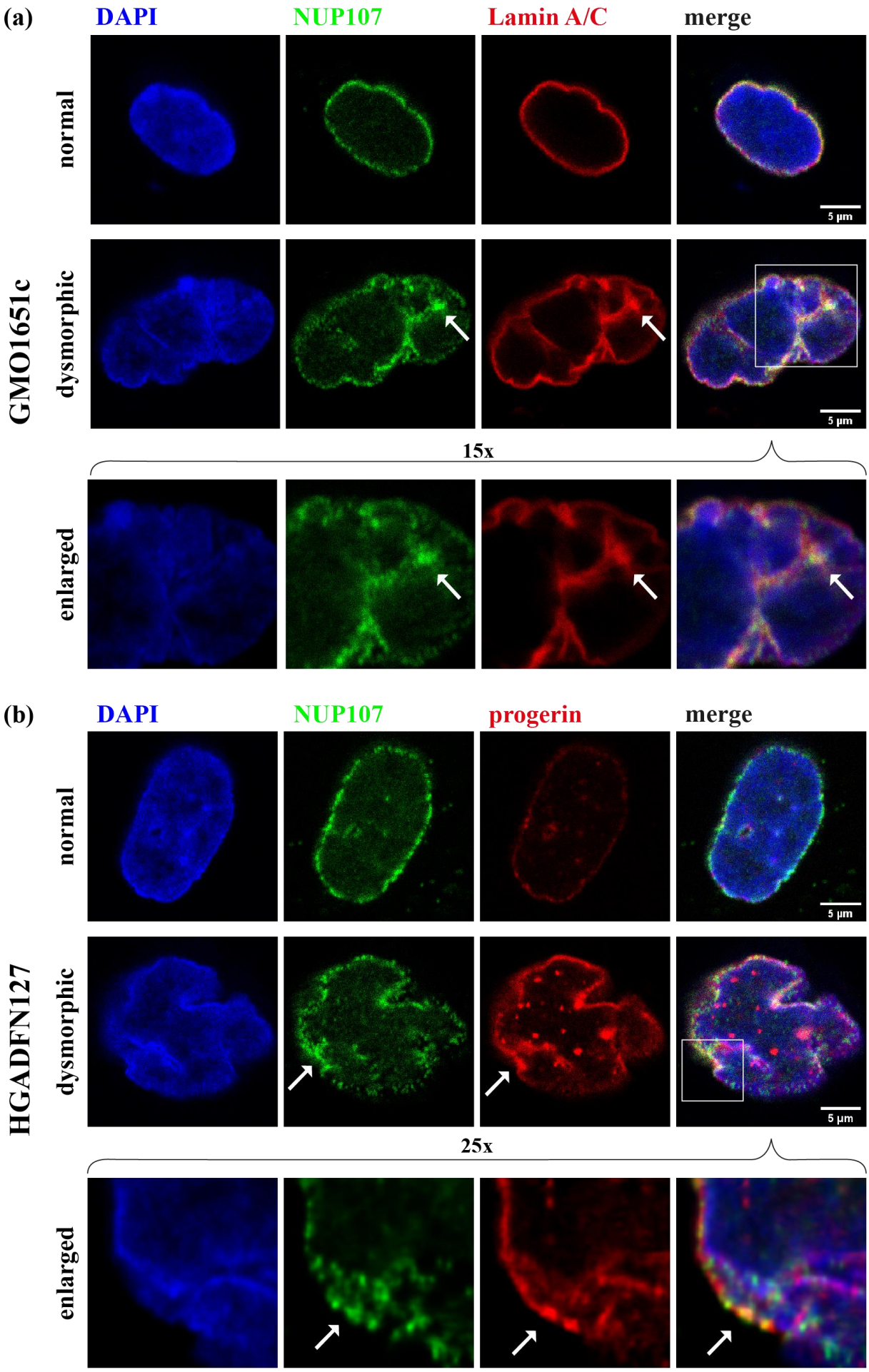
(a)
DAPI
NUP107
Lamin A/C
merge
normal
GM01651c
dysmorphic
5 µm
15x
enlarged
(b)
DAPI
NUP107
progerin
merge
normal
HGADFN127
dysmorphic
5 µm
25x
enlarged

Figure 3.20 NUP107 clustered in nuclear envelope folds of dysmorphic HGPS and control nuclei, co-localizing with trapped LA/C and progerin aggregates

Representative images of (a) GMO1651c and (b) HGADFN127 labeled with NUP107 (green) and LA/C or progerin (red), counterstained with DAPI (blue). White outlines indicate zoomed in regions and arrows indicate clustered NUP107 and aggregated LA/C or progerin. Images are taken from z-stack and provided as X-Z view. Zoom factors of each image are given as e.g., 25x above curly brackets.

To be able to analyze NPC clustering in relation to replicative senescence, I needed to elucidate which senescence marker would work best with my NUP antibodies. Therefore, I tested α-NUP107 with α-LB1 or α-POM121 with α-p16 or α-p21 antibodies in my control fibroblasts (Figure 3.22). Technical triplicates were performed in GMO1651c/GMO1652c with low or high SNS, determined by SA β-Gal. I counted how many dysmorphic nuclei had clustered NPCs and if those nuclei also had elevated p16/p21 or reduced LB1 (Figure 3.22 white arrows, Figure 3.23). All percentages in the following paragraph are given as the calculated average ($\bar{x}$) of the results for GMO1651c and GMO1651c.

An average of 29% of dysmorphic control nuclei displayed clustered POM121 (Figure 3.22 white arrows, Figure 3.23). With rising cellular age, the number of dysmorphic nuclei with abnormal POM121 distribution increased to about 63% in both control cell lines (Figure 3.23). In most old and young dysmorphic control nuclei with clustered NPCs, I also detected elevated p16/p21 or reduced LB1 (Figure 3.22 white arrows, Figure 3.23). However not all three senescence markers provided stable results (Figure 3.23), both LB1 and p21 proved to be unreliable in old cells (Figure 3.23). LB1 had a high standard deviation (SD), and it was not always reduced in highly dysmorphic nuclei (Figure 3.23), making LB1 an inaccurate judge of senescence in this instance. p21 presented another problem, it scored fewer nuclei than p16 and LB1 in old cultures (Figure 3.23). p16 had a lower standard deviation in old cells, was not elevated in normal nuclei, worked well with our homemade progerin antibody in previous experiments and the image quality was superior to p21 (Figure 3.22, Figure 3.23).

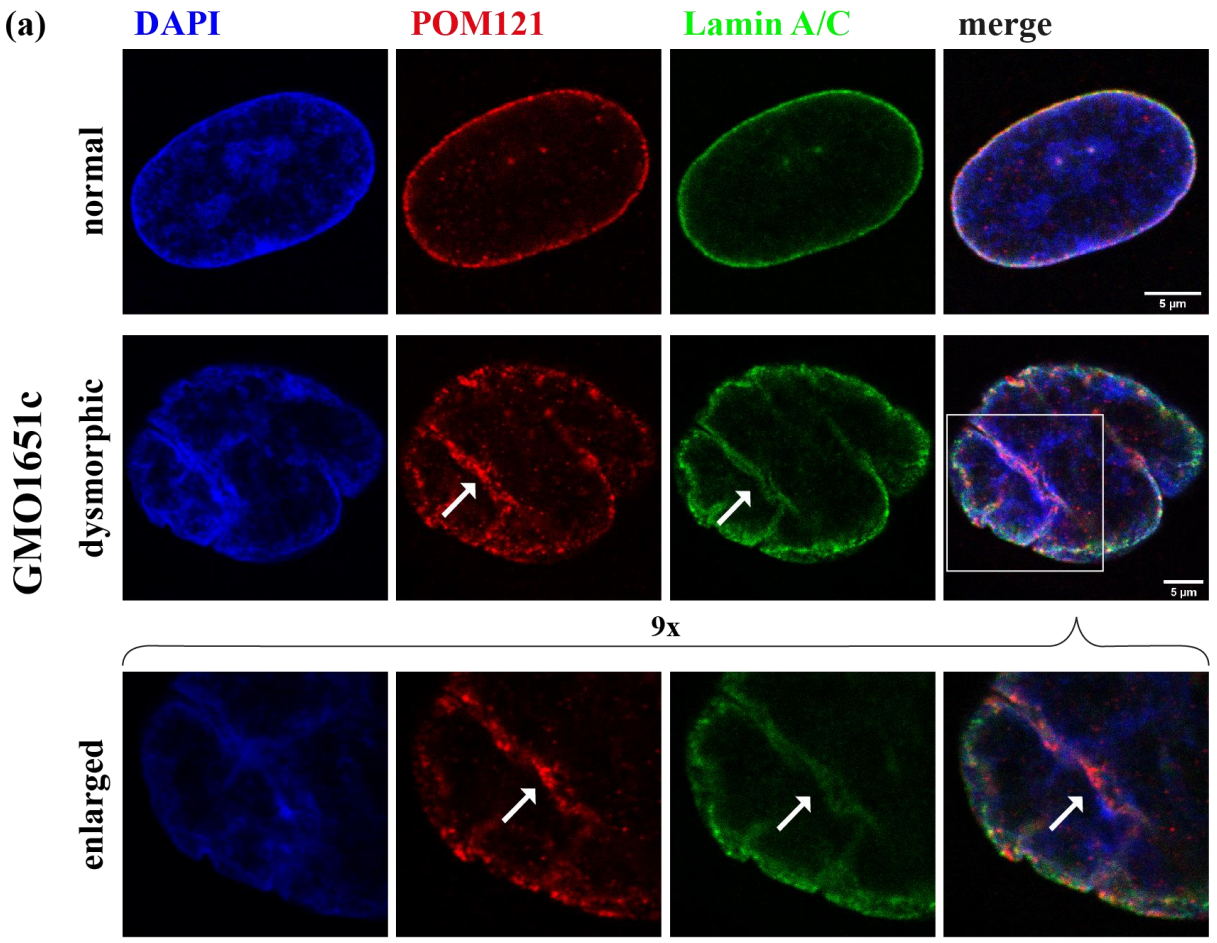
(a)
DAPI
POM121
Lamin A/C
merge
normal
GMO1651c
dysmorphic
5 µm
9x
enlarged

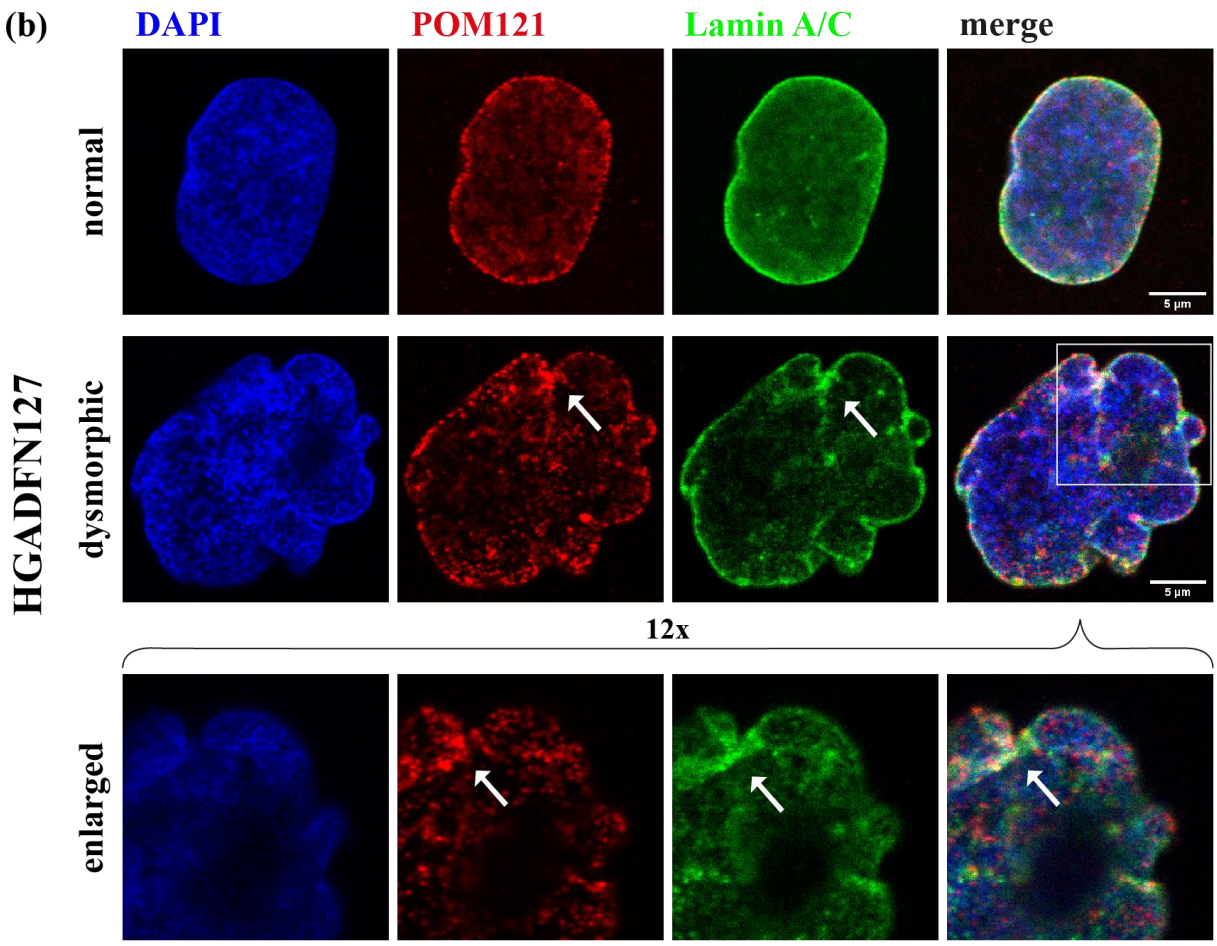
(b)
DAPI
POM121
Lamin A/C
merge
normal
HGADFN127
dysmorphic
5 µm
12x
enlarged

Figure 3.21 POM121 clustered in nuclear envelope folds of dysmorphic HGPS and control nuclei, co-localizing with trapped LA/C and progerin aggregates

Representative images of (a) GMO1651c and (b) HGADFN127 labeled with POM121 (red) and LA/C (green), counterstained with DAPI (blue). White outlines indicate zoomed in regions and arrows indicate clustered POM121 and aggregated LA/C or progerin. Images are taken from z-stack and provided as X-Z view. Zoom factors of each image are given as e.g., 9x above curly brackets.

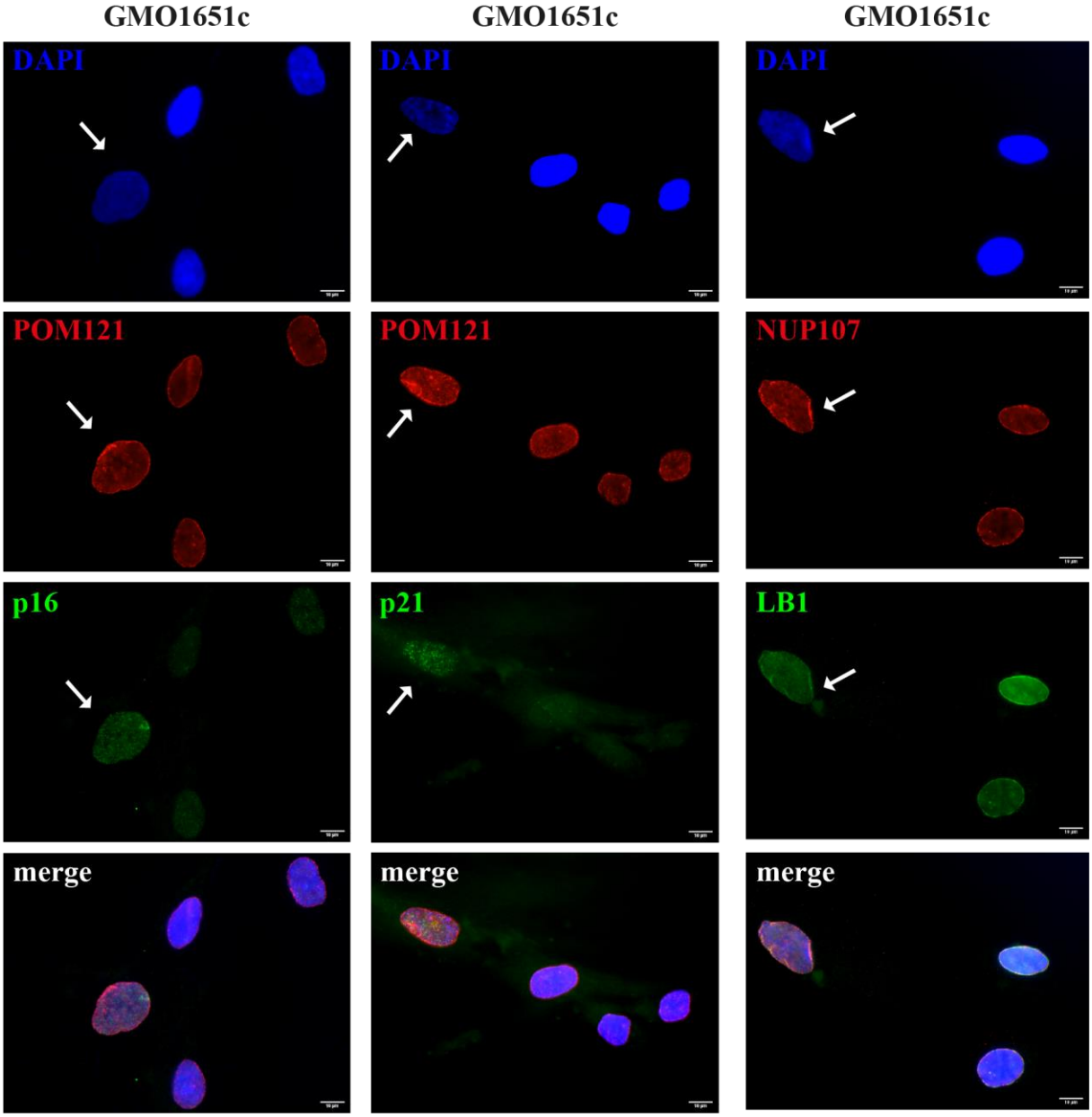

Figure 3.22 NPC clustering in dysmorphic control fibroblast nuclei in relation to the senescence markers p16, p21 and LB1

Representative images of GMO1651c labeled with α-NUP107/POM121 (red) and α-p16/p21/LB1 (green), counterstained with DAPI. White arrows indicate nuclei with clustered NPCs and positive for one of three senescence markers, namely elevated p16/p21 or reduced LB1. n≥3, scalebar 10 µm.

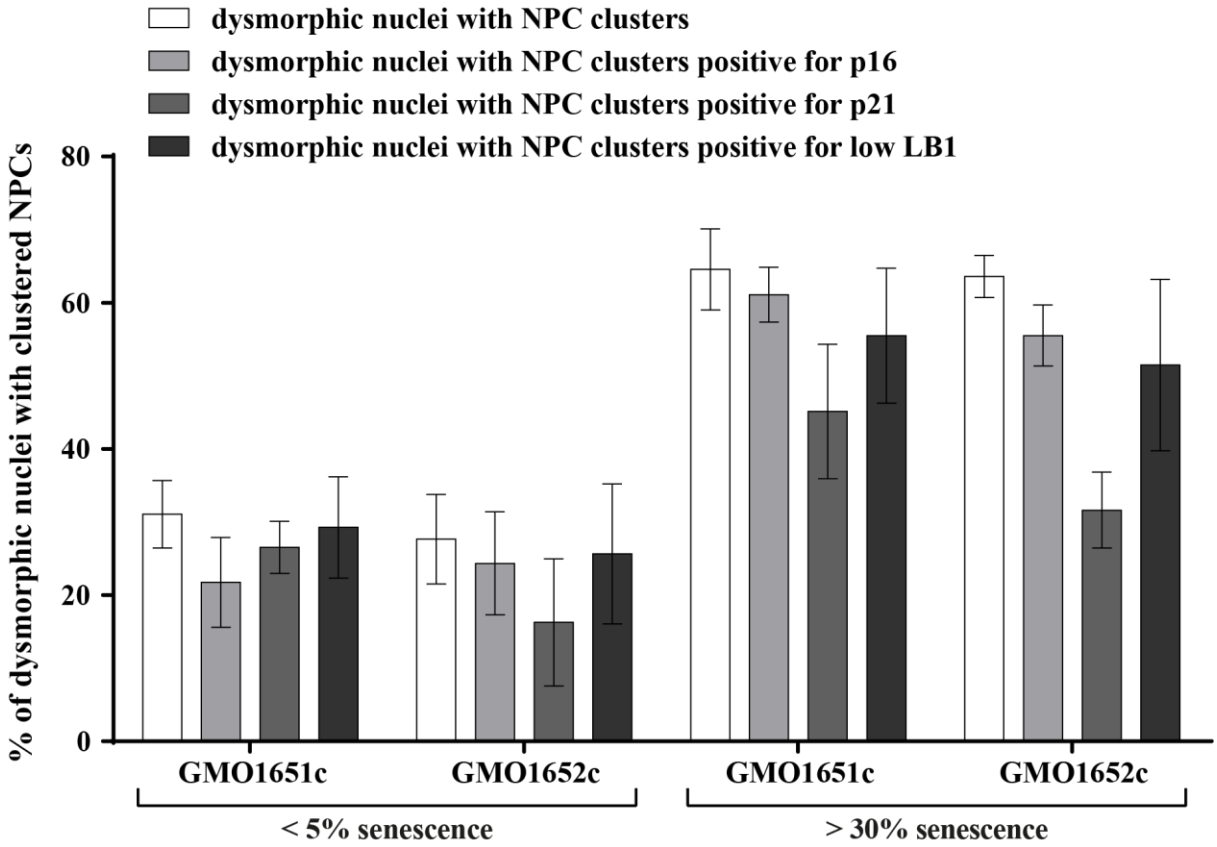

Figure 3.23 Analysis of replicative senescence and abnormal NPC distribution in control fibroblasts.

The number of dysmorphic nuclei with clustered NPCs in control <5% and >30% SNS was determined by counting dysmorphic nuclei positive for clustered POM121/NUP107 and positive for p16/p21/LB1, counterstained with DAPI. NUP107 was combined with LB1 and POM121 with p16 or p21. Passage number <5% SNS was ≤P21 and ≥P25 for >30% SNS. Values are presented as mean ± SD (n≥3).

Consequently, I decided to continue with the analysis of NPC distribution in aging control and HGPS fibroblasts using p16 as a senescence indicator in conjunction with abnormal nuclear morphology.

α-p16 was used in combination with α-POM121, a transmembrane NUP (Figure 3.24) to evaluate NPC clusters in control and HGPS fibroblasts. This ensured that I would not mistake clusters for nuclear foci, since POM121 is inserted into the membrane (Figure 1.4) (Soderqvist and Hallberg 1994). As clustering of NPCs occurred mostly in dysmorphic interphase nuclei with blebs or folds, I evaluated the statistics of this phenomenon and determined, if these dysmorphic cells were senescent. In the subsequent statistical evaluation of NPC clustering in re-

lation to replicative senescence, I used a standard wide-field fluorescence microscope to visually inspect and evaluate nuclei for alterations in morphology and NPC distribution (Figure 3.24). First, I compared the incidence of NPC clustering in control and HGPS cells with rising SNS (Figure 3.25). Here I observed the same trend as in my analysis of nuclear morphology (Figure 3.14), namely that I could only detect a significant difference in the incidence of clustered NPCs in young dysmorphic control and HGPS nuclei, but not in old cultures (Figure 3.14, Figure 3.25).

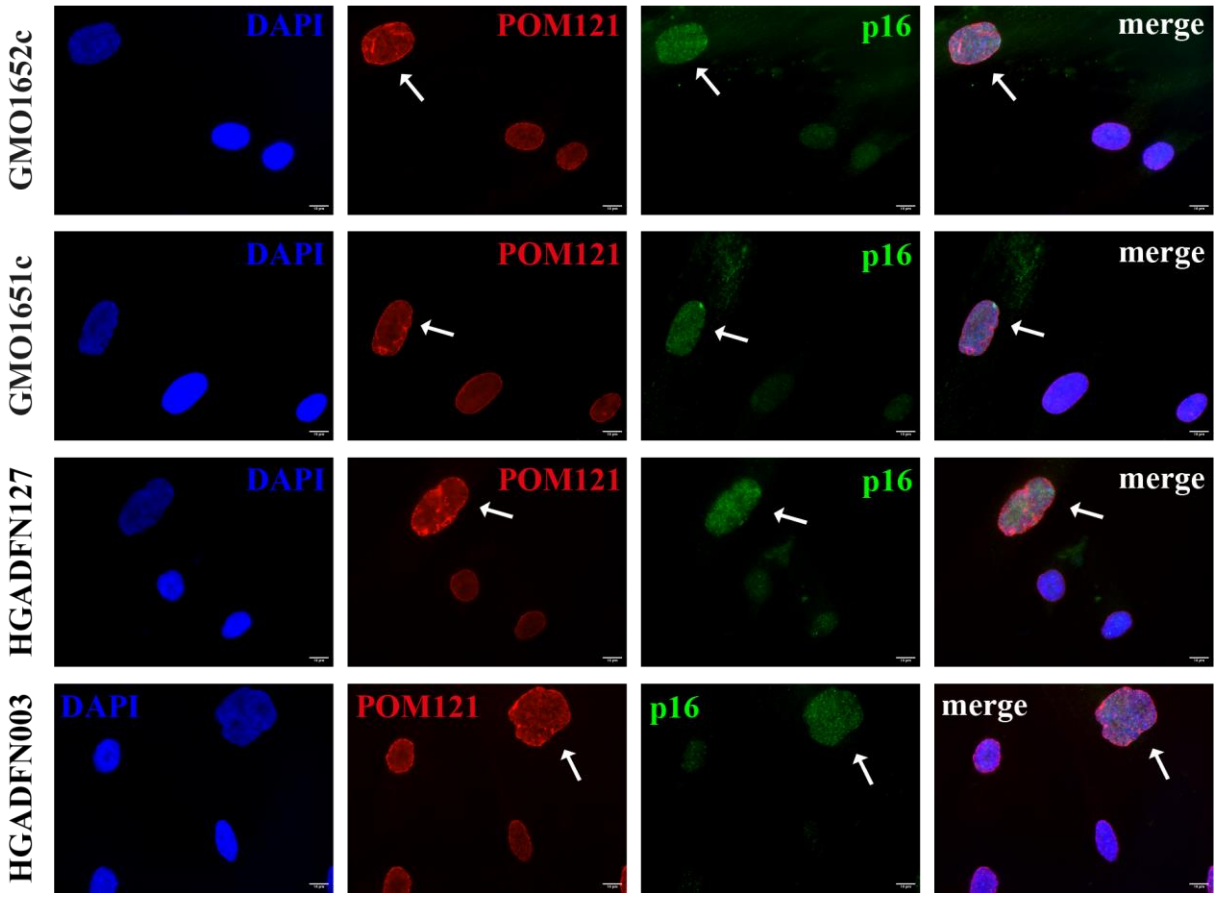

Figure 3.24 POM121 was clustered in dysmorphic control and HGPS nuclei with elevated p16

Representative images of GMO1651c, GMO1652c and HGADFN127, HGADFN003 labeled with α-POM121 (red) and α-p16 (green), counterstained with DAPI. White arrows indicate nuclei with clustered NPCs and positive for elevated p16. Scalebar 10 µm.

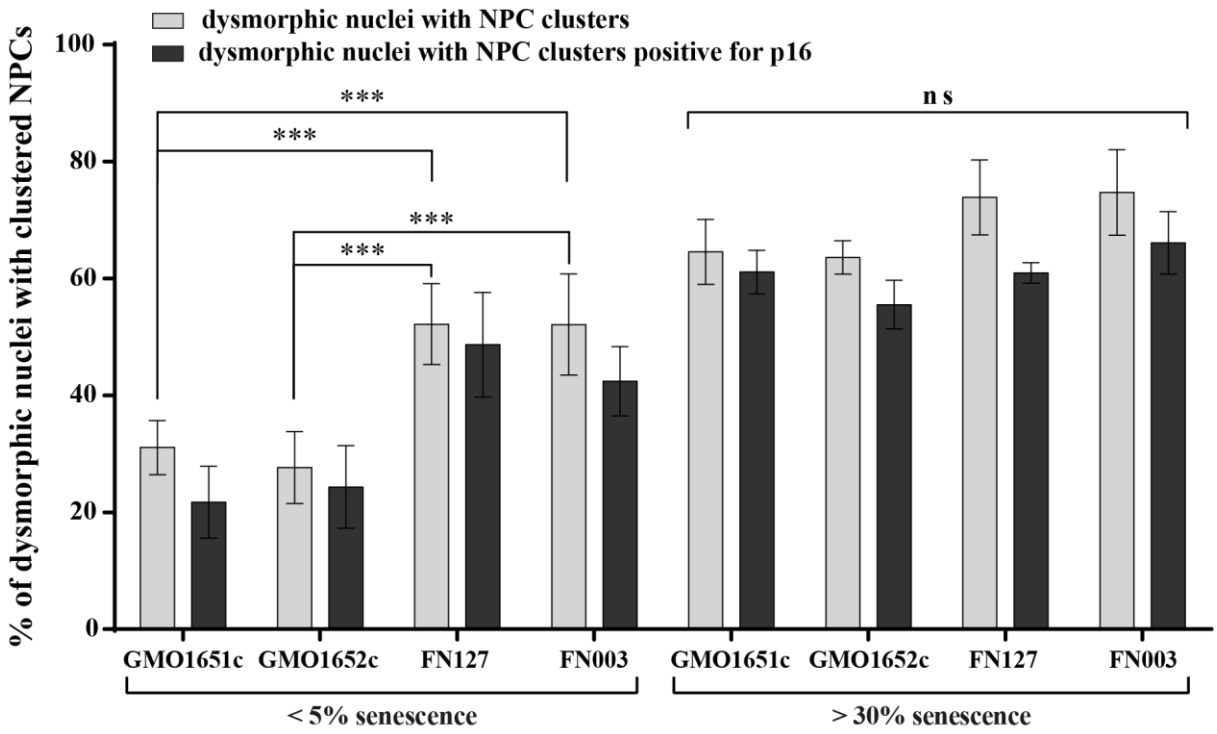

Figure 3.25 POM121 cluster in dysmorphic control and HGPS nuclei increased with replicative senescence

The number of dysmorphic nuclei with clustered NPCs in control/HGPS cultures <5% and >30% SNS was determined by counting dysmorphic nuclei positive for clustered POM121 and elevated p16 signal, counter-stained with DAPI. The difference within each cell line between young and old cultures was significant. Passage number <5% SNS was ≤P18 for HGPS and ≤P21 for control. Passage number >30% SNS was ≥P21 for HGPS and ≥P25 for control. Values are presented as mean ± SD (n≥3), ns (not significant) $p>0.05$, *** $p<0.001$ and were analyzed using a two-way ANOVA with Tukey's multiple comparison test.

In young control cultures approximately 29% of dysmorphic nuclei had clustered NPCs, in HGPS an average of 52% dysmorphic nuclei had unevenly distributed pores (Figure 3.25). The nearly 2-fold difference in cells with a SNS lower than 5% indicated that progerin likely plays a major role in clustering of NPCs, especially in young HGPS fibroblasts. In old cultures an average of 69% of dysmorphic control and HGPS nuclei had clustered pores in NE invaginations/folds, with no significant difference between the four fibroblast cell lines I analyzed (Figure 3.25). In addition, in both young and old cells, most dysmorphic nuclei with NPC clustering exhibited an elevated p16 signal, compared to healthy nuclei (Figure 3.26 a, b white arrows), potentially linking unevenly distributed pores to replicative senescence. The difference within

each cell line between dysmorphic nuclei with clusters and those who also had an elevated p16 signal was not significant (Figure 3.25).

Next, I ascertained progerin's influence on NPC clustering in young and old HGPS cells, to elucidate if progerin was the main cause for increased clustering in young HGPS. I performed a co-stain of progerin and the cyto-/nucleoplasmic ring nucleoporin NUP107 in HGPS fibroblasts with low (<5%) or high (>30%) SNS (Figure 3.26). I could not perform a co-stain of progerin and POM121, since both available antibodies at the time were from the same species. However, since NUP107 is part of the scaffolding of the NPC (Figure 1.4) it is unlikely to reside in the nucleoplasm.

I observed that most dysmorphic HGPS nuclei with clustered NUP107 also had a strong progerin signal (Figure 3.26 white arrows, b), but not all (Figure 3.26 green arrow). Despite not all dysmorphic nuclei with clustered NPCs displaying an elevated progerin signal, the difference was not significant. The incidence of NPC clustering rose with increased SNS, from ~ 52% in young to ~ 72% in old HGPS cells (Figure 3.27 a). In addition, I found that on average 87%

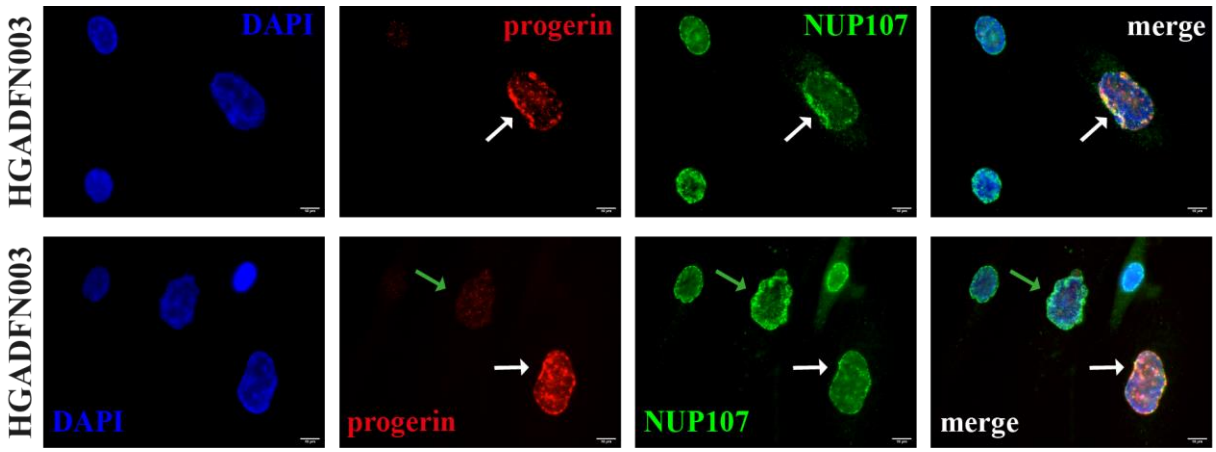

Figure 3.26 NUP107 clustered in most dysmorphic HGPS nuclei with elevated progerin levels

Representative images of HGADFN003 labeled with α-progerin (red) and α-NUP107 (green), counterstained with DAPI. White arrows indicate nuclei with clustered NPCs and positive for elevated progerin. Green arrows indicate nuclei with clustered NPCs and low progerin levels. Scalebar 10 µm.

of dysmorphic nuclei with clustered NUP107 displayed a strong progerin signal as well, independent of SNS (Figure 3.27 b). This proved that a high percentage of NPC clustering was

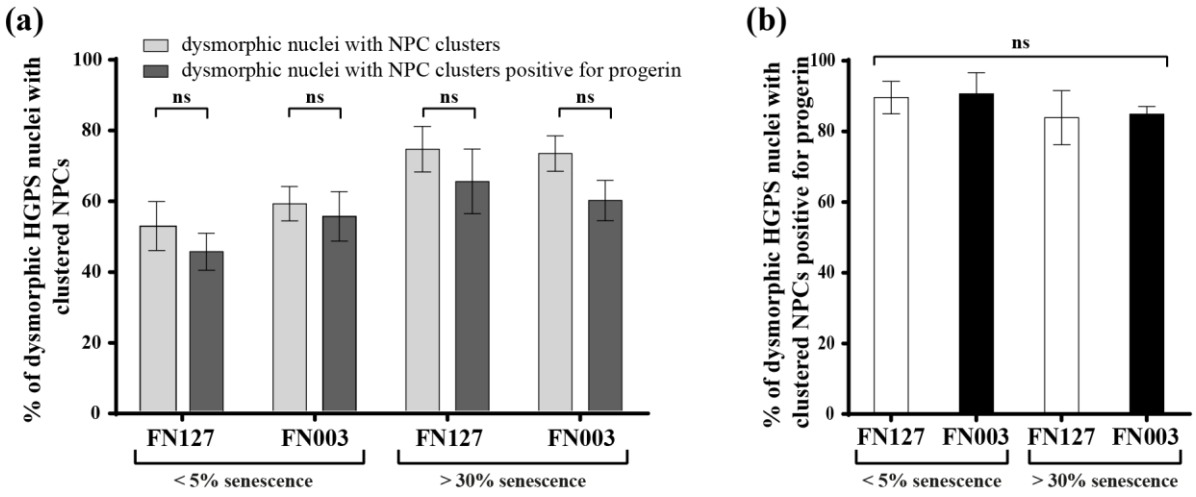

Figure 3.27 NPC clustering increased with rising replicative senescence in dysmorphic HGPS nuclei and correlated with progerin levels.

(a)The number of dysmorphic nuclei with clustered NPCs in HGPS cultures <5% and >30% SNS was determined by counting dysmorphic nuclei positive for clustered NUP107 and elevated progerin signal, counterstained with DAPI. (b) An average of 87% of dysmorphic HGPS nuclei with clustered NPCs had an elevated progerin signal, independent of replicative senescence. Passage number <5% SNS was ≤P18and ≥P21 for >30% SNS. Values are presented as mean ± SD (n≥3), ns (not significant) p>0.05 and were analyzed using an (a) unpaired Student's t-test or (b) one-way ANOVA with Sidak's multiple comparison test.

likely dependent on increased progerin content in individual nuclei, since no disturbed NPC distribution could be observed in normal ovoid nuclei with low/undetectable progerin (Figure 3.20 b, Figure 3.21 b). However, not all dysmorphic HGPS nuclei with clustered NPCs had a strong progerin signal, therefore other processes of replicative senescence might play a role in NPC clustering in HGPS cells as well.

In conclusion, clustering of pores increased simultaneously with rising replicative senescence in both control and HGPS cells. Only in young dysmorphic HGPS cells the incidence of NPC clustering was significantly higher than in dysmorphic control nuclei. In old control and HGPS cells this was no longer the case.

Since progerin was elevated in most dysmorphic HGPS nuclei with abnormal NPC distribution, progerin's presence in young cells was likely the cause for the higher incidence of

POM121 clustering in HGPS compared to control. The similar number of abnormal NPC distribution observed in older cultures was probably due to nuclear lamina defects precipitated by replicative senescence in control, with progerin playing a role in HGPS as well.

4. Discussion

Nuclear pore complex clustering is frequently listed as a typical cellular symptom in HGPS nuclei, however, up until now, nobody has found the exact cause (Goldman, Shumaker et al. 2004). NPCs associate with the nuclear lamina and therefore it is not surprising that NPC distribution is affected in HGPS (Goldberg and Allen 1996, Walther, Fornerod et al. 2001, Walther, Askjaer et al. 2003, Goldman, Shumaker et al. 2004, Al-Haboubi, Shumaker et al. 2011). In this thesis, I have explored possible mechanisms responsible for uneven NPC distribution e.g., a defect in post-mitotic NPC reassembly and changes in the NE due to progerin or replicative senescence. What I found was that NPC clustering was not just a symptom in HGPS fibroblasts, but also in normal cells entering replicative senescence.

First, I observed post-mitotic NPC reassembly to elucidate if progerin affected its progression. Since I found that progerin did not interfere with post-mitotic reassembly, I took a closer look at NPC clustering in aging cells. I discovered that with increasing replicative senescence NPC clustering increased and not just in HGPS cells, but also in control. This could be explained by e.g., deregulation of NE components such as LB1 and SUN1, the dysregulation of nuclear import/export pathway and increasing progerin content in the case of HGPS cells. In the following section I will analyze my findings in detail and place them in the context of the current knowledge on NPC distribution and replicative senescence.

4.1 NPC assembly in HGPS

4.1.1 Post-mitotic NPC reassembly in HGPS

The initial theory regarding the cause of NPC clustering in HGPS was a disturbance in post-mitotic NPC reassembly. Our group had previously demonstrated that progerin has a deleterious effect on various proteins, such as LA, LB1, SUN1, emerin, CENP-F and Aurora B during open mitosis in HGPS patient fibroblasts (Eisch, Lu et al. 2016). In addition, a slight delay in reintegration of mAb414 labeled nucleoporins was observed. mAb414 binds to FG-repeat nucleo-

porins such as basket nucleoporin NUP153, central FG-repeat NUP62 and the cytoplasmic filament nucleoporins NUP214 and NUP358 (Davis and Blobel 1986, Davis and Blobel 1987) (see Figure 1.4). Most NUPs bound by mAb414 are not fully incorporated into the NPC until early G1, however, seeding of NPCs across the separating chromosomes already begins in early anaphase (Dultz, Zanin et al. 2008). It is therefore unlikely that this slight delay at the very end of post-mitotic NPC reassembly is the cause for NPC clustering and was rather the result of progerin delaying incorporation of NE proteins such as SUN1, LB1 or LA (Eisch, Lu et al. 2016). So, to determine if post-mitotic NPC reassembly is affected by progerin, I looked into the induction of reassembly and likely nucleoporin candidates to be affected by progerin.

Seeding of the NPC is initiated by ELYS binding to the separating chromosomes in early anaphase via its' AT-hook DNA-binding motif (Kimura, Takizawa et al. 2002, Rasala, Orjalo et al. 2006, Franz, Walczak et al. 2007). In addition to seeding NPCs, as part of the NUP107-160 complex, ELYS plays a role in proper kinetochore-microtubule attachment and partially localizes to kinetochores in metaphase (Rasala, Orjalo et al. 2006, Zuccolo, Alves et al. 2007). This localization is moderately dependent on CENP-F, which is delocalized from kinetochores in HGPS cells (Eisch, Lu et al. 2016). The main interaction partner responsible for the localization of NUP107-160 to the kinetochores is the Ndc80 complex (Zuccolo, Alves et al. 2007). Depletion of the NUP107-160 complex from kinetochores causes chromosome-microtubule attachment errors, spindle midzone defects, misaligned and lagging chromosomes, Aurora B mislocalization and cytokinetic failure leading to binucleation (Zuccolo, Alves et al. 2007, Platani, Santarella-Mellwig et al. 2009). In HGPS cells we previously found that not only CENP-F is delocalized from kinetochores, but we observed an increased number of lagging chromosomes, binucleated cells and mislocalized Aurora B (Eisch, Lu et al. 2016). Yet, it remains unclear as to how exactly progerin causes these defects and I theorized that mislocalization of the NUP107-160 complex and thereby ELYS, was the origin of the aforementioned mitotic changes in HGPS. Even so, I could not observe any defect in ELYS localization to aligned metaphase chromosomes in HGPS compared to control cells, consequently, the function of the NUP107-160 complex was likely intact in mitotic HGPS cell. Further research is required to elucidate the mechanism underlying the remaining mitotic errors found in HGPS cells. In addition, ELYS

also localized properly to the dividing chromosomes starting in anaphase and therefore seeding of NPCs was not affected by progerin in HGPS either.

Following binding of ELYS to the chromosomes via its' AT-hook domain, it recruits the remainder of the NUP107-160 complex (Kimura, Takizawa et al. 2002, Franz, Walczak et al. 2007). This step of reassembly was also not perturbed, since NUP107 did not display any aggregates nor was its recruitment delayed in HGPS compared to control. Since the NUP107-160 complex remains mostly associated after NE dissolution in prophase, it is possible that no other members of the cytoplasmic/nucleoplasmic rings are affected by progerin's presence as well (Belgareh, Rabut et al. 2001, Loiodice, Alves et al. 2004).

One protein labeled by mAb414 does play a role in the initial stages of post-mitotic NPC reassembly, the basket nucleoporin NUP153. NUP153 is partially incorporated in anaphase and is a known interaction partner of LA and LB1 (Hase and Cordes 2003, Dultz, Zanin et al. 2008, Al-Haboubi, Shumaker et al. 2011). It was therefore a possible target for progerin interference during mitosis, yet like NUP107 and ELYS, NUP153 was properly recruited beginning in early anaphase and did not aggregate in the cytoplasm of dividing HPGS cells. NUP153 incorporation into the reforming NE was also not delayed in HGPS, however it might play a role in affecting interphase assembly in HGPS, which will be discussed in section 4.1.2.

Lastly, I observed the transmembrane nucleoporin POM121, since it remains associated with the ER membrane like progerin and acts in concert with SUN1 during interphase *de novo* NPC assembly (Daigle, Beaudouin et al. 2001, Talamas and Hetzer 2011). SUN1 aggregated in the ER of mitotic HGPS cells until cytokinesis, overlapping with progerin, even though association between SUN1 and the nuclear lamina is weakened by phosphorylation in mitotic cells (Patel, Bottrill et al. 2014, Eisch, Lu et al. 2016). It is possible that SUN1 preferred association with pre-Lamin A and progerin allows progerin to interfere with its localization, despite SUN1 being phosphorylated (Crisp, Liu et al. 2006, Eisch, Lu et al. 2016). Nevertheless, unlike SUN1, POM121 did not aggregate in mitotic HGPS cells and was properly recruited to the dividing chromosomes in late anaphase. This might be due to SUN1 and POM121 only working in concert during *de novo* interphase NPC assembly (Talamas and Hetzer 2011). What is more, POM121 may be a transmembrane protein, but it is only a known interaction partner of the

lamin B receptor (LBR) and not of nuclear lamins (Funakoshi, Clever et al. 2011). Consequently, progerin did not have a deleterious effect on POM121 localization or integration into the reforming NE in mitotic HGPS cells.

A possible explanation why progerin does not negatively influence post-mitotic NPC reassembly is the timing of NE reassembly. Previous studies of post-mitotic NE reassembly have demonstrated that NUP153 and POM121 localize at anaphase chromosomes before LB1. Following LB1, NUPs bound by mAb414 appear in late anaphase, before LA in telophase (Moir, Yoon et al. 2000, Daigle, Beaudouin et al. 2001). So, both nucleoporins that we theorized were likely to be affected by progerin, appear at the reforming envelope before LA and progerin would have no time to interfere. However, timing cannot be the only reason, since progerin clearly affects SUN1, which localized to the dividing chromosomes in early/late anaphase around the same time as NUP153, POM121 and LB1 (Moir, Yoon et al. 2000, Daigle, Beaudouin et al. 2001, Chi, Haller et al. 2007). It is therefore possible that the order of NE reassembly and lack of known direct LA/progerin association with the different nucleoporins during mitosis prevent progerin from interfering with post-mitotic NPC assembly.

Given that none of the nucleoporins involved in proper post-mitotic NPC assembly were affected by progerin during cellular division, NPC clustering likely happens sometime during interphase, possibly during *de novo* interphase insertion.

4.1.2 De novo interphase NPC assembly in HGPS

During interphase cells double their NPC numbers in preparation for cellular division and to replace dysfunctional pores (Maul, Maul et al. 1972). *De novo* interphase NPC assembly is a rare event, which makes it difficult to observe and therefore not as much is known about the exact mechanism as is for post-mitotic reassembly.

One recent discovery is that *de novo* assembly proceeds via an inside-out extrusion of new pores through the nuclear envelope (Otsuka, Bui et al. 2016). Unlike in healthy cells, accumulated progerin could block access of the required components to the INM and thereby prevent even NPC distribution. In addition, NPCs are stationary after mitosis, so if multiple NPCs were inserted into one area due to limited access, they would probably not be able to redistribute (Daigle, Beaudouin et al. 2001, Rabut, Doye et al. 2004). However, this scenario is unlikely since clustered pores tended to congregate in areas with a strong progerin signal and not areas devoid of progerin. This observation would suggest that progerin might limit mobility of NPCs or factors involved in *de novo* NPC assembly. For example, progerin reduces SUN1 mobility and Lamin A interacts with NUP153, both of which are involved in *de novo* NPC assembly (Al-Haboubi, Shumaker et al. 2011, Chen, Chi et al. 2012).

SUN1 interacts with NPCs and the lamina and is involved in *de novo* interphase NPC assembly, presenting a mechanism by which progerin could indirectly interfere with this process (Liu, Pante et al. 2007, Talamas and Hetzer 2011, Rothballer, Schwartz et al. 2013). SUN1 works in concert with the transmembrane nucleoporin POM121 to reduce the distance of the inner and outer nuclear membrane, thereby facilitating the required NE fusion. Knocking out either SUN1 or POM121 inhibits NPC doubling during G2 phase, alters nuclear shape and causes clustering of NPCs (Funakoshi, Maeshima et al. 2007, Liu, Pante et al. 2007, Talamas and Hetzer 2011). However, neither SUN1 nor POM121 are depleted in HGPS cells, rather SUN1 accumulates in HGPS cells (Chen, Chi et al. 2012, Eisch, Lu et al. 2016, Rohrl, Arnold et al. 2021). So, NPCs might be inserted into areas of high SUN1 concentration, where it is trapped by progerin (Chen, Wang et al. 2014). This idea is supported by the fact that SUN1 associates with ~50% of fully formed NPCs in interphase and 80% of intermediate NPCs (Talamas and Hetzer 2011). Post-mitotic NPCs are also immobile, so SUN1 being trapped by

progerin could prevent interphase redistribution of NPCs (Daigle, Beaudouin et al. 2001). Consequently, progerin would indirectly trap NPCs in areas with high progerin and therefore high SUN1 concentration, since SUN1 preferentially interacts with preLA (Crisp, Liu et al. 2006). Once cells no longer divide, then progerin's trapping effect on SUN1 might become even more pronounced, since NPCs can no longer be redistributed during mitosis (Talamas and Hetzer 2011). My observation that NPC clustering was elevated in senescing HGPS cells, would support this theory, especially since progerin and SUN1 accumulate in aging HGPS cells (Chen, Chi et al. 2012, Eisch, Lu et al. 2016, Liu, Arnold et al. 2019). However, SUN1 itself is also fairly immobile (Lu, Gotzmann et al. 2008), progerin simply limits its mobility even more (Chen, Chi et al. 2012). So reduced SUN1 mobility and accumulation in HGPS likely play a role, but other factors might influence NPC clustering as well.

One other factor of *de novo* NPC assembly might be involved in NPC clustering in HGPS cells, NUP153. NUP153 is part of the nuclear basket (see Figure 1.4) and directly interacts with pre-Lamin A, Lamin A and Lamin B1 (Al-Haboubi, Shumaker et al. 2011). However, unlike SUN1, NUP153 does not preferentially interact with pre-LA (Crisp, Liu et al. 2006, Al-Haboubi, Shumaker et al. 2011), so it is unlikely to be preferably recruited to areas with high progerin content. Therefore, progerin might affect its function via other mechanisms.

NUP153 needs an intact lamina for incorporation and maintenance in Xenopus cell free egg extract (Smythe, Jenkins et al. 2000). During interphase NPC insertion NUP153 interacts with the INM via its N-terminal amphipathic helix and recruits the NUP107-160 complex to the pre-pore (Vollmer, Lorenz et al. 2015). To fulfill its function, NUP153 needs to be imported into the nucleus by transportin and is then released from the transport receptor by binding of RanGTP (Vollmer, Lorenz et al. 2015). However, in HGPS cells the concentration of nuclear Ran is reduced, affecting import of large proteins such as TPR and ATM (Kelley, Datta et al. 2011, Snow, Dar et al. 2013, Dworak, Makosa et al. 2019). Consequently, NUP153 might not be properly released from transportin and might not function correctly during *de novo* interphase assembly.

Another factor affected by the Ran gradient disruption is the basket nucleoporin TPR, which is not properly imported into HGPS nuclei and needs NUP153 to bind to the NPCs basket

(Hase and Cordes 2003, Kelley, Datta et al. 2011, Snow, Dar et al. 2013). TPR is reportedly essential to determine NPC distribution and number (McCloskey, Ibarra et al. 2018, Fiserova, Maninova et al. 2019). Depletion of TPR does not prevent generation of new NPCs, it rather results in an increase of total NPC number and density (McCloskey, Ibarra et al. 2018). TPR negatively regulates NPC assembly by forming a complex with the kinase ERK, which phosphorylates the other basket nucleoporin NUP153. McCloskey *et al.* proposed a model in which phosphorylated NUP153 prevents insertion of new NPCs in direct vicinity of a fully assembled pore. In HGPS cells the reduction of nuclear TPR could reduce phosphorylation of NUP153 in newly assembled NPCs and allow insertion of new pores into regions already dense with pores. Since progerin limits SUN1 mobility and SUN1 is required for *de novo* insertion, these new pores could end up in the fold created by progerin accumulation. What is more, another component of *de novo* interphase assembly, POM121, also fails to localize to the inner nuclear membrane without an intact Ran gradient (Funakoshi, Clever et al. 2011), highlighting how important restoration of the Ran gradient in HGPS, by e.g., treatment with FTIs, is (Kelley, Datta et al. 2011).

In conclusion, progerin might interfere with *de novo* NPC assembly by negatively influencing the various components required for insertion and thereby affect NPC distribution. To prove that progerin affects NPC assembly in cycling HGPS cells, further studies are necessary. Otsuka *et. al.* used super-resolution and 3-dimensional electron tomography to observe the inside-out extrusion intermediates of *de novo* NPC assembly (Otsuka, Bui et al. 2016). Observing HGPS fibroblasts in the same manner might help clarify how and if progerin impacts this process. However, I mainly observed NPC clustering in dysmorphic senescent fibroblasts, both in control and HGPS. Senescent cells are unlikely to create and insert new pores since NPC doubling mainly happens during cell cycle progression from G1 to S-phase and transcription of some NUPs is downregulated in senescent cells (Hayflick and Moorhead 1961, Hayflick 1965, Maul, Maul et al. 1972, Kim, Ryu et al. 2010). In addition, the control fibroblasts I used did not contain detectable amounts of progerin. So, NPC clustering is unlikely to just depend on progerin's presence, there could be further mechanisms inherent to replicative senescence that play a role.

4.2 Replicative senescence, nuclear morphology and NPC clustering in HPGS

4.2.1 Nuclear morphology and replicative senescence

An abnormal nuclear morphology is considered one of the hallmarks of HGPS cells, however, I found that with increasing cellular age, control and HGPS nuclei started to strongly resemble each other. In young cultures, HGPS cells had nearly double the number of dysmorphic nuclei, compared to control. In old cultures both control and HGPS had the same percentage of dysmorphic nuclei, even without progerin stiffening the NE in control nuclei. In both HGPS and control, most of these dysmorphic nuclei were positive for one of the three senescence markers I analyzed: low LB1 or elevated p16/p21.

One explanation for the higher percentage of dysmorphic nuclei in young HGPS cultures is not only progerin but also SUN1. It is known that progerin stiffens the nuclear envelope and therefore negatively affects nuclear shape (Goldman, Shumaker et al. 2004). At the same time, SUN1 accumulates in HGPS cells and reduction ameliorates irregular shape of HGPS nuclei (Chen, Chi et al. 2012). In our experiments, young HGPS fibroblasts' SUN1 levels were increased compared to control (Rohrl, Arnold et al. 2021). So, the combination of progerin and elevated SUN1 was likely the reason for the higher number of dysmorphic nuclei in young HGPS cells compared to control. In old cells, we also observed a slight but insignificant increase of SUN1 in control fibroblasts, which might contribute to rising nuclear abnormalities in aging control fibroblasts (Rohrl, Arnold et al. 2021). Yet, this small rise of SUN1 alone cannot explain the dramatic increase of dysmorphic nuclei from 11% in young to 61% in old control cells.

Another possible contributor to the rise of nuclear abnormalities in aging control and HGPS could be a mechanism inherent to replicative senescence: the downregulation of LB1 (Freund, Laberge et al. 2012). LB1 confers elasticity of the NE and reduction can cause an increase in nuclear blebbing (Lammerding, Fong et al. 2006). So, a reduction of LB1 and a concomitant increase of SUN1 could disrupt the nuclear lamina properties sufficiently to lead to a rise in

nuclear abnormalities. To support this theory, I analyzed LB1 levels as potential immunofluorescence marker for senescent cells and found that most dysmorphic nuclei in both control and HGPS had reduced LB1 levels. It is therefore possible that reduction of LB1 due to senescence plays a prominent role in the increase of nuclear irregularities, especially in aging control cells. What is more, only 65% of dysmorphic HGPS nuclei in young and old cultures had an elevated progerin signal, raising the question what causes these changes in the remaining 35%. Since LB1 was also reduced in most dysmorphic HGPS nuclei, downregulation of LB1 could contribute to dysmorphism of HGPS nuclei as well. However, one has to keep in mind that lower amounts of progerin could already interfere with the nuclear lamina and my immunofluorescent experiments might not have been able to detect this effect.

One problem I faced when we decided to look into the relationship between NPC clustering and replicative senescence, was how to determine if a cell was senescent or not. Therefore, I analyzed three markers of senescence: elevated p16 or p21 and reduced LB1 (Alcorta, Xiong et al. 1996, Freund, Laberge et al. 2012). All three are considered hallmarks of senescent cells, but they all have their pitfalls. p16 and p21 are CDK inhibitors that are involved in the maintenance and initiation of senescence, in addition to their function during the cell cycle (Alcorta, Xiong et al. 1996, Jung, Qian et al. 2010, Witkiewicz, Knudsen et al. 2011). p21 presents with a further problem apart from its role during normal cell cycle progression, its levels are only elevated at the onset of senescence and decline over time. So, judging senescent state of a cell solely based on elevated p21 levels could have distorted my results by considering a cycling cell as senescent or missing senescent cells that no longer have elevated p21 levels. p16 maintains the senescent state, thus it is a later stage senescent marker than p21 (Alcorta, Xiong et al. 1996). Using p16 as a marker of senescence would mean missing cells that are just entering the senescent state, however unlike p21 its signal would not decline over time. Downregulation of LB1 on the mRNA level is dependent on stimulation of the p53 or pRB pathway (Freund, Laberge et al. 2012). Therefore, it is a late marker of senescence since decline on the protein level would take time after initiation of the aforementioned pathways. Consequently, one could miss cells in the earlier stages of senescence that have not reduced LB1 at the protein level yet.

To circumvent some of these issues, I pre-determined senescence of my cultures with a SA β-Gal assay. This allowed me to judge the accurateness of the three markers I was testing for my immunofluorescent experiments. Of note is that in young cultures (< 5% SA β-Gal) I generally detected more dysmorphic senescent nuclei with LB1, p16 and p21 then SA β-Gal positive cells before fixation and labelling. It is possible that these cells had already initiated senescence signaling, but lysosomal content had not increased enough yet to be detected by the SA β-Gal assay. This highlights the complexity of choosing the correct senescence indicator, depending on the mechanism or timepoint one is interested in observing.

An additional measure to prevent misidentifying senescent cells I took was that I only counted dysmorphic nuclei with elevated p16/p21 or reduced LB1. From analyzing my cultures, I observed that nuclear irregularities rose with increasing replicative senescence. Therefore, using both nuclear irregularities and a senescence marker could make it more difficult to misjudge a cycling cell for a senescent one. A high percentage of abnormal nuclei had elevated p16/p21 or low LB1 levels, in control and HGPS cells independent of their age. However, p21 labeled fewer dysmorphic nuclei as senescent in old cultures than p16 or LB1, likely due to p21 being an early senescence marker (Alcorta, Xiong et al. 1996). And not all abnormal nuclei I counted were positive for one of three senescence markers. This could mean that the cell was not senescent, but rather apoptotic or at a stage of senescence not labeled by the applied marker.

To conclude, using p16/p21 or LB1 and nuclear abnormalities in combination could be a more faithful marker to determine cellular senescence in immunofluorescent experiments than just observing p16/p21 or LB1. What is more, pre-determination of senescence with an SA β-Gal assay can also add an additional measure to ensure correct interpretation. One just needs to keep in mind at what stage of senescence the marker you are using is involved and what one wants to observe, before determining which of them to apply in combination with nuclear dysmorphism.

4.2.2 Progerin and replicative senescence

Even though I pre-determined senescence index with SA β-Gal, I detected an average of 5% more senescent nuclei labeled by p16, p21 or LB1 in young HGPS cells than in young control. Because SA β-Gal is a later stage senescence marker, it is possible that increased lysosomal content was not detectable yet in HGPS cells already suffering from progerin's deleterious effect on cellular health. To determine if this was the case, I needed to take a closer look at the relationship between progerin content and replicative senescence.

It was shown previously that progerin stiffens the nuclear envelope distorting its shape and HGPS cells senesce prematurely (Goldman, Shumaker et al. 2004, Liu, Arnold et al. 2019). I found that 65% of dysmorphic nuclei had a strong progerin signal in both young and old HGPS fibroblast, highlighting the dramatic effect progerin accumulation has on the morphology of the nucleus independent of cellular age.

To elucidate how progerin content affects replicative senescence in HGPS, I observed how many senescent nuclei also had elevated progerin levels. I labeled HGPS fibroblasts with progerin in combination with one of four senescence markers: SA β-Gal, LB1, p16 or p21. What I found was that the incidence of abnormal senescent HGPS nuclei rose with increasing age and that most of these nuclei also had a bright progerin signal. Depending on the marker applied, the number of dysmorphic senescent nuclei increased 2.8 to 5-fold from young to old HGPS cells.

The strongest increase from young to old was when I analyzed HGPS cells with a SA β-Gal assay (5-fold). SA β-Gal detects the elevated lysosomal content in senescent cells and is a late-stage senescence marker (Dimri, Lee et al. 1995). Consequently, SA β-Gal should detect fewer senescent nuclei in young cultures than an early-stage marker like p21 and more in old cultures, which was the case for both scenarios. In old cultures SA β-Gal detected a similar amount compared to LB1 and p16, which explains the 5-fold increase from young to old cultures.

In old cultures, SA β-Gal, LB1 and p16 labelled a similar amount of senescent dysmorphic nuclei (36,9 – 42,7%), whereas p21 detected only 32,7%. True for all four markers was that only a small number of senescent HGPS nuclei did not have a bright progerin signal both in

young and old cultures. The few senescent HGPS cells that did not have a bright progerin signal could have accumulated damage leading to induction of the irreversible cell cycle arrest independent of progerin.

Altogether my results indicate that a bright progerin signal was linked to replicative senescence in single cells and that progerin was the main cause for nuclear abnormalities in young and old HGPS cells. However, some HGPS cells enter replicative senescence without elevated progerin detectable. The question remains, if these cells senesce, due to f. ex. DNA damage caused by progerin even at low levels (Dreesen 2020) or due to defects independent of progerin inherent to natural aging e.g., telomer shortening, mitochondrial dysfunction, loss of proteostasis and epigenetic alterations (López-Otín, Blasco et al. 2013).

4.2.3 Replicative senescence and NPC clustering

One major discovery I made, was that NPC clustering was also detectable in aging control cells independent of progerin. To determine the cause of clustered pores, I analyzed if and how this phenomenon was related to replicative senescence and progerin levels.

In young cultures the incidence of clustered pores was nearly two-fold lower in control compared to HGPS, however, in old cultures, the number was almost the same. Approximately 29% of young dysmorphic control nuclei exhibited NPC clustering, whereas 52% were present in young dysmorphic HGPS nuclei. In old cells, an average of 69% of dysmorphic nuclei had clustered pores, trapped in invaginations and folds of the NE of all four fibroblast cell lines I analyzed. This raised two questions, why more NPCs clustered in young HGPS cells and what the cause of NPC clustering in aging control cells was.

Given that NPC clustering is considered a characteristic of HGPS cells, I investigated the direct relationship of progerin accumulation and unevenly distributed pores. To this end, I counted how many dysmorphic HGPS nuclei with clustered pores exhibited a strong progerin signal as well. I discovered that an average of 87% of dysmorphic nuclei with clustered NPCs had an elevated progerin signal in both fibroblast cell lines independent of their senescence index. Apparently, progerin content was strongly linked to NPC clustering, offering an explanation as to why more pores cluster in young HGPS cells than in control.

Nevertheless, progerin content cannot clarify why NPCs cluster in aging control cells as well. LB1 is downregulated during senescence (Freund, Laberge et al. 2012) and reduction in differentiated cells can cause asymmetric NPC distribution (Guo, Kim et al. 2014). So, reduced LB1 could allow pores to be trapped in folds and invagination of the NE in senescent cells. LB1 loss results in the nucleus losing its' elastic properties, so down-regulation in senescent cells could stiffen NE similar to progerin. Subsequently, pores would be trapped in the resulting folds of NE. What is curious, is that LB1 was also reduced in senescent HGPS cells, but I did not observe more clustered pores in old HGPS cells. Consequently, loss of LB1 and progerin accumulation at the same time did not have a cumulative effect on NPC clustering.

The nuclear lamina and the NPC interact in a highly complex and dependent manner. A recent in-depth analysis of NPC and nuclear lamina spatial relationship in mouse embryonic

fibroblasts revealed that both LA and LB1 fibers associate with the nucleoplasmic ring of the NPC (Kittisopikul, Shimi et al. 2021). Consequently, changes in the nuclear lamina can have dramatic effects on NPCs. Reduction of LB1 results in asymmetric NPC distribution or an increase in pore-free islands (Guo, Kim et al. 2014, Fiserova, Maninova et al. 2019) and loss or mutation of LA can lead to NPC clustering (Sullivan, Escalante-Alcalde et al. 1999, Goldman, Shumaker et al. 2004, Xie, Chojnowski et al. 2016).

But not just changes in the lamina can have an effect, changes in the NPC can alter the relationship as well. Depletion of the basket nucleoporin TPR causes fragmentation of the LB1 meshwork but does not affect LA/C network arrangement (Fiserova, Maninova et al. 2019). In addition, TPR depleted nuclei have large pore free islands, a phenotype that can be partially rescued by LB1 overexpression (Fiserova, Maninova et al. 2019). In further studies on TPR, McCloskey *et al.* detected an increase in NPC density following TPR down-regulation, yet Funasaka *et al.* observed the exact opposite and Fišerová *et al.* detected a slight decrease in overall NPC density (Funasaka, Tsuka et al. 2012, McCloskey, Ibarra et al. 2018).

TPR is not the only part of the nuclear basket that influences the lamina, NUP153 is involved as well. NUP153 depletion increases density of the lamin fiber meshwork. In cells lacking LA or LB1 loss of NUP153 detaches NPCs from lamin fibers and they cluster within the openings of the lamin network (Kittisopikul, Shimi et al. 2021). So, it is possible that NUP153 needs to interact with both LA and LB1 for proper NPC distribution.

All the above studies have one thing in common, they imply that NPCs and lamina structure are dependent on each other and changing one affects the other, be it mutation or downregulation. My results support this, however now one could add NPC clustering to the list of nuclear changes in cells undergoing replicative senescence. It remains to be seen, if this exclusively happens in senescent fibroblasts or if NPC distribution changes in other cell types as well. It is possible that in other cell types, NPC distribution is not affected by aging or progerin, since the stoichiometry of some NUPs is tissue-specific (Raices and D'Angelo 2012). In addition, it would be interesting to see if NPCs cluster in cells from old donors too, since my fibroblasts were extracted from young donors (see Table 2.1). Another interesting aspect to look into would

be the Ran gradient in aging fibroblasts, to see if this could also be an explanation for clustered pores in control cells and not just in HGPS.

In conclusion, my results describe a possible relationship between NPC clustering and replicative senescence. They also highlight the complexity of the interplay between the nuclear lamina and the NPC, and how this relationship can be affected by dysregulation. The conflicting information concerning e.g., TPRs exact involvement in regulating NPC density highlights that the relationship bears further investigation. However, the question remains, if treatment of HGPS cells shown to reduce progerin levels and improve abnormal nuclear envelope morphology, could ameliorate abnormal NPC distribution in young HGPS cultures and prevent problems arising due to defective nuclear transport.

5. Appendix

Table 2.1 Cell lines used in this study 21

Table 2.2 Primary antibodies used in this study 22

Table 2.3 Secondary antibodies used in this study 23

Table 5.1 Number of mitotic cells imaged in this study 85

Table 5.2 Frequency of mislocalized proteins in mitotic HGPS and control cells 86

Table 5.3 Number of young and old nuclei analyzed in this study 88

Table 5.4 Percentage of HGPS nuclei positive for senescence markers and strong progerin signal 88

Table 5.5 Abbreviations 89

5.1 Supplementary information

5.1.1 Tables

Table 5.1 Number of mitotic cells imaged in this study

SUN1/ mAb414	prophase	metaphase	anaphase	telophase	cytokinesis	number of experiments
1651c	10	20	26	27	45	11
1652c	16	30	19	22	59	11
FN003	9	12	20	25	34	10
FN127	19	26	39	26	36	11

ELYS/ LA	prophase	metaphase	anaphase	telophase	cytokinesis	number of experiments
1651c	8	31	24	14	31	4
1652c	9	17	15	10	24	5
FN003	8	22	15	22	36	6
FN127	7	43	47	23	22	6

POM121/ mAb414	prophase	metaphase	anaphase	telophase	cytokinesis	number of experiments
1651c	9	25	60	35	53	10
1652c	18	16	13	20	31	6

FN003	13	25	42	25	31	10
FN127	12	22	46	29	56	9

NUP153/ NUP107	prophase	metaphase	anaphase	telophase	cytokinesis	number of experiments
1651c	11	39	31	32	33	5
1652c	13	20	15	15	29	6
FN003	16	19	26	21	23	8
FN127	7	16	25	22	48	5

Table 5.2 Frequency of mislocalized proteins in mitotic HGPS and control cells

SUN1 localization in HGPS %	metaphase	anaphase	telophase	cytokinesis
no distribution changes	7,69 ± 7,69	16,54 ± 6,54	21,8 ± 10,23	21,24 ± 6,54
altered distribution	92,3 ± 7,69	83,46 ± 6,54	78,20 ± 10,23	78,76 ± 6,54
SUN1 localization in control %	metaphase	anaphase	telophase	cytokinesis
no distribution changes	79,17 ± 5,83	90,89 ± 1,42	80,39 ± 12,2	83,49 ± 1,26
altered distribution	20,8 ± 5,83	9,11 ± 1,42	19,61 ± 12,21	16,51 ± 1,26
Lamin A localization in HGPS %	metaphase	anaphase	telophase	cytokinesis
no distribution changes	16,28 ± 16,28	33,40 ± 13,40	30,93 ± 8,20	26,14 ± 11,36
altered distribution	83,72 ± 16,28	66,60 ± 13,40	69,07 ± 8,20	73,86 ± 11,36
Lamin A localization in control %	metaphase	anaphase	telophase	cytokinesis
no distribution changes	89,00 ± 5,12	89,27 ± 2,50	87,86 ± 2,14	95,77 ± 4,17
altered distribution	11,00 ± 5,12	10,83 ± 2,50	12,14 ± 2,14	4,17 ± 4,17
POM121 localization in HGPS versus control %	metaphase	anaphase	telophase	cytokinesis
no distribution changes	100,0 ± 0,0	100,0 ± 0,0	100,0 ± 0,0	100,0 ± 0,0
altered distribution	0,0 ± 0,0	0,0 ± 0,0	0,0 ± 0,0	0,0 ± 0,0
ELYS localization in HGPS versus control %	metaphase	anaphase	telophase	cytokinesis
no distribution changes	100,0 ± 0,0	100,0 ± 0,0	100,0 ± 0,0	100,0 ± 0,0
altered distribution	0,0 ± 0,0	0,0 ± 0,0	0,0 ± 0,0	0,0 ± 0,0
NUP107 localization in HGPS versus control %	metaphase	anaphase	telophase	cytokinesis
no distribution changes	100,0 ± 0,0	100,0 ± 0,0	100,0 ± 0,0	100,0 ± 0,0

altered distribution	0,0 ± 0,0	0,0 ± 0,0	0,0 ± 0,0	0,0 ± 0,0

NUP153 localization in HGPS versus control %	metaphase	anaphase	telophase	cytokinesis
no distribution changes	100,0 ± 0,0	100,0 ± 0,0	100,0 ± 0,0	100,0 ± 0,0
altered distribution	0,0 ± 0,0	0,0 ± 0,0	0,0 ± 0,0	0,0 ± 0,0

Table 5.3 Number of young and old nuclei analyzed in this study

Cells labelled with α-LB1/α-16/α-p21	**GMO1651c**	**GMO1652c**	**FN127**	**FN003**
α-LB1 <5% SNS	962	946	931	1329
α-LB1 >30% SNS	922	938	890	874
α-p16 <5% SNS	933	916	2187	2698
α-p16 >30% SNS	913	922	1799	1824
α-p21 <5% SNS	863	1010	964	1272
α-p21 >30% SNS	910	923	887	868

Table 5.4 Percentage of HGPS nuclei positive for senescence markers and strong progerin signal

% dysmorphic nuclei	SA β-Gal positive	SA β-Gal positive & progerin ↑	low LB1	low LB1 & progerin ↑
FN127 <5% SNS	8,35	7,59	15,22	9,27
FN003 <5% SNS	5,99	5,68	9,91	8,45
FN127 >30% SNS	38,00	33,28	43,63	32,99
FN003 >30% SNS	35,82	29,18	41,78	30,93
average <5% SNS	7,17 ± 1,67	6,64 ± 1,35	12,57 ± 3,75	8,86 ± 0,58
average > 30% SNS	36,91 ± 1,54	31,23 ± 2,90	42,71 ± 1,31	31,96 ± 1,46
% dysmorphic nuclei	p16 positive	p16 positive & progerin ↑	p21 positive	p21 positive & progerin ↑
FN127 <5% SNS	14,54	13,37	13,89	10,64
FN003 <5% SNS	10,08	7,01	8,97	6,75
FN127 >30% SNS	31,92	23,02	29,54	22,37
FN003 >30% SNS	42,63	34,33	35,76	21,97
average <5% SNS	12,31 ± 3,15	10,19 ± 4,50	11,43 ± 3,48	8,70 ± 2,75
average > 30% SNS	37,28 ± 7,57	28,68 ± 8,00	32,65 ± 4,40	22,17 ± 0,28

Table 5.5 Abbreviations

Abbreviation	Full context
1651c	GMO1651c
1652c	GMO1652c
AB	antibody
APS	Ammonium persulfate
AT-hook	DNA-binding motif
C	Cytosine
CDK	cyclin dependent kinase inhibitor
DCM-CD	familial dilated cardiomyopathy
DMSO	Dimethyl sulfoxide
EDMD	Emery-Dreifuss muscular dystrophy
ER	endoplasmic reticulum
FG-repeat NUPs	Phenylalanine-Glycine-repeat nucleoporins
FN003	HGADFN003
FN127	HGADFN127
FPLD	familial partial lipodystrophy
FT	Farnesyl transferase
FTI	Farnesyl transferase inhibitor
G	Glycine
HGPS	Hutchinson-Gilford progeria syndrome
ICMT	Isoprenylcysteine carboxyl methyltransferase
IF	intermediate filament
INM	inner nuclear membrane
LA	Lamin A
LAD	Lamina-associated domain
LAP1	Lamina-associated polypeptide 1
LB1	Lamin B1
LBR	Lamin B receptor
LC	Lamin C
NE	nuclear envelope
NPC	nuclear pore complex
NTR	nuclear transport receptor
NUP	nucleoporin
ONM	outer nuclear membrane
P	passage
p16	$p16^{INK4A}$
PBS	Phosphate buffered saline
PFA	Paraformaldehyde solution
PNS	perinuclear space
RanGAP	Ran GTPase-activating protein
RCC1	Ran guanine exchange factor
SA β-Gal	Senescence-associated -β-Galactosidase assay
SASP	senescence-associated secretory phenotype e
SD	standard deviation
SDS	Sodium dodecyl sulfate
T	Thymine
TBS	Tris-base buffered solution
Tyr	Tyrosine
VSMC	vascular smooth muscle cells
X-Gal	5-bromo-4-chloro-3-indolyl-β-D-galactopyranoside

5.2 List of figures

Figure 1.1 Schematic representation of the nuclear envelope 1

Figure 1.2 Schematic representation of the Lamin A and Progerin processing pathway 3

Figure 1.3 Schematic representation of the nuclear envelope in HGPS 7

Figure 1.4 Schematic representation of the Nuclear Pore Complex structure 10

Figure 3.1 NPCs clustered in dysmorphic HGADFN127 nuclei 28

Figure 3.2 NPCs clustered in dysmorphic HGADFN003 nuclei 29

Figure 3.3 NUP107 did not colocalize with progerin aggregates in mitotic HGPS cells 30

Figure 3.4 Seeding of NPCs by ELYS on anaphase chromosomes was not delayed in HGADFN003 compared to GMO1651c 33

Figure 3.5 Seeding of NPCs by ELYS on anaphase chromosomes was not delayed in HGADFN127 compared to GMO1652c 34

Figure 3.6 NUP153 and NUP107 recruitment and localization was not affected in HGADFN003 compared to GMO1652c 37

Figure 3.7 NUP153 and NUP107 recruitment and localization was not affected in HGADFN127 compared to GMO1651c 38

Figure 3.8 mAb414 did not colocalize with aggregated SUN1 in mitotic HGADFN127 cells 40

Figure 3.9 mAb414 did not colocalize with aggregated SUN1 in mitotic HGADFN003 cells 41

Figure 3.10 The transmembrane nucleoporin POM121 did not aggregate in mitotic HGADFN003 cells and incorporation into the NE was not delayed. 43

Figure 3.11 The transmembrane nucleoporin POM121 did not aggregate in mitotic HGADFN127 cells and incorporation into the NE was not delayed. 44

Figure 3.12 Dysmorphic nuclei in replicative senescence 47

Figure 3.13 Determination of senescence index using a Senescence associated β-Galactosidase assay 48

Figure 3.14 Nuclear abnormalities increase with rising replicative senescence in control and HGPS fibroblasts 49

Figure 3.15 Immunofluorescent determination of replicative senescence with p16, p21 or LB1 50

Figure 3.16 Comparison of the senescence markers p16, p21 and LB1 in young or old control and HGPS fibroblasts....52

Figure 3.17 Progerin was elevated in most dysmorphic HGPS nuclei independent of replicative senescence....54

Figure 3.18 HGPS fibroblasts with elevated progerin levels were positive for one of four different indicators of replicative senescence....55

Figure 3.19 HGPS fibroblasts with elevated progerin were senescent independent of cellular age.56

Figure 3.20 NUP107 clustered in nuclear envelope folds of dysmorphic HGPS and control nuclei, co-localizing with trapped LA/C and progerin aggregates....61

Figure 3.21 POM121 clustered in nuclear envelope folds of dysmorphic HGPS and control nuclei, co-localizing with trapped LA/C and progerin aggregates....63

Figure 3.22 NPC clustering in dysmorphic control fibroblast nuclei in relation to the senescence markers p16, p21 and LB1....63

Figure 3.23 Analysis of replicative senescence and abnormal NPC distribution in control fibroblasts. 64

Figure 3.24 POM121 was clustered in dysmorphic control and HGPS nuclei with elevated p16 ...65

Figure 3.25 POM121 cluster in dysmorphic control and HGPS nuclei increased with replicative senescence....66

Figure 3.26 NUP107 clustered in most dysmorphic HGPS nuclei with elevated progerin levels....67

Figure 3.27 NPC clustering increased with rising replicative senescence in dysmorphic HGPS nuclei and correlated with progerin levels.....68

5.3 List of tables

Table 2.1 Cell lines used in this study 21

Table 2.2 Primary antibodies used in this study 22

Table 2.3 Secondary antibodies used in this study 23

Table 5.1 Number of mitotic cells imaged in this study 85

Table 5.2 Frequency of mislocalized proteins in mitotic HGPS and control cells 86

Table 5.3 Number of young and old nuclei analyzed in this study 88

Table 5.4 Percentage of HGPS nuclei positive for senescence markers and strong progerin signal 88

Table 5.5 Abbreviations 89

6. References

Acosta, J. C., A. Banito, T. Wuestefeld, A. Georgilis, P. Janich, J. P. Morton, D. Athineos, T. W. Kang, F. Lasitschka, M. Andrulis, G. Pascual, K. J. Morris, S. Khan, H. Jin, G. Dharmalingam, A. P. Snijders, T. Carroll, D. Capper, C. Pritchard, G. J. Inman, T. Longerich, O. J. Sansom, S. A. Benitah, L. Zender and J. Gil (2013). "A complex secretory program orchestrated by the inflammasome controls paracrine senescence." Nat Cell Biol **15**(8): 978-990.

Adam, S. A. and R. D. Goldman (2012). "Insights into the differences between the A- and B-type nuclear lamins." Adv Biol Regul **52**(1): 108-113.

Aebi, U., J. Cohn, L. Buhle and L. Gerace (1986). "The nuclear lamina is a meshwork of intermediate-type filaments." Nature **323**(6088): 560-564.

Al-Haboubi, T., D. K. Shumaker, J. Koser, M. Wehnert and B. Fahrenkrog (2011). "Distinct association of the nuclear pore protein Nup153 with A- and B-type lamins." Nucleus **2**(5): 500-509.

Alcorta, D. A., Y. Xiong, D. Phelps, G. Hannon, D. Beach and J. C. Barrett (1996). "Involvement of the cyclin-dependent kinase inhibitor p16 (INK4a) in replicative senescence of normal human fibroblasts." Proc Natl Acad Sci U S A **93**(24): 13742-13747.

Antonin, W., C. Franz, U. Haselmann, C. Antony and I. W. Mattaj (2005). "The integral membrane nucleoporin pom121 functionally links nuclear pore complex assembly and nuclear envelope formation." Mol Cell **17**(1): 83-92.

Ashapkin, V. V., L. I. Kutueva, S. Y. Kurchashova and Kireev, II (2019). "Are There Common Mechanisms Between the Hutchinson-Gilford Progeria Syndrome and Natural Aging?" Front Genet **10**: 455.

Baker, D. J., T. Wijshake, T. Tchkonia, N. K. LeBrasseur, B. G. Childs, B. van de Sluis, J. L. Kirkland and J. M. van Deursen (2011). "Clearance of p16Ink4a-positive senescent cells delays ageing-associated disorders." Nature **479**(7372): 232-236.

Banerjee, I., J. Zhang, T. Moore-Morris, E. Pfeiffer, K. S. Buchholz, A. Liu, K. Ouyang, M. J. Stroud, L. Gerace, S. M. Evans, A. McCulloch and J. Chen (2014). "Targeted ablation of nesprin 1 and nesprin 2 from murine myocardium results in cardiomyopathy, altered nuclear morphology and inhibition of the biomechanical gene response." PLoS Genet **10**(2): e1004114.

Bayliss, R., K. Ribbeck, D. Akin, H. M. Kent, C. M. Feldherr, D. Görlich and M. Stewart (1999). "Interaction between NTF2 and xFxFG-containing nucleoporins is required to mediate nuclear import of RanGDP." J Mol Biol **293**(3): 579-593.

Beck, M. and E. Hurt (2017). "The nuclear pore complex: understanding its function through structural insight." Nat Rev Mol Cell Biol **18**(2): 73-89.

Belgareh, N., G. Rabut, S. W. Bai, M. van Overbeek, J. Beaudouin, N. Daigle, O. V. Zatsepina, F. Pasteau, V. Labas, M. Fromont-Racine, J. Ellenberg and V. Doye (2001). "An evolutionarily conserved NPC subcomplex, which redistributes in part to kinetochores in mammalian cells." J Cell Biol **154**(6): 1147-1160.

Benson, E. K., S. W. Lee and S. A. Aaronson (2010). "Role of progerin-induced telomere dysfunction in HGPS premature cellular senescence." J Cell Sci **123**(Pt 15): 2605-2612.

Bernad, R., H. van der Velde, M. Fornerod and H. Pickersgill (2004). "Nup358/RanBP2 attaches to the nuclear pore complex via association with Nup88 and Nup214/CAN and plays a supporting role in CRM1-mediated nuclear protein export." Mol Cell Biol **24**(6): 2373-2384.

Bischoff, F. R. and H. Ponstingl (1991). "Catalysis of guanine nucleotide exchange on Ran by the mitotic regulator RCC1." Nature **354**(6348): 80-82.

Bodoor, K., S. Shaikh, D. Salina, W. H. Raharjo, R. Bastos, M. Lohka and B. Burke (1999). "Sequential recruitment of NPC proteins to the nuclear periphery at the end of mitosis." J Cell Sci **112 (Pt 13)**: 2253-2264.

Buchwalter, A., J. M. Kaneshiro and M. W. Hetzer (2019). "Coaching from the sidelines: the nuclear periphery in genome regulation." Nat Rev Genet **20**(1): 39-50.

Cao, K., B. C. Capell, M. R. Erdos, K. Djabali and F. S. Collins (2007). "A lamin A protein isoform overexpressed in Hutchinson-Gilford progeria syndrome interferes with mitosis in progeria and normal cells." Proc Natl Acad Sci U S A **104**(12): 4949-4954.

Capell, B. C., M. R. Erdos, J. P. Madigan, J. J. Fiordalisi, R. Varga, K. N. Conneely, L. B. Gordon, C. J. Der, A. D. Cox and F. S. Collins (2005). "Inhibiting farnesylation of progerin prevents the characteristic nuclear blebbing of Hutchinson-Gilford progeria syndrome." Proc Natl Acad Sci U S A **102**(36): 12879-12884.

Chellappan, S. P., S. Hiebert, M. Mudryj, J. M. Horowitz and J. R. Nevins (1991). "The E2F transcription factor is a cellular target for the RB protein." Cell **65**(6): 1053-1061.

Chen, C. Y., Y. H. Chi, R. A. Mutalif, M. F. Starost, T. G. Myers, S. A. Anderson, C. L. Stewart and K. T. Jeang (2012). "Accumulation of the inner nuclear envelope protein Sun1 is pathogenic in progeric and dystrophic laminopathies." Cell **149**(3): 565-577.

Chen, Z. J., W. P. Wang, Y. C. Chen, J. Y. Wang, W. H. Lin, L. A. Tai, G. G. Liou, C. S. Yang and Y. H. Chi (2014). "Dysregulated interactions between lamin A and SUN1 induce abnormalities in the nuclear envelope and endoplasmic reticulum in progeric laminopathies." Journal of Cell Science **127**: 1792-17804.

Chi, Y. H., K. Haller, J. M. Peloponese, Jr. and K. T. Jeang (2007). "Histone acetyltransferase hALP and nuclear membrane protein hsSUN1 function in de-condensation of mitotic chromosomes." J Biol Chem **282**(37): 27447-27458.

Childs, B. G., M. Durik, D. J. Baker and J. M. van Deursen (2015). "Cellular senescence in aging and age-related disease: from mechanisms to therapy." Nat Med **21**(12): 1424-1435.

Christie, M., C. W. Chang, G. Róna, K. M. Smith, A. G. Stewart, A. A. Takeda, M. R. Fontes, M. Stewart, B. G. Vértessy, J. K. Forwood and B. Kobe (2016). "Structural Biology and Regulation of Protein Import into the Nucleus." J Mol Biol **428**(10 Pt A): 2060-2090.

Cobb, A. M., D. Larrieu, D. T. Warren, Y. Liu, S. Srivastava, A. J. O. Smith, R. P. Bowater, S. P. Jackson and C. M. Shanahan (2016). "Prelamin A impairs 53BP1 nuclear entry by mislocalizing NUP153 and disrupting the Ran gradient." Aging Cell **15**(6): 1039-1050.

Corrigan, D. P., D. Kuszczak, A. E. Rusinol, D. P. Thewke, C. A. Hrycyna, S. Michaelis and M. S. Sinensky (2005). "Prelamin A endoproteolytic processing in vitro by recombinant Zmpste24." Biochem J **387**(Pt 1): 129-138.

Crisp, M., Q. Liu, K. Roux, J. B. Rattner, C. Shanahan, B. Burke, P. D. Stahl and D. Hodzic (2006). "Coupling of the nucleus and cytoplasm: role of the LINC complex." Journal of Cell Biology **172**: 43-51.

Cross, M. K. and M. A. Powers (2011). "Nup98 regulates bipolar spindle assembly through association with microtubules and opposition of MCAK." Mol Biol Cell **22**(5): 661-672.

D'Angelo, M. A., M. Raices, S. H. Panowski and M. W. Hetzer (2009). "Age-dependent deterioration of nuclear pore complexes causes a loss of nuclear integrity in postmitotic cells." Cell **136**(2): 284-295.

Dahl, K. N., P. Scaffidi, M. F. Islam, A. G. Yodh, K. L. Wilson and T. Misteli (2006). "Distinct structural and mechanical properties of the nuclear lamina in Hutchinson-Gilford progeria syndrome." Proc Natl Acad Sci U S A **103**(27): 10271-10276.

Daigle, N., J. Beaudouin, L. Hartnell, G. Imreh, E. Hallberg, J. Lippincott-Schwartz and J. Ellenberg (2001). "Nuclear pore complexes form immobile networks and have a very low turnover in live mammalian cells." J Cell Biol **154**(1): 71-84.

Davis, L. I. and G. Blobel (1986). "Identification and characterization of a nuclear pore complex protein." Cell **45**(5): 699-709.

Davis, L. I. and G. Blobel (1987). "Nuclear pore complex contains a family of glycoproteins that includes p62: glycosylation through a previously unidentified cellular pathway." Proc Natl Acad Sci U S A **84**(21): 7552-7556.

Dawson, T. R., M. D. Lazarus, M. W. Hetzer and S. R. Wente (2009). "ER membrane-bending proteins are necessary for de novo nuclear pore formation." J Cell Biol **184**(5): 659-675.

de Leeuw, R., Y. Gruenbaum and O. Medalia (2017). "Nuclear Lamins: Thin Filaments with Major Functions." Trends Cell Biol.

de Magalhães, J. P. and J. F. Passos (2018). "Stress, cell senescence and organismal ageing." Mech Ageing Dev **170**: 2-9.

De Sandre-Giovannoli, A., R. Bernard, P. Cau, C. Navarro, J. Amiel, I. Boccaccio, S. Lyonnet, C. L. Stewart, A. Munnich, M. Le Merrer and N. Levy (2003). "Lamin a truncation in Hutchinson-Gilford progeria." Science **300**(5628): 2055.

DeBusk, F. L. (1972). "The Hutchinson-Gilford progeria syndrome. Report of 4 cases and review of the literature." J Pediatr **80**(4): 697-724.

Denning, D. P., S. S. Patel, V. Uversky, A. L. Fink and M. Rexach (2003). "Disorder in the nuclear pore complex: the FG repeat regions of nucleoporins are natively unfolded." Proc Natl Acad Sci U S A **100**(5): 2450-2455.

Dhillon, S. (2021). "Lonafarnib: First Approval." Drugs **81**(2): 283-289.

Di Micco, R., V. Krizhanovsky, D. Baker and F. d'Adda di Fagagna (2021). "Cellular senescence in ageing: from mechanisms to therapeutic opportunities." Nat Rev Mol Cell Biol **22**(2): 75-95.

Dimri, G. P., X. Lee, G. Basile, M. Acosta, G. Scott, C. Roskelley, E. E. Medrano, M. Linskens, I. Rubelj, O. Pereira-Smith and et al. (1995). "A biomarker that identifies senescent human cells in culture and in aging skin in vivo." Proc Natl Acad Sci U S A **92**(20): 9363-9367.

Doucet, C. M., J. A. Talamas and M. W. Hetzer (2010). "Cell cycle-dependent differences in nuclear pore complex assembly in metazoa." Cell **141**(6): 1030-1041.

Dreesen, O. (2020). "Towards delineating the chain of events that cause premature senescence in the accelerated aging syndrome Hutchinson-Gilford progeria (HGPS)." Biochem Soc Trans **48**(3): 981-991.

Dultz, E. and J. Ellenberg (2010). "Live imaging of single nuclear pores reveals unique assembly kinetics and mechanism in interphase." J Cell Biol **191**(1): 15-22.

Dultz, E., E. Zanin, C. Wurzenberger, M. Braun, G. Rabut, L. Sironi and J. Ellenberg (2008). "Systematic kinetic analysis of mitotic dis- and reassembly of the nuclear pore in living cells." J Cell Biol **180**(5): 857-865.

Dworak, N., D. Makosa, M. Chatterjee, K. Jividen, C. S. Yang, C. Snow, W. C. Simke, I. G. Johnson, J. B. Kelley and B. M. Paschal (2019). "A nuclear lamina-chromatin-Ran GTPase axis modulates nuclear import and DNA damage signaling." Aging Cell **18**(1): e12851.

Dyson, N. (1998). "The regulation of E2F by pRB-family proteins." Genes Dev **12**(15): 2245-2262.

Eisch, V., X. Lu, D. Gabriel and K. Djabali (2016). "Progerin impairs chromosome maintenance by depleting CENP-F from metaphase kinetochores in Hutchinson-Gilford progeria fibroblasts." Oncotarget **7**(17): 24700-24718.

Eisenhardt, N., J. Redolfi and W. Antonin (2014). "Interaction of Nup53 with Ndc1 and Nup155 is required for nuclear pore complex assembly." J Cell Sci **127**(Pt 4): 908-921.

Eriksson, M., W. T. Brown, L. B. Gordon, M. W. Glynn, J. Singer, L. Scott, M. R. Erdos, C. M. Robbins, T. Y. Moses, P. Berglund, A. Dutra, E. Pak, S. Durkin, A. B. Csoka, M. Boehnke, T. W. Glover and F. S. Collins (2003). "Recurrent de novo point mutations in lamin A cause Hutchinson-Gilford progeria syndrome." Nature **423**(6937): 293-298.

Faria, A. M., A. Levay, Y. Wang, A. O. Kamphorst, M. L. Rosa, D. R. Nussenzveig, W. Balkan, Y. M. Chook, D. E. Levy and B. M. Fontoura (2006). "The nucleoporin Nup96 is required for proper expression of interferon-regulated proteins and functions." Immunity **24**(3): 295-304.

Fawcett, D. W. (1966). "On the occurrence of a fibrous lamina on the inner aspect of the nuclear envelope in certain cells of vertebrates." Am J Anat **119**(1): 129-145.

Fernandez, P., P. Scaffidi, E. Markert, J. H. Lee, S. Rane and T. Misteli (2014). "Transformation resistance in a premature aging disorder identifies a tumor-protective function of BRD4." Cell Rep **9**(1): 248-260.

Fiserova, J., M. Maninova, T. Sieger, J. Uhlirova, L. Sebestova, M. Efenberkova, M. Capek, K. Fiser and P. Hozak (2019). "Nuclear pore protein TPR associates with lamin B1 and affects nuclear lamina organization and nuclear pore distribution." Cell Mol Life Sci **76**(11): 2199-2216.

Fisher, D. Z., N. Chaudhary and G. Blobel (1986). "cDNA sequencing of nuclear lamins A and C reveals primary and secondary structural homology to intermediate filament proteins." Proc Natl Acad Sci U S A **83**(17): 6450-6454.

Floer, M., G. Blobel and M. Rexach (1997). "Disassembly of RanGTP-karyopherin beta complex, an intermediate in nuclear protein import." J Biol Chem **272**(31): 19538-19546.

Forbes, D. J., A. Travesa, M. S. Nord and C. Bernis (2015). "Nuclear transport factors: global regulation of mitosis." Curr Opin Cell Biol **35**: 78-90.

Franz, C., R. Walczak, S. Yavuz, R. Santarella, M. Gentzel, P. Askjaer, V. Galy, M. Hetzer, I. W. Mattaj and W. Antonin (2007). "MEL-28/ELYS is required for the recruitment of nucleoporins to chromatin and postmitotic nuclear pore complex assembly." EMBO Rep **8**(2): 165-172.

Freund, A., R. M. Laberge, M. Demaria and J. Campisi (2012). "Lamin B1 loss is a senescence-associated biomarker." Mol Biol Cell **23**(11): 2066-2075.

Frey, S. and D. Görlich (2007). "A saturated FG-repeat hydrogel can reproduce the permeability properties of nuclear pore complexes." Cell **130**(3): 512-523.

Frey, S. and D. Görlich (2009). "FG/FxFG as well as GLFG repeats form a selective permeability barrier with self-healing properties." Embo j **28**(17): 2554-2567.

Frey, S., R. P. Richter and D. Görlich (2006). "FG-rich repeats of nuclear pore proteins form a three-dimensional meshwork with hydrogel-like properties." Science **314**(5800): 815-817.

Funakoshi, T., M. Clever, A. Watanabe and N. Imamoto (2011). "Localization of Pom121 to the inner nuclear membrane is required for an early step of interphase nuclear pore complex assembly." Mol Biol Cell **22**(7): 1058-1069.

Funakoshi, T., K. Maeshima, K. Yahata, S. Sugano, F. Imamoto and N. Imamoto (2007). "Two distinct human POM121 genes: requirement for the formation of nuclear pore complexes." FEBS Lett **581**(25): 4910-4916.

Funasaka, T., E. Tsuka and R. W. Wong (2012). "Regulation of autophagy by nucleoporin Tpr." Sci Rep **2**: 878.

Gall, J. G. (1967). "Octagonal nuclear pores." J Cell Biol **32**(2): 391-399.

Gerhard-Herman, M., L. B. Smoot, N. Wake, M. W. Kieran, M. E. Kleinman, D. T. Miller, A. Schwartzman, A. Giobbie-Hurder, D. Neuberg and L. B. Gordon (2012). "Mechanisms of premature vascular aging in children with Hutchinson-Gilford progeria syndrome." Hypertension **59**(1): 92-97.

Goldberg, M. W. and T. D. Allen (1996). "The nuclear pore complex and lamina: three-dimensional structures and interactions determined by field emission in-lens scanning electron microscopy." J Mol Biol **257**(4): 848-865.

Goldman, R. D., D. K. Shumaker, M. R. Erdos, M. Eriksson, A. E. Goldman, L. B. Gordon, Y. Gruenbaum, S. Khuon, M. Mendez, R. Varga and F. S. Collins (2004). "Accumulation of mutant lamin A causes progressive changes in nuclear architecture in Hutchinson-Gilford progeria syndrome." Proceedings of the National Academy of Sciences **101**: 8963-8968.

Gonzalo, S., R. Kreienkamp and P. Askjaer (2017). "Hutchinson-Gilford Progeria Syndrome: A premature aging disease caused by LMNA gene mutations." Ageing Res Rev **33**: 18-29.

Gordon, L. B., J. Massaro, R. B. D'Agostino, Sr., S. E. Campbell, J. Brazier, W. T. Brown, M. E. Kleinman, M. W. Kieran and C. Progeria Clinical Trials (2014). "Impact of farnesylation inhibitors on survival in Hutchinson-Gilford progeria syndrome." Circulation **130**(1): 27-34.

Gorgoulis, V., P. D. Adams, A. Alimonti, D. C. Bennett, O. Bischof, C. Bishop, J. Campisi, M. Collado, K. Evangelou, G. Ferbeyre, J. Gil, E. Hara, V. Krizhanovsky, D. Jurk, A. B. Maier, M. Narita, L. Niedernhofer, J. F. Passos, P. D. Robbins, C. A. Schmitt, J. Sedivy, K. Vougas, T. von Zglinicki, D. Zhou, M. Serrano and M. Demaria (2019). "Cellular Senescence: Defining a Path Forward." Cell **179**(4): 813-827.

Görlich, D., N. Panté, U. Kutay, U. Aebi and F. R. Bischoff (1996). "Identification of different roles for RanGDP and RanGTP in nuclear protein import." Embo j **15**(20): 5584-5594.

Görlich, D., S. Prehn, R. A. Laskey and E. Hartmann (1994). "Isolation of a protein that is essential for the first step of nuclear protein import." Cell **79**(5): 767-778.

Gruenbaum, Y., Y. Landesman, B. Drees, J. W. Bare, H. Saumweber, M. R. Paddy, J. W. Sedat, D. E. Smith, B. M. Benton and P. A. Fisher (1988). "Drosophila nuclear lamin precursor Dm0 is

translated from either of two developmentally regulated mRNA species apparently encoded by a single gene." J Cell Biol **106**(3): 585-596.

Guo, Y., Y. Kim, T. Shimi, R. D. Goldman and Y. Zheng (2014). "Concentration-dependent lamin assembly and its roles in the localization of other nuclear proteins." Mol Biol Cell **25**(8): 1287-1297.

Hänzelmann, S., F. Beier, E. G. Gusmao, C. M. Koch, S. Hummel, I. Charapitsa, S. Joussen, V. Benes, T. H. Brümmendorf, G. Reid, I. G. Costa and W. Wagner (2015). "Replicative senescence is associated with nuclear reorganization and with DNA methylation at specific transcription factor binding sites." Clin Epigenetics **7**(1): 19.

Haque, F., D. J. Lloyd, D. T. Smallwood, C. L. Dent, C. M. Shanahan, A. M. Fry, R. C. Trembath and S. Shackleton (2006). "SUN1 interacts with nuclear lamin A and cytoplasmic nesprins to provide a physical connection between the nuclear lamina and the cytoskeleton." Molecular and Cellular Biology **26**: 3738-3751.

Hase, M. E. and V. C. Cordes (2003). "Direct interaction with nup153 mediates binding of Tpr to the periphery of the nuclear pore complex." Mol Biol Cell **14**(5): 1923-1940.

Hayflick, L. (1965). "THE LIMITED IN VITRO LIFETIME OF HUMAN DIPLOID CELL STRAINS." Exp Cell Res **37**: 614-636.

Hayflick, L. and P. S. Moorhead (1961). "The serial cultivation of human diploid cell strains." Exp Cell Res **25**: 585-621.

Hennekam, R. C. (2006). "Hutchinson-Gilford progeria syndrome: review of the phenotype." Am J Med Genet A **140**(23): 2603-2624.

Hernandez-Segura, A., J. Nehme and M. Demaria (2018). "Hallmarks of Cellular Senescence." Trends Cell Biol **28**(6): 436-453.

Hetzer, M., D. Bilbao-Cortés, T. C. Walther, O. J. Gruss and I. W. Mattaj (2000). "GTP hydrolysis by Ran is required for nuclear envelope assembly." Mol Cell **5**(6): 1013-1024.

Hoelz, A., J. S. Glavy and M. Beck (2016). "Toward the atomic structure of the nuclear pore complex: when top down meets bottom up." Nat Struct Mol Biol **23**(7): 624-630.

Hu, X. T., H. C. Song, H. Yu, Z. C. Wu, X. G. Liu and W. C. Chen (2020). "Overexpression of Progerin Results in Impaired Proliferation and Invasion of Non-Small Cell Lung Cancer Cells." Onco Targets Ther **13**: 2629-2642.

Huang, S., R. A. Risques, G. M. Martin, P. S. Rabinovitch and J. Oshima (2008). "Accelerated telomere shortening and replicative senescence in human fibroblasts overexpressing mutant and wild-type lamin A." Exp Cell Res **314**(1): 82-91.

Huebner, A., A. M. Kaindl, K. P. Knobeloch, H. Petzold, P. Mann and K. Koehler (2004). "The triple A syndrome is due to mutations in ALADIN, a novel member of the nuclear pore complex." Endocr Res **30**(4): 891-899.

Imamoto, N., T. Shimamoto, S. Kose, T. Takao, T. Tachibana, M. Matsubae, T. Sekimoto, Y. Shimonishi and Y. Yoneda (1995). "The nuclear pore-targeting complex binds to nuclear pores after association with a karyophile." FEBS Lett **368**(3): 415-419.

Izaurralde, E., U. Kutay, C. von Kobbe, I. W. Mattaj and D. Görlich (1997). "The asymmetric distribution of the constituents of the Ran system is essential for transport into and out of the nucleus." Embo j **16**(21): 6535-6547.

Janota, C. S., F. J. Calero-Cuenca and E. R. Gomes (2020). "The role of the cell nucleus in mechanotransduction." Curr Opin Cell Biol **63**: 204-211.

Joseph, J., S. T. Liu, S. A. Jablonski, T. J. Yen and M. Dasso (2004). "The RanGAP1-RanBP2 complex is essential for microtubule-kinetochore interactions in vivo." Curr Biol **14**(7): 611-617.

Jung, H. J., C. Coffinier, Y. Choe, A. P. Beigneux, B. S. Davies, S. H. Yang, R. H. Barnes, 2nd, J. Hong, T. Sun, S. J. Pleasure, S. G. Young and L. G. Fong (2012). "Regulation of prelamin A but not lamin C by miR-9, a brain-specific microRNA." Proc Natl Acad Sci U S A **109**(7): E423-431.

Jung, Y. S., Y. Qian and X. Chen (2010). "Examination of the expanding pathways for the regulation of p21 expression and activity." Cell Signal **22**(7): 1003-1012.

Kalab, P., K. Weis and R. Heald (2002). "Visualization of a Ran-GTP gradient in interphase and mitotic Xenopus egg extracts." Science **295**(5564): 2452-2456.

Kelley, J. B., S. Datta, C. J. Snow, M. Chatterjee, L. Ni, A. Spencer, C. S. Yang, C. Cubenas-Potts, M. J. Matunis and B. M. Paschal (2011). "The defective nuclear lamina in Hutchinson-gilford progeria syndrome disrupts the nucleocytoplasmic Ran gradient and inhibits nuclear localization of Ubc9." Mol Cell Biol **31**(16): 3378-3395.

Kim, S. Y., S. J. Ryu, H. J. Ahn, H. R. Choi, H. T. Kang and S. C. Park (2010). "Senescence-related functional nuclear barrier by down-regulation of nucleo-cytoplasmic trafficking gene expression." Biochem Biophys Res Commun **391**(1): 28-32.

Kimura, N., M. Takizawa, K. Okita, O. Natori, K. Igarashi, M. Ueno, K. Nakashima, I. Nobuhisa and T. Taga (2002). "Identification of a novel transcription factor, ELYS, expressed predominantly in mouse foetal haematopoietic tissues." Genes Cells **7**(4): 435-446.

Kinoshita, D., A. Nagasawa, I. Shimizu, T. K. Ito, Y. Yoshida, M. Tsuchida, A. Iwama, T. Hayano and T. Minamino (2017). "Progerin impairs vascular smooth muscle cell growth via the DNA damage response pathway." Oncotarget **8**(21): 34045-34056.

Kittisopikul, M., T. Shimi, M. Tatli, J. R. Tran, Y. Zheng, O. Medalia, K. Jaqaman, S. A. Adam and R. D. Goldman (2021). "Computational analyses reveal spatial relationships between nuclear pore complexes and specific lamins." J Cell Biol **220**(4).

Knockenhauer, K. E. and T. U. Schwartz (2016). "The Nuclear Pore Complex as a Flexible and Dynamic Gate." Cell **164**(6): 1162-1171.

Kreienkamp, R. and S. Gonzalo (2019). "Hutchinson-Gilford Progeria Syndrome: Challenges at Bench and Bedside." Subcell Biochem **91**: 435-451.

Krizhanovsky, V., M. Yon, R. A. Dickins, S. Hearn, J. Simon, C. Miething, H. Yee, L. Zender and S. W. Lowe (2008). "Senescence of activated stellate cells limits liver fibrosis." Cell **134**(4): 657-667.

Krohne, G., S. L. Wolin, F. D. McKeon, W. W. Franke and M. W. Kirschner (1987). "Nuclear lamin LI of Xenopus laevis: cDNA cloning, amino acid sequence and binding specificity of a member of the lamin B subfamily." EMBO J **6**(12): 3801-3808.

Krull, S., J. Dörries, B. Boysen, S. Reidenbach, L. Magnius, H. Norder, J. Thyberg and V. C. Cordes (2010). "Protein Tpr is required for establishing nuclear pore-associated zones of heterochromatin exclusion." Embo j **29**(10): 1659-1673.

Kudlow, B. A., M. N. Stanfel, C. R. Burtner, E. D. Johnston and B. K. Kennedy (2008). "Suppression of proliferative defects associated with processing-defective lamin A mutants by hTERT or inactivation of p53." Mol Biol Cell **19**(12): 5238-5248.

Kutay, U., F. R. Bischoff, S. Kostka, R. Kraft and D. Görlich (1997). "Export of importin alpha from the nucleus is mediated by a specific nuclear transport factor." Cell **90**(6): 1061-1071.

Lammerding, J., L. G. Fong, J. Y. Ji, K. Reue, C. L. Stewart, S. G. Young and R. T. Lee (2006). "Lamins A and C but not lamin B1 regulate nuclear mechanics." J Biol Chem **281**(35): 25768-25780.

Lammerding, J., P. C. Schulze, T. Takahashi, S. Kozlov, T. Sullivan, R. D. Kamm, C. L. Stewart and R. T. Lee (2004). "Lamin A/C deficiency causes defective nuclear mechanics and mechanotransduction." J Clin Invest **113**(3): 370-378.

Laurell, E., K. Beck, K. Krupina, G. Theerthagiri, B. Bodenmiller, P. Horvath, R. Aebersold, W. Antonin and U. Kutay (2011). "Phosphorylation of Nup98 by multiple kinases is crucial for NPC disassembly during mitotic entry." Cell **144**(4): 539-550.

Lee, Y. L. and B. Burke (2018). "LINC complexes and nuclear positioning." Semin Cell Dev Biol **82**: 67-76.

Lehner, C. F., R. Stick, H. M. Eppenberger and E. A. Nigg (1987). "Differential expression of nuclear lamin proteins during chicken development." J Cell Biol **105**(1): 577-587.

Lin, D. H. and A. Hoelz (2019). "The Structure of the Nuclear Pore Complex (An Update)." Annu Rev Biochem **88**: 725-783.

Lin, F. and H. J. Worman (1993). "Structural organization of the human gene encoding nuclear lamin A and nuclear lamin C." J Biol Chem **268**(22): 16321-16326.

Liu, B., J. Wang, K. M. Chan, W. M. Tjia, W. Deng, X. Guan, J. D. Huang, K. M. Li, P. Y. Chau, D. J. Chen, D. Pei, A. M. Pendas, J. Cadinanos, C. Lopez-Otin, H. F. Tse, C. Hutchison, J. Chen, Y.

Cao, K. S. Cheah, K. Tryggvason and Z. Zhou (2005). "Genomic instability in laminopathy-based premature aging." Nat Med **11**(7): 780-785.

Liu, C., R. Arnold, G. Henriques and K. Djabali (2019). "Inhibition of JAK-STAT Signaling with Baricitinib Reduces Inflammation and Improves Cellular Homeostasis in Progeria Cells." Cells **8**(10).

Liu, Q., N. Pante, T. Misteli, M. Elsagga, M. Crisp, D. Hodzic, B. Burke and K. J. Roux (2007). "Functional association of Sun1 with nuclear pore complexes." J Cell Biol **178**(5): 785-798.

Loiodice, I., A. Alves, G. Rabut, M. Van Overbeek, J. Ellenberg, J. B. Sibarita and V. Doye (2004). "The entire Nup107-160 complex, including three new members, is targeted as one entity to kinetochores in mitosis." Mol Biol Cell **15**(7): 3333-3344.

Lombardi, M. L., D. E. Jaalouk, C. M. Shanahan, B. Burke, K. J. Roux and J. Lammerding (2011). "The interaction between nesprins and sun proteins at the nuclear envelope is critical for force transmission between the nucleus and cytoskeleton." J Biol Chem **286**(30): 26743-26753.

López-Otín, C., M. A. Blasco, L. Partridge, M. Serrano and G. Kroemer (2013). "The hallmarks of aging." Cell **153**(6): 1194-1217.

Lounsbury, K. M. and I. G. Macara (1997). "Ran-binding protein 1 (RanBP1) forms a ternary complex with Ran and karyopherin beta and reduces Ran GTPase-activating protein (RanGAP) inhibition by karyopherin beta." J Biol Chem **272**(1): 551-555.

Lu, W., J. Gotzmann, L. Sironi, V. M. Jaeger, M. Schneider, Y. Luke, M. Uhlen, C. A. Szigyarto, A. Brachner, J. Ellenberg, R. Foisner, A. A. Noegel and I. Karakesisoglou (2008). "Sun1 forms immobile macromolecular assemblies at the nuclear envelope." Biochim Biophys Acta **1783**(12): 2415-2426.

Lu, X. and K. Djabali (2018). "Autophagic Removal of Farnesylated Carboxy-Terminal Lamin Peptides." Cells **7**(4).

Lussi, Y. C., D. K. Shumaker, T. Shimi and B. Fahrenkrog (2010). "The nucleoporin Nup153 affects spindle checkpoint activity due to an association with Mad1." Nucleus **1**(1): 71-84.

Mackay, D. R., S. W. Elgort and K. S. Ullman (2009). "The nucleoporin Nup153 has separable roles in both early mitotic progression and the resolution of mitosis." Mol Biol Cell **20**(6): 1652-1660.

Maeshima, K., H. Iino, S. Hihara, T. Funakoshi, A. Watanabe, M. Nishimura, R. Nakatomi, K. Yahata, F. Imamoto, T. Hashikawa, H. Yokota and N. Imamoto (2010). "Nuclear pore formation but not nuclear growth is governed by cyclin-dependent kinases (Cdks) during interphase." Nat Struct Mol Biol **17**(9): 1065-1071.

Mallampalli, M. P., G. Huyer, P. Bendale, M. H. Gelb and S. Michaelis (2005). "Inhibiting farnesylation reverses the nuclear morphology defect in a HeLa cell model for Hutchinson-Gilford progeria syndrome." Proc Natl Acad Sci U S A **102**(40): 14416-14421.

Mansfeld, J., S. Guttinger, L. A. Hawryluk-Gara, N. Pante, M. Mall, V. Galy, U. Haselmann, P. Muhlhausser, R. W. Wozniak, I. W. Mattaj, U. Kutay and W. Antonin (2006). "The conserved transmembrane nucleoporin NDC1 is required for nuclear pore complex assembly in vertebrate cells." Molecular Cell **22**.

Matsuura, Y. (2016). "Mechanistic Insights from Structural Analyses of Ran-GTPase-Driven Nuclear Export of Proteins and RNAs." J Mol Biol **428**(10 Pt A): 2025-2039.

Maul, G. G., H. M. Maul, J. E. Scogna, M. W. Lieberman, G. S. Stein, B. Y. Hsu and T. W. Borun (1972). "Time sequence of nuclear pore formation in phytohemagglutinin-stimulated lymphocytes and in HeLa cells during the cell cycle." J Cell Biol **55**(2): 433-447.

McClintock, D., D. Ratner, M. Lokuge, D. M. Owens, L. B. Gordon, F. S. Collins and K. Djabali (2007). "The Mutant Form of Lamin A that Causes Hutchinson-Gilford Progeria Is a Biomarker of Cellular Aging in Human Skin." PLoS ONE **2**: e1269.

McCloskey, A., A. Ibarra and M. W. Hetzer (2018). "Tpr regulates the total number of nuclear pore complexes per cell nucleus." Genes Dev **32**(19-20): 1321-1331.

McKeon, F. D., M. W. Kirschner and D. Caput (1986). "Homologies in both primary and secondary structure between nuclear envelope and intermediate filament proteins." Nature **319**(6053): 463-468.

Mehta, I. S., M. Figgitt, C. S. Clements, I. R. Kill and J. M. Bridger (2007). "Alterations to nuclear architecture and genome behavior in senescent cells." Ann N Y Acad Sci **1100**: 250-263.

Melchior, F., B. Paschal, J. Evans and L. Gerace (1993). "Inhibition of nuclear protein import by nonhydrolyzable analogues of GTP and identification of the small GTPase Ran/TC4 as an essential transport factor." J Cell Biol **123**(6 Pt 2): 1649-1659.

Merideth, M. A., L. B. Gordon, S. Clauss, V. Sachdev, A. C. Smith, M. B. Perry, C. C. Brewer, C. Zalewski, H. J. Kim, B. Solomon, B. P. Brooks, L. H. Gerber, M. L. Turner, D. L. Domingo, T. C. Hart, J. Graf, J. C. Reynolds, A. Gropman, J. A. Yanovski, M. Gerhard-Herman, F. S. Collins, E. G. Nabel, R. O. Cannon, 3rd, W. A. Gahl and W. J. Introne (2008). "Phenotype and course of Hutchinson-Gilford progeria syndrome." N Engl J Med **358**(6): 592-604.

Mitchell, J. M., J. Mansfeld, J. Capitanio, U. Kutay and R. W. Wozniak (2010). "Pom121 links two essential subcomplexes of the nuclear pore complex core to the membrane." J Cell Biol **191**(3): 505-521.

Mitsui, Y. and E. L. Schneider (1976). "Increased nuclear sizes in senescent human diploid fibroblast cultures." Exp Cell Res **100**(1): 147-152.

Moir, R. D., M. Yoon, S. Khuon and R. D. Goldman (2000). "Nuclear lamins A and B1: different pathways of assembly during nuclear envelope formation in living cells." J Cell Biol **151**(6): 1155-1168.

Moore, M. S. and G. Blobel (1993). "The GTP-binding protein Ran/TC4 is required for protein import into the nucleus." Nature **365**(6447): 661-663.

Najdi, F., P. Krüger and K. Djabali (2021). "Impact of Progerin Expression on Adipogenesis in Hutchinson-Gilford Progeria Skin-Derived Precursor Cells." Cells **10**(7).

Olins, A. L., G. Rhodes, D. B. Welch, M. Zwerger and D. E. Olins (2010). "Lamin B receptor: multi-tasking at the nuclear envelope." Nucleus **1**(1): 53-70.

Orjalo, A. V., A. Arnaoutov, Z. Shen, Y. Boyarchuk, S. G. Zeitlin, B. Fontoura, S. Briggs, M. Dasso and D. J. Forbes (2006). "The Nup107-160 nucleoporin complex is required for correct bipolar spindle assembly." Mol Biol Cell **17**(9): 3806-3818.

Otsuka, S., K. H. Bui, M. Schorb, M. J. Hossain, A. Z. Politi, B. Koch, M. Eltsov, M. Beck and J. Ellenberg (2016). "Nuclear pore assembly proceeds by an inside-out extrusion of the nuclear envelope." Elife **5**.

Otsuka, S. and J. Ellenberg (2018). "Mechanisms of nuclear pore complex assembly - two different ways of building one molecular machine." FEBS Lett **592**(4): 475-488.

Pappas, G. D. (1956). "The fine structure of the nuclear envelope of Amoeba proteus." J Biophys Biochem Cytol **2**(4 Suppl): 431-434.

Paradisi, M., D. McClintock, R. L. Boguslavsky, C. Pedicelli, H. J. Worman and K. Djabali (2005). "Dermal fibroblasts in Hutchinson-Gilford progeria syndrome with the lamin A G608G mutation have dysmorphic nuclei and are hypersensitive to heat stres." BioMed Central Cell Biology **6**: 27.

Parry, D. A., J. F. Conway and P. M. Steinert (1986). "Structural studies on lamin. Similarities and differences between lamin and intermediate-filament proteins." Biochem J **238**(1): 305-308.

Patel, J. T., A. Bottrill, S. L. Prosser, S. Jayaraman, K. Straatman, A. M. Fry and S. Shackleton (2014). "Mitotic phosphorylation of SUN1 loosens its connection with the nuclear lamina while the LINC complex remains intact." Nucleus **5**(5): 462-473.

Pendás, A. M., Z. Zhou, J. Cadiñanos, J. M. Freije, J. Wang, K. Hultenby, A. Astudillo, A. Wernerson, F. Rodríguez, K. Tryggvason and C. López-Otín (2002). "Defective prelamin A processing and muscular and adipocyte alterations in Zmpste24 metalloproteinase-deficient mice." Nat Genet **31**(1): 94-99.

Peter, M., G. T. Kitten, C. F. Lehner, K. Vorburger, S. M. Bailer, G. Maridor and E. A. Nigg (1989). "Cloning and sequencing of cDNA clones encoding chicken lamins A and B1 and comparison of the primary structures of vertebrate A- and B-type lamins." J Mol Biol **208**(3): 393-404.

Platani, M., R. Santarella-Mellwig, M. Posch, R. Walczak, J. R. Swedlow and I. W. Mattaj (2009). "The Nup107-160 nucleoporin complex promotes mitotic events via control of the localization state of the chromosome passenger complex." Mol Biol Cell **20**(24): 5260-5275.

Port, S. A., T. Monecke, A. Dickmanns, C. Spillner, R. Hofele, H. Urlaub, R. Ficner and R. H. Kehlenbach (2015). "Structural and Functional Characterization of CRM1-Nup214 Interactions Reveals Multiple FG-Binding Sites Involved in Nuclear Export." Cell Rep **13**(4): 690-702.

Rabut, G., V. Doye and J. Ellenberg (2004). "Mapping the dynamic organization of the nuclear pore complex inside single living cells." Nat Cell Biol **6**(11): 1114-1121.

Ragnauth, C. D., D. T. Warren, Y. Liu, R. McNair, T. Tajsic, N. Figg, R. Shroff, J. Skepper and C. M. Shanahan (2010). "Prelamin A acts to accelerate smooth muscle cell senescence and is a novel biomarker of human vascular aging." Circulation **121**(20): 2200-2210.

Raices, M. and M. A. D'Angelo (2012). "Nuclear pore complex composition: a new regulator of tissue-specific and developmental functions." Nat Rev Mol Cell Biol **13**(11): 687-699.

Raices, M. and M. A. D'Angelo (2017). "Nuclear pore complexes and regulation of gene expression." Curr Opin Cell Biol **46**: 26-32.

Rasala, B. A., A. V. Orjalo, Z. Shen, S. Briggs and D. J. Forbes (2006). "ELYS is a dual nucleoporin/kinetochore protein required for nuclear pore assembly and proper cell division." Proc Natl Acad Sci U S A **103**(47): 17801-17806.

Rasala, B. A., C. Ramos, A. Harel and D. J. Forbes (2008). "Capture of AT-rich chromatin by ELYS recruits POM121 and NDC1 to initiate nuclear pore assembly." Mol Biol Cell **19**(9): 3982-3996.

Reichelt, R., A. Holzenburg, E. L. Buhle, Jr., M. Jarnik, A. Engel and U. Aebi (1990). "Correlation between structure and mass distribution of the nuclear pore complex and of distinct pore complex components." J Cell Biol **110**(4): 883-894.

Ribbeck, K. and D. Görlich (2001). "Kinetic analysis of translocation through nuclear pore complexes." Embo j **20**(6): 1320-1330.

Rivera-Torres, J., R. Acín-Perez, P. Cabezas-Sánchez, F. G. Osorio, C. Gonzalez-Gómez, D. Megias, C. Cámara, C. López-Otín, J. A. Enríquez, J. L. Luque-García and V. Andrés (2013). "Identification of mitochondrial dysfunction in Hutchinson-Gilford progeria syndrome through use of stable isotope labeling with amino acids in cell culture." J Proteomics **91**: 466-477.

Rober, R. A., K. Weber and M. Osborn (1989). "Differential timing of nuclear lamin A/C expression in the various organs of the mouse embryo and the young animal: a developmental study." Development **105**(2): 365-378.

Rohrl, J. M., R. Arnold and K. Djabali (2021). "Nuclear Pore Complexes Cluster in Dysmorphic Nuclei of Normal and Progeria Cells during Replicative Senescence." Cells **10**(1).

Rotem, A., R. Gruber, H. Shorer, L. Shaulov, E. Klein and A. Harel (2009). "Importin beta regulates the seeding of chromatin with initiation sites for nuclear pore assembly." Mol Biol Cell **20**(18): 4031-4042.

Rothballer, A., T. U. Schwartz and U. Kutay (2013). "LINCing complex functions at the nuclear envelope: what the molecular architecture of the LINC complex can reveal about its function." Nucleus **4**(1): 29-36.

Ryu, S. J., Y. S. Oh and S. C. Park (2007). "Failure of stress-induced downregulation of Bcl-2 contributes to apoptosis resistance in senescent human diploid fibroblasts." Cell Death Differ **14**(5): 1020-1028.

Sachdev, R., C. Sieverding, M. Flotenmeyer and W. Antonin (2012). "The C-terminal domain of Nup93 is essential for assembly of the structural backbone of nuclear pore complexes." Mol Biol Cell **23**(4): 740-749.

Sadaie, M., R. Salama, T. Carroll, K. Tomimatsu, T. Chandra, A. R. Young, M. Narita, P. A. Pérez-Mancera, D. C. Bennett, H. Chong, H. Kimura and M. Narita (2013). "Redistribution of the Lamin B1 genomic binding profile affects rearrangement of heterochromatic domains and SAHF formation during senescence." Genes Dev **27**(16): 1800-1808.

Sagiv, A. and V. Krizhanovsky (2013). "Immunosurveillance of senescent cells: the bright side of the senescence program." Biogerontology **14**(6): 617-628.

Sakuma, S. and M. A. D'Angelo (2017). "The roles of the nuclear pore complex in cellular dysfunction, aging and disease." Semin Cell Dev Biol **68**: 72-84.

Salamat, M., P. K. Dhar, D. L. Neagu and J. B. Lyon (2010). "Aortic calcification in a patient with hutchinson-gilford progeria syndrome." Pediatr Cardiol **31**(6): 925-926.

Salina, D., P. Enarson, J. B. Rattner and B. Burke (2003). "Nup358 integrates nuclear envelope breakdown with kinetochore assembly." J Cell Biol **162**(6): 991-1001.

Schellhaus, A. K., P. De Magistris and W. Antonin (2016). "Nuclear Reformation at the End of Mitosis." J Mol Biol **428**(10 Pt A): 1962-1985.

Schindelin, J., I. Arganda-Carreras, E. Frise, V. Kaynig, M. Longair, T. Pietzsch, S. Preibisch, C. Rueden, S. Saalfeld, B. Schmid, J. Y. Tinevez, D. J. White, V. Hartenstein, K. Eliceiri, P. Tomancak and A. Cardona (2012). "Fiji: an open-source platform for biological-image analysis." Nat Methods **9**(7): 676-682.

Schmidt, H. B. and D. Gorlich (2016). "Transport Selectivity of Nuclear Pores, Phase Separation, and Membraneless Organelles." Trends Biochem Sci **41**(1): 46-61.

Shimi, T., M. Kittisopikul, J. Tran, A. E. Goldman, S. A. Adam, Y. Zheng, K. Jaqaman and R. D. Goldman (2015). "Structural organization of nuclear lamins A, C, B1, and B2 revealed by superresolution microscopy." Mol Biol Cell **26**(22): 4075-4086.

Shumaker, D. K., T. Dechat, A. Kohlmaier, S. A. Adam, M. R. Bozovsky, M. R. Erdos, M. Eriksson, A. E. Goldman, S. Khuon, F. S. Collins, T. Jenuwein and R. D. Goldman (2006). "Mutant nuclear

lamin A leads to progressive alterations of epigenetic control in premature aging." Proc Natl Acad Sci U S A **103**(23): 8703-8708.

Sinensky, M., K. Fantle, M. Trujillo, T. McLain, A. Kupfer and M. Dalton (1994). "The processing pathway of prelamin A." J Cell Sci **107 (Pt 1)**: 61-67.

Smythe, C., H. E. Jenkins and C. J. Hutchison (2000). "Incorporation of the nuclear pore basket protein nup153 into nuclear pore structures is dependent upon lamina assembly: evidence from cell-free extracts of Xenopus eggs." Embo j **19**(15): 3918-3931.

Snow, C. J., A. Dar, A. Dutta, R. H. Kehlenbach and B. M. Paschal (2013). "Defective nuclear import of Tpr in Progeria reflects the Ran sensitivity of large cargo transport." J Cell Biol **201**(4): 541-557.

Soderqvist, H. and E. Hallberg (1994). "The large C-terminal region of the integral pore membrane protein, POM121, is facing the nuclear pore complex." Eur J Cell Biol **64**(1): 186-191.

Sola-Carvajal, A., G. Revêchon, H. T. Helgadottir, D. Whisenant, R. Hagblom, J. Döhla, P. Katajisto, D. Brodin, F. Fagerström-Billai, N. Viceconte and M. Eriksson (2019). "Accumulation of Progerin Affects the Symmetry of Cell Division and Is Associated with Impaired Wnt Signaling and the Mislocalization of Nuclear Envelope Proteins." J Invest Dermatol **139**(11): 2272-2280.e2212.

Sosa, B. A., A. Rothballer, U. Kutay and T. U. Schwartz (2012). "LINC complexes form by binding of three KASH peptides to domain interfaces of trimeric SUN proteins." Cell **149**(5): 1035-1047.

Stade, K., C. S. Ford, C. Guthrie and K. Weis (1997). "Exportin 1 (Crm1p) is an essential nuclear export factor." Cell **90**(6): 1041-1050.

Stehbens, W. E., B. Delahunt, T. Shozawa and E. Gilbert-Barness (2001). "Smooth muscle cell depletion and collagen types in progeric arteries." Cardiovasc Pathol **10**(3): 133-136.

Stehbens, W. E., S. J. Wakefield, E. Gilbert-Barness, R. E. Olson and J. Ackerman (1999). "Histological and ultrastructural features of atherosclerosis in progeria." Cardiovasc Pathol **8**(1): 29-39.

Stein, G. H., L. F. Drullinger, A. Soulard and V. Dulić (1999). "Differential roles for cyclin-dependent kinase inhibitors p21 and p16 in the mechanisms of senescence and differentiation in human fibroblasts." Mol Cell Biol **19**(3): 2109-2117.

Stewart, C. and B. Burke (1987). "Teratocarcinoma stem cells and early mouse embryos contain only a single major lamin polypeptide closely resembling lamin B." Cell **51**(3): 383-392.

Sullivan, T., D. Escalante-Alcalde, H. Bhatt, M. Anver, N. Bhat, K. Nagashima, C. L. Stewart and B. Burke (1999). "Loss of A-type lamin expression compromises nuclear envelope integrity leading to muscular dystrophy." J Cell Biol **147**(5): 913-920.

Swift, J., I. L. Ivanovska, A. Buxboim, T. Harada, P. C. Dingal, J. Pinter, J. D. Pajerowski, K. R. Spinler, J. W. Shin, M. Tewari, F. Rehfeldt, D. W. Speicher and D. E. Discher (2013). "Nuclear

lamin-A scales with tissue stiffness and enhances matrix-directed differentiation." Science **341**(6149): 1240104.

Tajik, A., Y. Zhang, F. Wei, J. Sun, Q. Jia, W. Zhou, R. Singh, N. Khanna, A. S. Belmont and N. Wang (2016). "Transcription upregulation via force-induced direct stretching of chromatin." Nat Mater **15**(12): 1287-1296.

Talamas, J. A. and M. W. Hetzer (2011). "POM121 and Sun1 play a role in early steps of interphase NPC assembly." Journal of Cell Biology **194**: 27-37.

Timney, B. L., B. Raveh, R. Mironska, J. M. Trivedi, S. J. Kim, D. Russel, S. R. Wente, A. Sali and M. P. Rout (2016). "Simple rules for passive diffusion through the nuclear pore complex." J Cell Biol **215**(1): 57-76.

Toth, J. I., S. H. Yang, X. Qiao, A. P. Beigneux, M. H. Gelb, C. L. Moulson, J. H. Miner, S. G. Young and L. G. Fong (2005). "Blocking protein farnesyltransferase improves nuclear shape in fibroblasts from humans with progeroid syndromes." Proc Natl Acad Sci U S A **102**(36): 12873-12878.

Turgay, Y., M. Eibauer, A. E. Goldman, T. Shimi, M. Khayat, K. Ben-Harush, A. Dubrovsky-Gaupp, K. T. Sapra, R. D. Goldman and O. Medalia (2017). "The molecular architecture of lamins in somatic cells." Nature **543**(7644): 261-264.

Ullrich, N. J. and L. B. Gordon (2015). "Hutchinson-Gilford progeria syndrome." Handb Clin Neurol **132**: 249-264.

Vergnes, L., M. Péterfy, M. O. Bergo, S. G. Young and K. Reue (2004). "Lamin B1 is required for mouse development and nuclear integrity." Proc Natl Acad Sci U S A **101**(28): 10428-10433.

Verstraeten, V. L., J. Y. Ji, K. S. Cummings, R. T. Lee and J. Lammerding (2008). "Increased mechanosensitivity and nuclear stiffness in Hutchinson-Gilford progeria cells: effects of farnesyltransferase inhibitors." Aging Cell **7**(3): 383-393.

Vollmer, B., M. Lorenz, D. Moreno-Andres, M. Bodenhofer, P. De Magistris, S. A. Astrinidis, A. Schooley, M. Flotenmeyer, S. Leptihn and W. Antonin (2015). "Nup153 Recruits the Nup107-160 Complex to the Inner Nuclear Membrane for Interphasic Nuclear Pore Complex Assembly." Dev Cell **33**(6): 717-728.

Vollmer, B., A. Schooley, R. Sachdev, N. Eisenhardt, A. M. Schneider, C. Sieverding, J. Madlung, U. Gerken, B. Macek and W. Antonin (2012). "Dimerization and direct membrane interaction of Nup53 contribute to nuclear pore complex assembly." EMBO J **31**(20): 4072-4084.

Vorburger, K., C. F. Lehner, G. T. Kitten, H. M. Eppenberger and E. A. Nigg (1989). "A second higher vertebrate B-type lamin. cDNA sequence determination and in vitro processing of chicken lamin B2." J Mol Biol **208**(3): 405-415.

Walther, T. C., P. Askjaer, M. Gentzel, A. Habermann, G. Griffiths, M. Wilm, I. W. Mattaj and M. Hetzer (2003). "RanGTP mediates nuclear pore complex assembly." Nature **424**(6949): 689-694.

Walther, T. C., M. Fornerod, H. Pickersgill, M. Goldberg, T. D. Allen and I. W. Mattaj (2001). "The nucleoporin Nup153 is required for nuclear pore basket formation, nuclear pore complex anchoring and import of a subset of nuclear proteins." EMBO J **20**(20): 5703-5714.

Watson, M. L. (1959). "Further observations on the nuclear envelope of the animal cell." J Biophys Biochem Cytol **6**(2): 147-156.

Weber, K., U. Plessmann and P. Traub (1989). "Maturation of nuclear lamin A involves a specific carboxy-terminal trimming, which removes the polyisoprenylation site from the precursor; implications for the structure of the nuclear lamina." FEBS Lett **257**(2): 411-414.

Wheaton, K., D. Campuzano, W. Ma, M. Sheinis, B. Ho, G. W. Brown and S. Benchimol (2017). "Progerin-Induced Replication Stress Facilitates Premature Senescence in Hutchinson-Gilford Progeria Syndrome." Mol Cell Biol **37**(14).

Witkiewicz, A. K., K. E. Knudsen, A. P. Dicker and E. S. Knudsen (2011). "The meaning of p16(ink4a) expression in tumors: functional significance, clinical associations and future developments." Cell Cycle **10**(15): 2497-2503.

Worman, H. J. and G. Bonne (2007). ""Laminopathies": a wide spectrum of human diseases." Exp Cell Res **313**(10): 2121-2133.

Worman, H. J., C. Ostlund and Y. Wang (2010). "Diseases of the nuclear envelope." Cold Spring Harb Perspect Biol **2**(2): a000760.

Xie, W., A. Chojnowski, T. Boudier, J. S. Lim, S. Ahmed, Z. Ser, C. Stewart and B. Burke (2016). "A-type Lamins Form Distinct Filamentous Networks with Differential Nuclear Pore Complex Associations." Curr Biol **26**(19): 2651-2658.

Young, S. G., L. G. Fong and S. Michaelis (2005). "Prelamin A, Zmpste24, misshapen cell nuclei, and progeria--new evidence suggesting that protein farnesylation could be important for disease pathogenesis." J Lipid Res **46**(12): 2531-2558.

Zhang, X., S. Chen, S. Yoo, S. Chakrabarti, T. Zhang, T. Ke, C. Oberti, S. L. Yong, F. Fang, L. Li, R. de la Fuente, L. Wang, Q. Chen and Q. K. Wang (2008). "Mutation in nuclear pore component NUP155 leads to atrial fibrillation and early sudden cardiac death." Cell **135**(6): 1017-1027.

Zuccolo, M., A. Alves, V. Galy, S. Bolhy, E. Formstecher, V. Racine, J. B. Sibarita, T. Fukagawa, R. Shiekhattar, T. Yen and V. Doye (2007). "The human Nup107-160 nuclear pore subcomplex contributes to proper kinetochore functions." EMBO J **26**(7): 1853-1864.